Electronic Thesis and Dissertation Repository

6-22-2022 10:00 AM

Characterization of galectin-16 expression and function in placental cells

Jennifer Kaminker, *The University of Western Ontario*

Supervisor: Alexander Timoshenko, *The University of Western Ontario*
A thesis submitted in partial fulfillment of the requirements for the Master of Science degree in Biology
© Jennifer Kaminker 2022

Follow this and additional works at: https://ir.lib.uwo.ca/etd

Part of the Biology Commons, and the Cell Biology Commons

Recommended Citation

Abstract

The processes of cellular differentiation and apoptosis are critical for placental development. The galectin-16 gene (*LGALS16*) is associated with these processes in the placenta, but the mechanism by which it acts is poorly characterized. My bioinformatics analysis revealed that *LGALS16* expression was limited to specific tissues including the placenta and identified multiple regulatory molecules (transcription factors and miRNAs), which could potentially control relevant transcriptional and post-transcriptional mechanisms. Considering the predominant expression of *LGALS16* in placenta, I examined the expression, regulation, and function of *LGALS16* in BeWo and JEG-3 cell lines representing *in vitro* models of trophoblast differentiation. In both models, *LGALS16* was significantly upregulated in parallel with human chorionic gonadotropin beta (*CGB*) during trophoblastic differentiation induced by 8-Br-cAMP. Inhibition of p38 MAPK and Epac significantly altered *LGALS16* expression during differentiation, while modulation of *O*-GlcNAc homeostasis failed to change *LGALS16* and *CGB* expression. Lastly, CRISPR/Cas9 *LGALS16* knockouts suppressed expression of CGB. These findings suggest that *LGALS16* may play a role in trophoblastic differentiation through p38 MAPK and Epac signaling pathways.

Keywords

Summary for Lay Audience

Galectins are a group of carbohydrate binding proteins with roles in cell growth, differentiation, and cell death. Of the galectins characterized in humans, galectins-13, -14, and -16 are highly expressed in the placenta, suggesting that they play a unique role in placental development. Furthermore, improper expression of these three galectins leads to disorders such as preeclampsia, a condition characterized by high blood pressure in pregnant mothers that can be fatal. Limited literature exists on galectin-16 (encoded by the *LGALS16* gene) and thus it is the focus of the current study. Datasets from other studies were extracted and analyzed to determine the level of galectin-16 in different tissues. This revealed that galectin-16 expression is expressed at a high level in two tissues, the placenta and brain. I also used a program to align the upstream sequence of galectin-16 with sequences of binding sites for specific transcription factors. I determined predicted transcription factors by identifying binding site sequences which matched with 100% similarity to a part of the upstream sequence. Using placental culture models, I induced placental differentiation with cAMP and examined the effects on *LGALS16* expression. Additionally, I treated cells with biochemical inhibitors and stimulators of transcription factors, cAMP signaling molecules, and enzymes responsible for adding and removing sugars to proteins. I analyzed how these inhibitors/stimulators affected galectin gene and protein expression, particularly *LGALS16*, and the biomarker of differentiation, chorionic gonadotropin. Finally, cell pools were genetically modified to knockout galectin-16 and then treated with cAMP to test whether cells could still undergo differentiation. In placental cell models, *LGALS16* expression was significantly increased during placental differentiation. Inhibition of two cAMP signaling molecules led to significant changes in *LGALS16* expression while no changes were observed in response to drugs changing glycosylation of intracellular proteins. Knocking out galectin-16 in placental cells changed the morphology of cells and inhibited gene expression of chorionic gonadotropin. These findings provide insights into the significance of galectin-16 as a critical regulator of placental differentiation which may serve as a tool to identify dysregulated placental differentiation in cancers and pregnancy disorders.

Co-Authorship Statement

Chapter 2: This chapter was published in Biomolecules, 2021; 11(12): 1909. I contributed to methodology, investigation, formal analysis, and writing under the supervision of Dr. Alexander Timoshenko.

Acknowledgments

First and foremost, I would like to thank my supervisor, Dr. Alexander Timoshenko. Thank you for your mentorship, encouragement, and unwavering support over these past four years. I am greatly appreciative for the amazing learning opportunities of new techniques and skills that I was given throughout my project. Thank you for pushing me to ask new questions and to continuously seek out ways to expand my project. With your direction and feedback, I have grown immensely both as an individual and a researcher.

Thank you to my advisors, Dr. Robert Cumming and Dr. Jim Karagiannis. I am grateful for your guidance and constructive feedback on how to improve and enhance my project. Thank you for the use of your labs and equipment which was essential to completing my project.

I would also like to thank Dr. Stephen Renaud for providing us with the BeWo and JEG-3 cell lines. Thank you for sharing your expertise in placental biology and for your support in my endeavours. Thank you, Gargi Jaju, for training me to learn techniques and your patience in answering all of my questions. Thank you for your assistance and advice through multiple obstacles over these past few years.

Thank you to Danielle Spice for your help and instruction to assist me with CRISPR/Cas9 techniques and analyses. I am extremely fortunate for your knowledge and tips which proved extremely useful to ensure I was able to complete my analyses effectively and on time.

Thank you, Ahmad Butt, for all of the hard work you put in and for your contributions to this project including completing bioinformatics analysis, carrying out cell treatments, as well as performing and quantifying MTT assays and qPCR experiments. You were an integral part of this project, and I am grateful to have collaborated with you over the past year.

Finally, thank you to all of the members of the Timoshenko lab: Adam McTague, Jolaine Smith, Rada Tazhitdinova, Philipp Guevorguian, and Haya Tawfik. Thank you for sharing your knowledge, teaching me techniques, and providing technical assistance when I faced roadblocks. I am grateful for your thought-provoking questions about my project and for your encouragement over the years.

Table of Contents

List of Tables

List of Figures

List of Appendices

List of Abbreviations

8-Br-cAMP	8-Bromoadenosine-3',5'-cyclic monophosphate
AC	2-acetamido-1,3,4,6-tetra-O-acetyl-2-deoxy-5-thio-α-D-glucopyranose
AEBSF	4-(2-Aminoethyl)benzenesulfonyl fluoride hydrochloride
ANOVA	Analysis of variance
BeWo	Human placental choriocarcinoma cell line
BSA	Bovine serum albumin
CGB	Chorionic gonadotropin beta
CGB3/5	Chorionic gonadotropin beta subunits 3 and 5
cPCR	Conventional polymerase chain reaction
CRD	Carbohydrate recognition domain
CTB	Cytotrophoblasts
DMSO	Dimethyl sulfoxide
DPBS	Dulbecco's phosphate buffered saline
EDTA	Ethylenediaminetetraacetic acid
Epac	Exchange protein directly activated by cAMP
FBS	Fetal bovine serum
GFAT	Glutamine fructose-6-phosphate aminotransferase
HBP	Hexosamine biosynthesis pathway
hCG	Human chorionic gonadotropin
JEG-3	Human placental choriocarcinoma cell line
KO	Knockout
MAPK	Mitogen activated protein kinase
NF-κB	Nuclear factor kappa B
O-GlcNAc	O-linked β-N-acetyl-D-glucosamine
OGA	O-GlcNAcase
OGT	O-GlcNAc transferase
PAM	Protospacer adjacent motif
PKA	Protein kinase A
PMSF	Phenylmethylsulfonyl fluoride
PVDF	Polyvinylidene difluoride
RT-qPCR	Quantitative reverse transcription polymerase chain reaction
SD	Standard deviation
SDS-PAGE	Sodium dodecyl sulfate polyacrylamide gel electrophoresis
STB	Syncytiotrophoblasts
TBS	Tris-buffered saline
TBS-T	Tris-buffered saline with Tween
TF	Transcription factor
TG	Thiamet G
UDP	Uridine diphosphate
VT	Villous cytotrophoblasts
WT	Wildtype

Chapter 1

1   Introduction

1.1   Galectins

Galectins are a family of soluble glycan-binding proteins that share a conserved carbohydrate-recognition domain (CRD) consisting of ~130 amino acids and are characterized by their affinity for β-galactosides. Glycoproteins, proteoglycans and glycolipids contain glycan groups that can be dynamically exposed as a post-translational modification in response to various stimuli resulting in "glycosylation signatures". Galectins are responsible for decoding the "glycosylation signatures" via N-acetyllactosamine units of glycoproteins and glycolipids to stimulate a signal transduction cascade. This mechanism allows galectins to play a key role in the regulation of fundamental biological processes including cell growth, differentiation, migration, death, and immune responses (Laderach et al., 2010; Timoshenko, 2015).

Galectins exist in all metazoans and are the most widely expressed class of lectins (Cummings & Liu, 2009). Initially termed an electrolectin, galectins were first discovered in 1975 in the electric eel (Teichberg et al., 1975). In 1976, galectins were identified in vertebrates from chick muscle as well as calf heart and lung (de Waard et al., 1976). Studies have since identified 16 galectin genes in the animal kingdom, 12 of which are expressed in humans (Timoshenko, 2015). Galectin expression and localization patterns vary in different cell and tissue types, disease states, and stress responses (Cummings & Liu, 2009; Johannes et al., 2018; Hong et al., 2021). Moreover, some galectins are abundantly expressed in a variety of tissues while others are uniquely expressed in a limited number of tissues suggesting they may have evolved to serve a tissue-specific function (Johannes et al., 2018).

Three subcategories of galectins have been defined based on domain structure: prototype, tandem-repeat, and chimeric types (**Figure 1**) (Timoshenko, 2015). Prototype galectins contain one CRD and include galectins-1, -2, -5, -7, -10, -11, -13, -14, -15, and -16
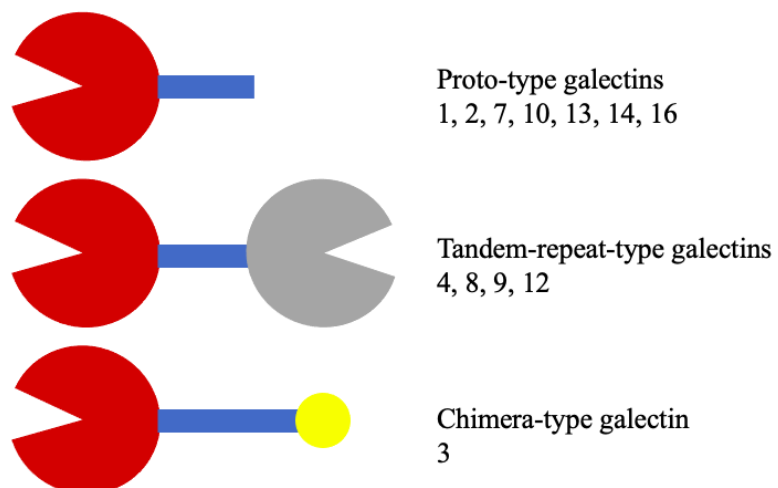
Figure 1. Three structural subcategories of galectins in humans.

Galectins are subcategorized according to their carbohydrate recognition domains (red and grey). Prototype galectins contain one CRD, tandem-repeat galectins contain two non-identical CRDs linked by a non-lectin linker domain (blue), and chimera-type contain an N-terminal end domain (yellow). Adapted figure from (Timoshenko, 2015).

(Laderach et al., 2010; Timoshenko, 2015) with galectins-13, 14, and -16 sharing over 60% similarity in their amino acid sequences (Si et al., 2021). Tandem-repeat galectins contain two homologous CRDs connected by a linker of 70 amino acids and include galectins-4, -6, -8, -9, and -12 (Laderach et al., 2010). Chimera-type galectins contain one CRD linked to a non-lectin N terminal proline and glycine rich domain and only includes galectin-3 (Laderach et al., 2010). The CRD forms a β-sandwich and contains a conserved galactose-binding site consisting of approximately seven amino acids in addition to non-carbohydrate binding sites (Johannes et al., 2018). These amino acids next to the galactose-binding site of the CRD are less conserved and these differences confer varying specificities and affinities of galectins for longer glycoconjugates (Johannes et al., 2018). These non-carbohydrate binding sites can also lead to dimerization (e.g., galectin-1) (Johannes et al., 2018). Furthermore, some galectins share homology with the galectin family but do not bind β-galactosides, such as galectin-10 which has a higher affinity for β-mannosides, or may not bind carbohydrates (Cummings & Liu, 2009).

Galectins are synthesized in the cytosol and then widely distributed throughout the cell in the nucleus, cytoplasm, outer plasma membrane, and extracellular matrix (Johannes, 2018). The localization of galectins plays a key role in governing their function (Vladoiu et al., 2014). Galectins do not contain a signal sequence for secretion and are found intracellularly in nuclear, cytoplasmic, or mitochondrial compartments to affect cell growth and apoptosis (Vladoiu et al., 2014). Extracellular galectins are non-classically secreted independent of the ER and Golgi via galectin-rich vesicles, exosomes, oligomerisation, and direct translocation (He & Baum, 2006; Johannes, 2018; Popa et al., 2018). Secreted galectins can bind to glycan ligands on the cell surface or glycoproteins (i.e. fibronectin and laminin) in the extracellular matrix to promote cell adhesion and migration (He & Baum, 2006). Other extracellular galectins bind to cell surface receptors as dimers or oligomers to facilitate cross-linking and transmembrane signaling (Vladoiu et al., 2014; Nabi et al., 2015).

Galectins primarily use carbohydrate-independent pathways inside the cell via cytosolic or nuclear targets as well as carbohydrate-dependent signaling extracellularly to carry out

their function (Johannes, 2018). However, some extracellular carbohydrate-independent signaling occurs, while other galectins signal intracellularly through glycan-dependent mechanisms (Tazhitdinova & Timoshenko, 2020).

1.2   *O*-GlcNAcylation

O-linked N-acetyl-D-glucosamine (*O*-GlcNAc) can be added post-translationally to serine/threonine residues of proteins in a process called *O*-GlcNAcylation (**Figure 2**) (Kim et al., 2017). These modifications may determine the localization of galectins and ultimately affect their function. The process relies on glucose utilized through the hexosamine biosynthetic pathway (HBP) (Buse, 2006). This involves the conversion of fructose-6-phosphate to glucosamine-6-phosphate, which is catalyzed by glutamine:fructose-6-phosphate amidotransferase (GFAT) to generate UDP-N-acetylglucosamine (UDP-GlcNAc) (Buse, 2006). *O*-GlcNAc transferase (OGT) uses UDP-GlcNAc as a substrate to add *O*-GlcNAc while *O*-GlcNAcase (OGA) removes *O*-GlcNAc (Yang & Qian, 2017). Therefore, the activity of OGA and OGT affects the level of *O*-GlcNAcylated proteins in a cell (Yang & Qian, 2017).

O-GlcNAcylation levels vary in different cell types and during differentiation. Undifferentiated stem cells exhibit a high level of *O*-GlcNAc as transcription factors important in maintaining pluripotency (i.e. OCT4, GATA-1, SOX2, NANOG, C-MYC, and KLF4) are *O*-GlcNAcylated (Jang et al., 2012). HL-60 and HT-29 cells that differentiate into neutrophils and enterocytes, respectively, display decreased *O*-GlcNAc (Sherazi et al., 2018). However, osteogenic (Koyama & Kamemura, 2015), adipocytic (Ishihara et al., 2010), chondrocytic (Andrés-Bergós et al., 2012), and corneal epithelial (McColgan et al., 2020) cellular differentiation are associated with an increase in global *O*-GlcNAc. These changes in *O*-GlcNAcylation during differentiation are linked to the secretion and accumulation of galectins. For instance, increased galectin secretion was shown during the differentiation of plasma cells (Tsai et al., 2011), macrophages (Novak et al., 2012), granulocytes (Barrow et al., 2011), muscle cells (Cooper & Barondes, 1990; Harrison & Wilson, 1992), and adipocytes (Wang et al., 2004). Additionally, galectin gene
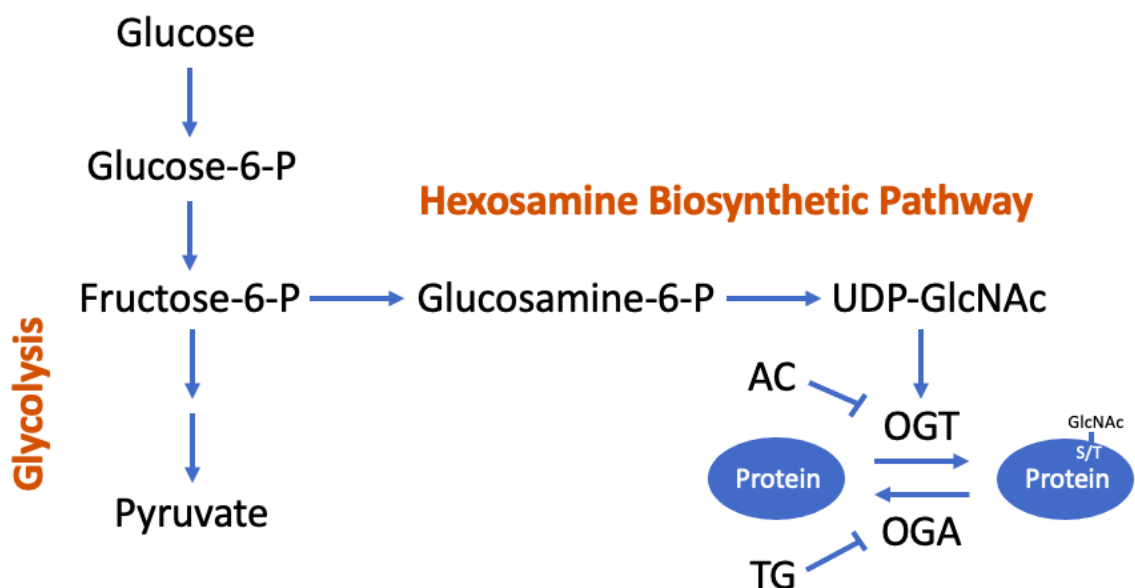
Figure 2. Diagram of the generation of UDP-GlcNAc in the hexosamine biosynthetic pathway and *O*-GlcNAcylation.

UDP-GlcNAc is used as a substrate for *O*-GlcNAcylation, which is carried out by enzymes OGT and OGA. OGT adds GlcNAc to serine/threonine residues of proteins and can be inhibited by AC. OGA removes GlcNAc and can be inhibited by thiamet G (modified from Kim et al., 2017).

expression profiles differ when global *O*-GlcNAcylated levels of proteins are high or low in cells. A model has been proposed suggesting that stem cells have a high *O*-GlcNAc level and an intracellular accumulation of galectins while differentiated cells have a low *O*-GlcNAc level and an increase in galectin secretion (Tazhitdinova & Timoshenko, 2020). *O*-GlcNAcylation levels have also been associated with placental development and pathologies during pregnancy. For example, maternal hyperglycemia is associated with an increase in *O*-GlcNAcylation which may affect human fetal development (Ning & Yang, 2021). Moreover, changes in *O*-GlcNAcylation levels occur in the placentas of mothers with diabetes which can result in endocytosis of trophoblast cells and altered fetal growth (Palin et al., 2021). *O*-GlcNAcylation has also been shown to regulate decidualization, transcription factors, and maternal stress in the placentas of mice (Lima et al., 2018).

1.3 Placenta

During pregnancy, the placenta is formed as an interface between the mother and fetus and is responsible for transport, metabolism, protection, and endocrine functions. This specialized organ is vital for successful embryonic development. The placenta transfers oxygen and nutrients to the fetus and utilizes these for its own function while it removes carbon dioxide and waste from the fetus (Gude, 2004). Amino acids and lipids are metabolized by the placenta and these products are released back into circulation (Gude, 2004). Additionally, the placenta protects the fetus from toxic substances with a variety of mechanisms, such as export pumps, and transports maternal antibodies to regulate passive immunity of the fetus (Gude, 2004). Hormones are also produced by the placenta and released into maternal and fetal circulation (Gude, 2004). These include the glycoprotein, human chorionic gonadotropin (hCG), and the steroid hormone, progesterone, which are tightly linked to each other (Gude, 2004). In early pregnancy, syncytiotrophoblasts (STBs) are the primary producers of hCG to maintain the corpus luteum and promote progesterone secretion for embryo implantation and growth as well as proper capillary development (Cole, 2010; Fournier, Guibourdenche, & Evain-Brion, 2015). Progesterone is responsible for supporting decidualization; inhibiting uterine contraction, menstruation, and labour; and suppressing immune responses (Cole, 2010; Ku et al., 2018; Peavey et al., 2021). hCG is a dimer comprised of an α and β subunit (Kardana & Cole, 1994). hCG peaks at 10

weeks of pregnancy leading to an increase in progesterone (Cole, 2010). However, hCG decreases in the second and third trimesters which results in a decrease of the luteal production of progesterone (Cole, 2010). Consequently, trophoblasts become the primary producers of progesterone to sustain high levels of progesterone later in pregnancy which peak at the end of gestation (Tuckey, 2005; Cole, 2010). Dysregulation of progesterone and hCG can have harmful effects during pregnancy. Reduced levels of progesterone are associated with threatened miscarriage (Ku et al., 2018) and trophoblastic disease can lead to significant increases in a subunit of hCG, chorionic gonadotropin beta (CGB) (Kumar & Magon, 2012). Therefore, trophoblasts are critical in the regulation of hormones and proper placental development.

1.3.1　Placental differentiation

Implantation occurs when the blastocyst attaches to the uterine lumen epithelium (Ji et al., 2013). Following implantation, proliferative, undifferentiated cytotrophoblast (CTB) cells are derived from trophectodermal cells comprising the outer layer of the blastocyst (Pollheimer et al., 2018). CTBs differentiate through two predominant pathways into villous cytotrophoblasts (VT) or extravillous cytotrophoblasts (EVTs) (**Figure 3**) (Ji et al., 2013). In the VT pathway, CTBs differentiate and fuse into multinucleated syncytiotrophoblasts (STBs) to form a layer on chorionic villi that is in direct contact with maternal blood and thus lacks the expression of the classical class I human leukocyte antigens (HLA) to provide immune tolerance (Ji et al., 2013). CTBs continuously fuse with the overlaying syncytium to provide fresh cellular components as apoptotic material is released as syncytial knots (Ji et al., 2013). The syncytium at the maternal-fetal interface produces and regulates hormones (i.e., hCG); regulates immunological responses; and facilitates the transfer of nutrients, hormones, gases, and wastes (Than et al., 2014). Differentiated EVTs proliferate and invade the decidua and myometrium as interstitial EVTs which fuse into the terminally differentiated giant cells (Al-Nasiry, 2009; Ji et al., 2013). Alternatively, differentiated endovascular EVTs can invade the maternal spiral arteries to remodel the vasculature providing increased blood and oxygen flow to the fetus (Ji et al., 2013).
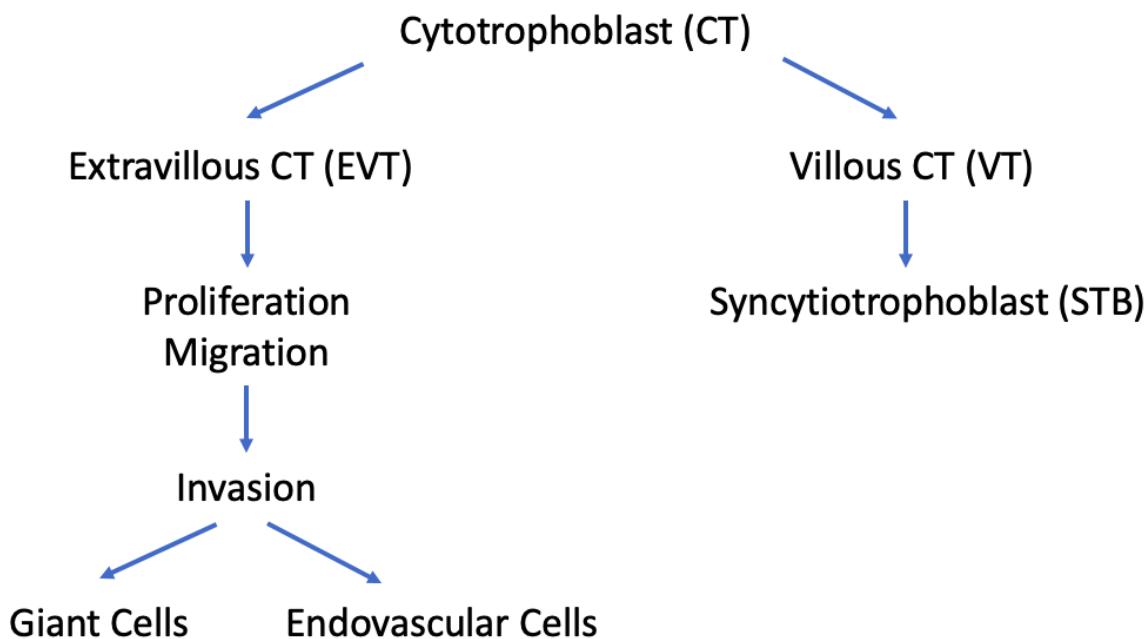
Figure 3. Cytotrophoblast differentiation occurs through two main pathways: villous cytotrophoblasts and extravillous cytotrophoblasts.

CTB progenitor cells differentiating towards the EVT pathway proliferate and migrate to invade the decidua and myometrium and become giant cells or promote maternal vascularization as endovascular EVTs. CTBs can also differentiate towards the VT pathway to fuse into STBs which has a variety of functions. Adapted from (Tarrade et al., 2001).

STB differentiation is initiated by increased 3',5'-cyclic adenosine monophosphate (cAMP) levels via activated adenylyl cyclase which converts adenosine triphosphate (ATP) to cAMP (Ji et al., 2013). cAMP induces downstream molecules including protein kinase A (PKA) and exchange protein directly activated by cAMP (Epac) (**Figure 4**) (Kusama et al., 2018). PKA mediates the phosphorylation of cyclic AMP response element binding protein (CREB) as well as activates p38 MAPK leading to increased transcription of glial cells missing-1 (*GCM1*), a transcription factor essential for cell fusion, and Ovo like transcriptional repressor 1 (*OVOL1*) (Kusama et al., 2018). Other pathways including MAPK kinases and transforming growth factor β (TGF-β)–activating kinase 1 are also reported to activate p38 kinase (Zhang & Liu, 2002). Signal transducer and activator of transcription 5B (STAT5B) has also been shown to regulate cell fusion and is suggested to target GCM1. GCM1 then activates *ERVWE1*, an endogenous retroviral gene abundantly expressed in placental tissues (Hua et al., 2018). This gene codes for syncytin-1 which is upregulated along with syncytin 2 to promote CTB fusion into STBs (Blond et al., 2000; Hua et al., 2018). The PKA-CREB pathway also leads to an increase of NR4A3 which can result in a decrease in syncytin 2 to regulate the degree of syncytialization (Kusama et al., 2018). Alternatively, Epac may induce cell fusion through Ras-related protein 1 (RAP1) activation (Kusama et al., 2018). RAP1 in turn activates calcium/calmodulin-dependent protein kinase 1 (CaMK1) which phosphorylates GCM1 (Gupta et al., 2015). A variety of other signaling pathways are involved in STB fusion and differentiation including the p38 mitogen-activated protein kinases (MAPK), wingless-related integration site (Wnt), janus kinase-signal transducer and activator of transcription (JAK/STAT), phosphatidylinositol-3-kinase (PI3K)/Akt and the mammalian target of rapamycin (mTOR), and TGF-β superfamily pathways (Gupta et al., 2015). However, these associations are less well characterized. Cell fusion ultimately leads to increased hCG and *LGALS13* expression (Orendi et al., 2010; Kusama et al., 2018). Whether *LGALS16* is upregulated in a manner similar to the closely related *LGALS13* gene remains to be elucidated. Previous literature has also found that cytokines, hormones, protein kinases, transcription factors (i.e., KLF6), proteases and fusion proteins regulate the fusion of VTs (Ji et al., 2013; Racca et al., 2015). Myosin-II and tissue stiffness may also mechanically regulate STB morphology, fusion, and hormone release (Ma et al., 2020).
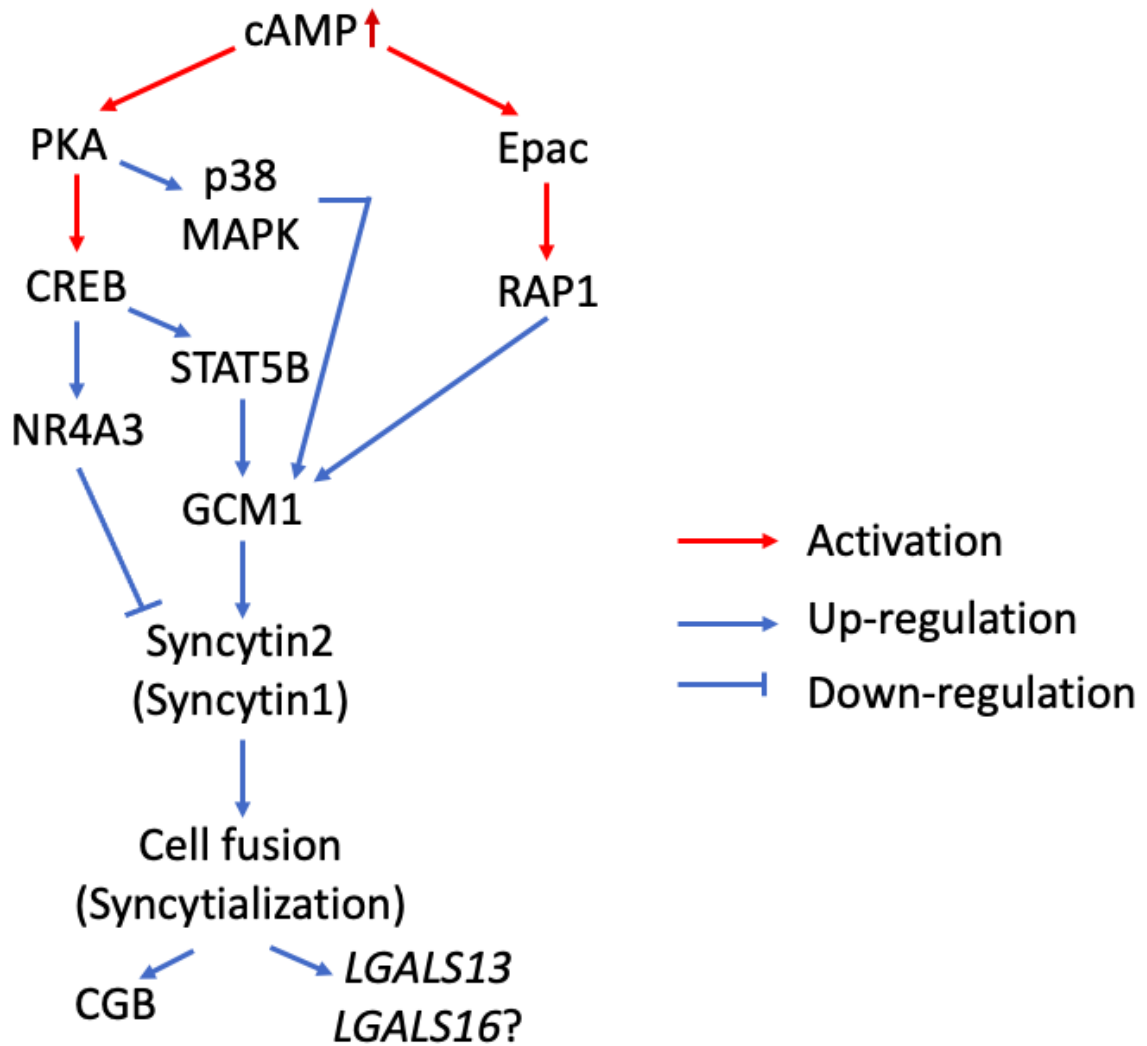
Figure 4. cAMP-mediated differentiation signaling pathway.

cAMP induces placental differentiation via PKA and Epac mediated pathways. Downstream effector molecules upregulate the transcription of genes essential for cell fusion (i.e. GCM1) leading to an increase in hCG, *LGALS13* and potentially *LGALS16*. Adapted from (Kusama et al., 2018).

Improper trophoblast differentiation and placental function can result in the development of miscarriage, stillbirth, recurrent pregnancy loss, and preeclampsia, a disorder characterized by hypertension and proteinurea during pregnancy (Pabinger et al., 2001; Than et al., 2014; Huppertz, 2018). For example, errors in trophoblast fusion can result in the release of apoptotic material activating an inflammatory maternal response leading to preeclampisa (Gauster et al., 2009). Despite their importance, the molecular mechanisms governing human trophoblast differentiation require further investigation. Galectins have been found to be associated with placental development and thus may be involved in mechanisms underlying this pathology.

1.3.2   Placental immune tolerance

Placental immune tolerance is an essential adaptation that suppresses the maternal immune response to the fetus while maintaining normal infection defense against non-self-antigens (Wang & Li, 2020). In pregnancy, the embryo and placenta are semi-allografts, exposing the maternal immune system to paternal-fetal antigens (Kieffer et al., 2019). Despite the direct contact between the placental/fetal membranes and maternal blood/tissues, immunological rejection is not triggered (Kanellopoulos-Langevin et al., 2003; Bai et al, 2022). Various mechanisms exist to suppress the immune response. Trophoblasts regulate the activity, differentiation, and induction of uterine natural killer (NK) cells, decidual macrophages, and regulatory T cells (Treg), respectively (Wang & Li, 2020). Moreover, trophoblasts express and secrete immune inhibitory molecules targeting macrophages, natural killer cells, dendritic cells (DCs), T cells, or myeloid-derived suppressor cells (MDSCs) (Wang & Li, 2020). The syncytiotrophoblast is also densely covered with glycoproteins which inhibits activated maternal leukocytes (Arkwright et al., 1994; Petty et al., 2006). Galectin expression in trophoblasts also serves to regulate placental immune tolerance (Than et al., 2009).

1.3.3   Galectin expression in the placenta

Placental trophoblasts express galectins-1, -3, -7, -10, -13, -14, and -16. This intricate network of galectins is regulated by fetal sex, hormones, oxygen tension, epigenetics, pathogens, and inflammatory mediators (Jovanović Krivokuća et al., 2021). Consequently, galectin expression profiles vary in different trophoblast cell populations as well as during development and differentiation. For example, VT cells express galectins -1, -3 and -8 and CTBs express galectins-3 and -9 (Jovanović Krivokuća et al., 2021). STBs and EVTs express galectins-1, -3, -7, and -8. STBs also express galectins-10, -13, -14, and -16 (Than et al., 2009; Jovanović Krivokuća et al., 2021). While many galectins are widely expressed in a variety of tissues (i.e., galectins-1 and -3), galectins-13, -14, and -16 are placenta-specific which may indicate their uniquely evolved role at the feto-maternal interface.

Studies have shown galectins to be involved in trophoblast differentiation processes including placental immune tolerance, invasion, proliferation, angiogenesis, and cell fusion (**Figure 5**). Altered and incorrect galectin expression is also associated with different pregnancy pathologies. These include pregnancy loss, gestational diabetes mellitus, inflammation, infection, pre-eclampsia, and intrauterine growth restriction (Jovanović Krivokuća et al., 2021).

Placental specific galectins (*LGALS13, LGALS14, LGALS16*), particularly *LGALS16*, are exclusively expressed in STBs and they are proposed to play a key role in regulating and preventing the maternal immune response through T cell apoptosis (Than et al., 2014). These three galectin genes are highly conserved and located in a cluster on chromosome 19 (Than et al., 2014). The correct expression of galectins-13, -14, and -16 has been shown to be essential for proper reprogramming of the transcriptional activity of the trophoblast. If the expression of this placenta specific gene cluster is impaired, disorders such as pre-eclampsia can occur (Than et al., 2014). The predicted loci, LOC148003, was distinguished as galectin-16 in 2009 and its monomeric structure was only elucidated in 2021 (Than et al., 2009; Si et al., 2021). Given its recent discovery, extremely limited literature exists on *LGALS16* and its role in trophoblastic differentiation. Therefore, it is a novel feature of my
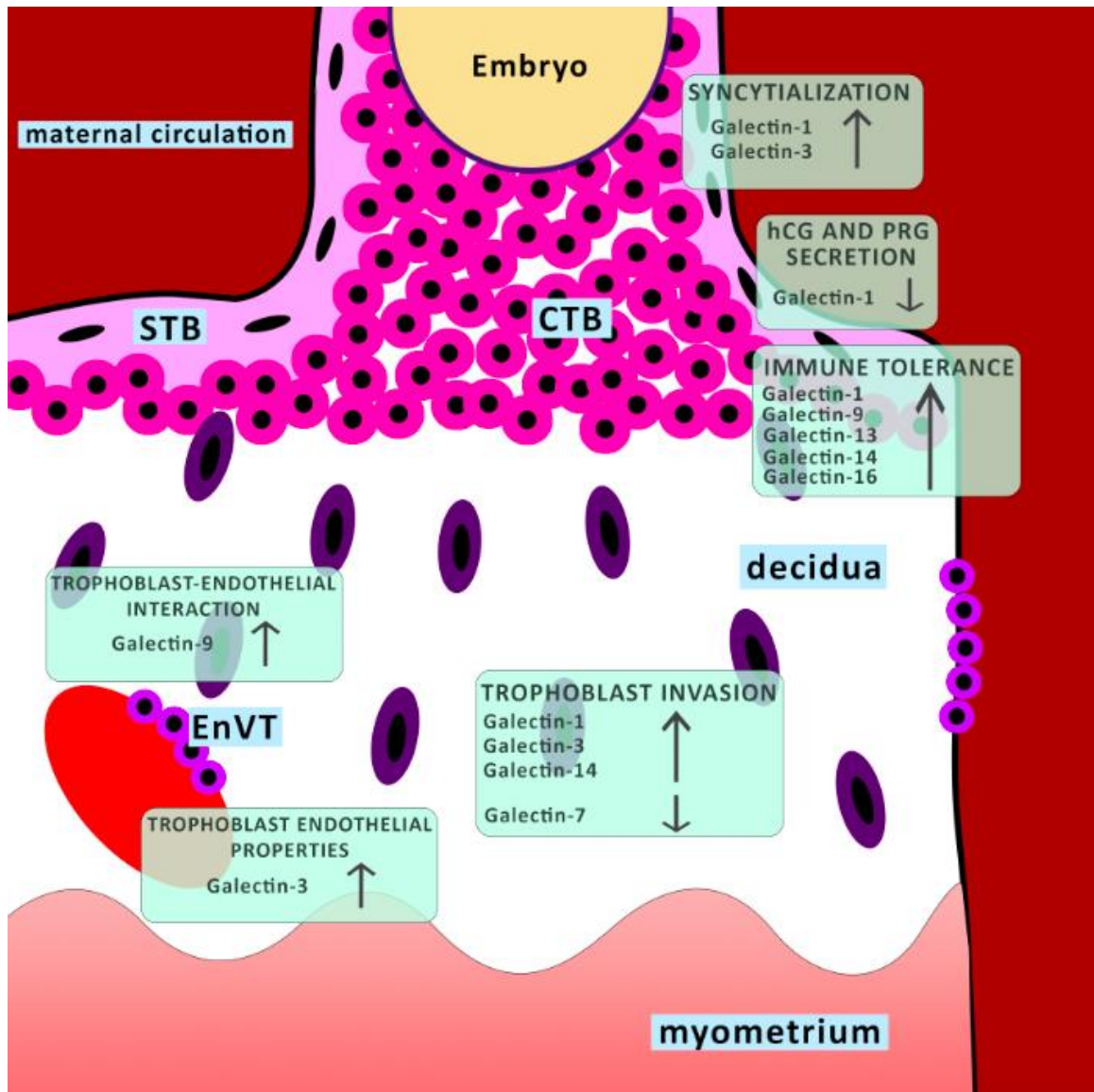
Figure 5. Overview of galectin functions in the placenta.

Proposed galectin functions during placental development. Syncytiotrophoblast (STB); cytotrophoblast (CTB); extravillous trophoblast (EVT); endovascular trophoblast (EnVT); progesterone (PRG); human chorionic gonadotropin (hCG). Adapted from (Jovanović Krivokuća et al., 2021).

study.

1.3.4   Cell models of trophoblastic differentiation

The human placental choriocarcinoma cell lines, BeWo and JEG-3, are well-established *in vitro* models for investigating the role of galectins in the differentiation of CTB cells (Orendi et al., 2010; Poloski et al., 2016). These two cell models differ as BeWo cells are more similar to VTs and undergo fusion during differentiation, while JEG-3 cells are more similar to EVTs as they express some EVT markers (i.e. HLA-G), are invasive, and undergo little fusion compared to BeWo cells (Collett et al., 2012; Tilburgs et al., 2015; Drwal et al., 2018). A study comparing gene expression in BeWo and JEG-3 cells treated with forskolin to induce cAMP and ultimately differentiation found 32 altered genes between the two cell lines highlighting their differences and genes which may play key roles in cell fusion (Msheik et al., 2019).

Upon treatment with 8-bromo-cyclic adenosine 3′,5′-monophosphate (8-Br-cAMP), both BeWo and JEG-3 cells are stimulated to differentiate into STB-like cells (Burnside et al., 1985; Chen et al., 2013). This occurs via PKA-induced activation which upregulates fusogenic transcription factors, certain galectins (i.e., *LGALS13*), and the biomarker of differentiation, *CGB* (Orendi et al., 2010). However, *CGB* is also expressed independently of PKA and cell fusion (Orendi et al., 2010) which allows JEG-3 cells to express this marker despite undergoing little fusion. These cell models are thus excellent tools that can be used in experiments investigating the role, function, and regulation of *LGALS16* during 8-Br-cAMP-induced differentiation.

1.4   Thesis Overview

Galectins are involved in the differentiation of a variety of cell types (Tazhitdinova & Timoshenko, 2020). Current literature has shown that galectin-16 is tissue-specific to the placenta and is significantly upregulated in differentiated STBs treated with cAMP directly, or forskolin, an inducer of cAMP. However, the reasoning for this relationship between *LGALS16* and placental development is unclear. Gaining a better understanding

of the regulation and expression of galectin-16 during placental differentiation can help elucidate its potential role as an important regulator of placental development. Transcription factors unique to the promoter region of *LGALS16* and molecules upstream in the cAMP pathway may mediate *LGALS16* expression during trophoblastic differentiation. Moreover, recent studies from the Timoshenko laboratory have shown that galectin expression and secretion can be driven by *O*-GlcNAcylation, which alters in differentiated versus progenitor cells (Sherazi et al., 2018; Tazhitdinova & Timoshenko, 2020; Gatie et al., 2022). Therefore, understanding how inhibitors of upstream transcription factors and *O*-GlcNAcylation affect *LGALS16* expression during differentiation can reveal the regulatory mechanisms of *LGALS16*. Additionally, generating *LGALS16* CRISPR/Cas9 knockout cells and examining phenotypic effects on STB differentiation can unveil the functional role of galectin-16 and whether it plays a critical role in placental differentiation processes.

This study aims to examine the effects of transcription factor inhibitors, *O*-GlcNAc modulation, and galectin-16 knockouts on *LGALS16* and *CGB* expression to provide novel insights into the regulation and functional role of galectin-16. Considering a unique association of galectin-16 with placental development, **I will test the hypothesis that galectin-16 is an essential regulator of trophoblast differentiation which is guided through different cAMP-mediated signaling pathways.** The rationale behind this study is that galectin-16 is highly restricted in its expression to differentiated placental cells. Chapter 2 provides bioinformatics analysis of available databases on galectin-16 and insights into *LGALS16* expression in different cell lines and tissues. Experimental techniques were also used to identify *LGALS16* and transcription factor expression during placental differentiation using two cell lines, BeWo and JEG-3. Chapter 3 dives deeper into the regulation and function of galectin-16 by examining the effects of biochemical inhibitors of predicted transcription factors and *O*-GlcNAc enzymes to examine their effects on *LGALS16* during differentiation. Further, *LGALS16* CRISPR/Cas9 knockouts were generated to determine phenotypic consequences on placental differentiation. Together, these chapters provide a comprehensive overview into the regulation and role of galectin-16 as a novel biomarker of placental differentiation.

Objective 1: To perform bioinformatics analysis of available databases on galectin-16 expression in different human tissues and cells as well as potential transcriptional and post-transcriptional regulators of galectin-16 expression.

Objective 2: To study changes in the expression of *LGALS16* in BeWo and JEG-3 cell lines in the context of trophoblastic differentiation.

Objective 3: To examine the role of potential transcription factors and *O*-GlcNAc homeostasis in regulating *LGALS16* expression and trophoblastic differentiation.

Objective 4: To characterize how the *LGALS16* CRISPR/Cas9 knockout changes the capacity of JEG-3 cells for trophoblastic differentiation.

1.5   References

Al-Nasiry S, Vercruysse L, Hanssens M, Luyten C, Pijnenborg R. Interstitial trophoblastic cell fusion and E-cadherin immunostaining in the placental bed of normal and hypertensive pregnancies. Placenta. 2009 Aug;30(8):719-725.

Andrés-Bergós J, Tardio L, Larranaga-Vera A, Gómez R, Herrero-Beaumont G, Largo R. The increase in O-linked N-acetylglucosamine protein modification stimulates chondrogenic differentiation both in vitro and in vivo. J Biol Chem. 2012 Sep 28;287(40):33615-33628.

Arkwright PD, Rademacher TW, Boutignon F, Dwek RA, Redman CWG. Suppression of allogenic reactivity in vitm by the syncytiotrophoblast membrane glycocalyx of the human term placenta is carbohydrate dependent. Glycobiology. 1994 Feb;4(1):39–47.

Barrow H, Guo X, Wandall HH, Pedersen JW, Fu B, Zhao Q, Chen C, Rhodes JM, Yu L-G. Serum galectin-2, -4, and -8 are greatly increased in colon and breast cancer patients

and promote cancer cell adhesion to blood vascular endothelium. Clin Cancer Res. 2011;17:7035–7046.

Blond JL, Lavillette D, Cheynet V, et al. An envelope glycoprotein of the human endogenous retrovirus HERV-W is expressed in the human placenta and fuses cells expressing the type D mammalian retrovirus receptor. J Virol. 2000 Apr;74(7):3321-3329.

Bode CJ, Jin H, Rytting E, Silverstein PS, Young AM, Audus KL. In vitro models for studying trophoblast transcellular transport. Methods Mol Med. 2006;122:225-239.

Burnside J, Nagelberg SB, Lippman SS, Weintraub BD. Differential regulation of hCG alpha and beta subunit mRNAs in JEG-3 choriocarcinoma cells by 8-bromo-cAMP. J Biol Chem. 1985 Oct 15;260(23):12705-12709.

Buse MG. Hexosamines, insulin resistance, and the complications of diabetes: current status. Am J Physiol Endocrinol Metab. 2006 Jan;290(1):E1-E8.

Chen Y, Allars M, Pan X, et al. Effects of corticotrophin releasing hormone (CRH) on cell viability and differentiation in the human BeWo choriocarcinoma cell line: a potential syncytialisation inducer distinct from cyclic adenosine monophosphate (cAMP). Reprod Biol Endocrinol. 2013 Apr 15;11:30.

Cole LA. Biological functions of hCG and hCG-related molecules. Reprod Biol Endocrinol. 2010 Aug 24;8:102.

Collett GP, Goh XF, Linton EA, Redman CW, Sargent IL. RhoE is regulated by cyclic AMP and promotes fusion of human BeWo choriocarcinoma cells. PLoS One. 2012 Jan 17;7(1):e30453.

Cooper DN, Barondes SH. Evidence for export of a muscle lectin from cytosol to extracellular matrix and for a novel secretory mechanism. J Cell Biol. 1990 May;110(5):1681-1691.

Cummings RD, Liu FT. Galectins. In: Varki A, Cummings RD, Esko JK, et al., editors. Essentials of glycobiology. 2nd edition. Cold Spring Harbor (NY): Cold Spring Harbor Laboratory Press. 2009. Chapter 33.

de Waard A, Hickman S, Kornfeld S. Isolation and properties of beta-galactoside binding lectins of calf heart and lung. J Biol Chem. 1976 Dec 10;251(23):7581-7587.

Drwal E, Rak A, Gregoraszczuk E. Co-culture of JEG-3, BeWo and syncBeWo cell lines with adrenal H295R cell line: an alternative model for examining endocrine and metabolic properties of the fetoplacental unit. Cytotechnology. 2018 Feb;70(1):285-297.

Fournier T, Guibourdenche J, Evain-Brion D. Review: hCGs: different sources of production, different glycoforms and functions. Placenta. 2015 Apr;36 Suppl 1:S60-S65.

Gatie MI, Spice DM, Garha A, McTague A, Ahmer M, Timoshenko AV, Kelly GM. O-GlcNAcylation and regulation of galectin-3 in extraembryonic endoderm differentiation. Biomolecules. 2022 Apr 22;12(5):623.

Gauster M, Moser G, Orendi K, Huppertz B. Factors involved in regulating trophoblast fusion: potential role in the development of preeclampsia. Placenta. 2009 Mar;30 Suppl A:S49-S54.

Gude NM, Roberts CT, Kalionis B, King RG. Growth and function of the normal human placenta. Thromb Res. 2004 Jan 1;114(5-6):397-407.

Gupta SK, Malhotra SS, Malik A, Verma S, Chaudhary P. Cell signaling pathways involved during invasion and syncytialization of trophoblast cells. Am J Reprod Immunol. 2016 Mar;75(3):361-371.

Harrison FL, Wilson TJ. The 14 kDa beta-galactoside binding lectin in myoblast and myotube cultures: localization by confocal microscopy. J Cell Sci. 1992 Mar;101:635-646.

He J, Baum LG. Galectin interactions with extracellular matrix and effects on cellular function. Methods Enzymol. 2006 Nov 26;417:247–256.

Hua Y, Wang J, Yuan DL, et al. A tag SNP in syncytin-2 3-UTR significantly correlates with the risk of severe preeclampsia. Clin Chim Acta. 2018 Aug;483:265-270.

Huppertz B. The critical role of abnormal trophoblast development in the etiology of preeclampsia. Curr Pharm Biotechnol. 2018 Aug;19(10):771-780.

Ishihara K, Takahashi I, Tsuchiya Y, Hasegawa M, Kamemura K. Characteristic increase in nucleocytoplasmic protein glycosylation by O-GlcNAc in 3T3-L1 adipocyte differentiation. Biochem Biophys Res Commun. 2010 Jul 30;398(3):489-494.

Jang H, Kim TW, Yoon S, et al. O-GlcNAc regulates pluripotency and reprogramming by directly acting on core components of the pluripotency network. Cell Stem Cell. 2012 July 6;11(1):62-74.

Ji L, Brkić J, Liu M, Fu G, Peng C, Wang YL. Placental trophoblast cell differentiation: physiological regulation and pathological relevance to preeclampsia. Mol Aspects Med. 2013 Oct;34(5):981-1023.

Johannes L, Jacob R, Leffler H. Galectins at a glance. J Cell Sci. 2018 May 1;131(9):jcs208884.

Jovanović Krivokuća M, Vilotić A, Nacka-Aleksić M, et al. Galectins in early pregnancy and pregnancy-associated pathologies. Int J Mol Sci. 2021 Dec 22;23(1):69.

Kanellopoulos-Langevin C, Caucheteux SM, Verbeke P, Ojcius DM. Tolerance of the fetus by the maternal immune system: role of inflammatory mediators at the feto-maternal interface. Reprod Biol Endocrinol. 2003 Dec 2;1:121.

Kieffer TEC, Laskewitz A, Scherjon SA, Faas MM, Prins JR. Memory T cells in pregnancy. Front Immunol. 2019 Apr 2;10:625.

Kim G, Cao L, Reece EA, Zhao Z. Impact of protein O-GlcNAcylation on neural tube malformation in diabetic embryopathy. Sci Rep. 2017 Sep 11;7(1):11107.

Kardana A, Cole LA. Human chorionic gonadotropin beta-subunit nicking enzymes in pregnancy and cancer patient serum. J Clin Endocrinol Metab. 1994 Sep;79(3):761-767.

Koyama T, Kamemura K. Global increase in O-linked N-acetylglucosamine modification promotes osteoblast differentiation. Exp Cell Res. 2015 Nov 1;338(2):194-202.

Ku CW, Allen JC Jr, Lek SM, Chia ML, Tan NS, Tan TC. Serum progesterone distribution in normal pregnancies compared to pregnancies complicated by threatened miscarriage from 5 to 13 weeks gestation: a prospective cohort study. BMC Pregnancy Childbirth. 2018 Sep 5;18(1):360.

Kumar P, Magon N. Hormones in pregnancy. Niger Med J. 2012 Oct-Dec;53(4):179-183.

Kusama K, Bai R, Imakawa K. Regulation of human trophoblast cell syncytialization by transcription factors STAT5B and NR4A3. J Cell Biochem. 2018 Jun;119(6):4918-4927.

Laderach DJ, Compagno D, Toscano MA, et al. Dissecting the signal transduction pathways triggered by galectin-glycan interactions in physiological and pathological settings. IUBMB Life. 2010 Jan;62(1):1-13.

Lima VV, Dela Justina V, Dos Passos RR Jr, et al. O-GlcNAc modification during pregnancy: focus on placental environment. Front Physiol. 2018 Sep 12;9:1263.

Ma Z, Sagrillo-Fagundes L, Mok, S. et al. Mechanobiological regulation of placental trophoblast fusion and function through extracellular matrix rigidity. Sci Rep. 2020 Apr 3;10:5837.

McColgan NM, Feeley MN, Woodward AM, Guindolet D, Argüeso P. The O-GlcNAc modification promotes terminal differentiation of human corneal epithelial cells. Glycobiology. 2020 Oct 21;30(11):872-880.

Msheik H, El Hayek S, Bari MF, et al. Transcriptomic profiling of trophoblast fusion using BeWo and JEG-3 cell lines. Mol Hum Reprod. 2019 Dec 1;25(12):811-824.

Nabi IR, Shankar J, Dennis JW. The galectin lattice at a glance. J Cell Sci. 2015 Jul 1;128(13):2213–2219.

Ning J, Yang H. O-GlcNAcylation in hyperglycemic pregnancies: impact on placental function. Front Endocrinol (Lausanne). 2021 Jun 1;12:659733.

Novak R, Dabelic S, Dumic J. Galectin-1 and galectin-3 expression profiles in classically and alternatively activated human macrophages. Biochim Biophys Acta. 2012 Sep;1820(9):1383-1390.

Orendi K, Gauster M, Moser G, Meiri H, Huppertz B. The choriocarcinoma cell line BeWo: syncytial fusion and expression of syncytium-specific proteins. Reproduction. 2010 Nov;140(5):759-766.

Pabinger I, Grafenhofer H, Kaider A, et al. Preeclampsia and fetal loss in women with a history of venous thromboembolism. Arterioscler Thromb Vasc Biol. 2001 May;21(5):874-879.

Palin V, Russell M, Graham R, Aplin JD, Westwood M. Altered protein O-GlcNAcylation in placentas from mothers with diabetes causes aberrant endocytosis in placental trophoblast cells. Sci Rep. 2021 Oct 19;11(1):20705.

Peavey MC, Wu SP, Li R, et al. Progesterone receptor isoform B regulates the Oxtr-Plcl2-Trpc3 pathway to suppress uterine contractility. Proc Natl Acad Sci U S A. 2021 Mar 16;118(11):e2011643118.

Petty HR, Kindzelskii AL, Espinoza J, Romero R. Trophoblast contact deactivates human neutrophils. J Immunol. 2006 Mar 1;176(5):3205-3214.

Pollheimer J, Vondra S, Baltayeva J, Beristain AG, Knöfler M. Regulation of placental extravillous trophoblasts by the maternal uterine environment. Front Immunol. 2018 Nov 13;9:2597.

Poloski E, Oettel A, Ehrentraut S, et al. JEG-3 Trophoblast cells producing human chorionic gonadotropin promote conversion of human CD4+FOXP3- T cells into CD4+FOXP3+ regulatory T cells and foster T cell suppressive activity. Biol Reprod. 2016 May 1;94(5):106.

Popa SJ, Stewart SE, Moreau K. Unconventional secretion of annexins and galectins. Semin Cell Dev Biol. 2018 Nov;83:42-50.

Racca AC, Ridano ME, Camolotto S, Genti-Raimondi S, Panzetta-Dutari GM. A novel regulator of human villous trophoblast fusion: the Krüppel-like factor 6. Mol Hum Reprod. 2015 Apr;21(4):347-358.

Sherazi AA, Jariwala KA, Cybulski AN, Lewis JW, Karagiannis J, Cumming RC, Timoshenko AV. Effects of global O-GlcNAcylation on galectin gene-expression profiles in human cancer cell lines. Anticancer Res. 2018 Dec;38(12):6691–6697.

Si Y, Yao Y, Jaramillo Ayala G, et al. Human galectin-16 has a pseudo ligand binding site and plays a role in regulating c-Rel-mediated lymphocyte activity. Biochim Biophys Acta Gen Subj. 2021 Jan;1865(1):129755.

Tarrade A, Lai Kuen R, Malassiné A, et al. Characterization of human villous and extravillous trophoblasts isolated from first trimester placenta. Lab Invest. 2001 Sep;81(9):1199-1211.

Tazhitdinova R, Timoshenko AV. The emerging role of galectins and O-GlcNAc homeostasis in processes of cellular differentiation. Cells. 2020 Jul 28;9(8):1792.

Teichberg VI, Silman I, Beitsch DD, Resheff G. A beta-D-galactoside binding protein from electric organ tissue of Electrophorus electricus. Proc Natl Acad Sci U S A. 1975 Apr;72(4):1383-1387.

Than NG, Romero R, Goodman M, Weckle A, Xing J, Dong Z, Xu Y, Tarquini F, Szilagyi A, Gal P, et al. A primate subfamily of galectins expressed at the maternal-fetal interface that promote immune cell death. Proc. Natl. Acad. Sci. USA. 2009 Jun 16;106(24):9731–9736.

Than NG, Romero R, Xu Y, Erez O, Xu Z, Bhatti G, Leavitt R, Chung TH. El-Azzamy H, LaJeunesse C, et al. Evolutionary origins of the placental expression of chromosome 19 cluster galectins and their complex dysregulation in preeclampsia. Placenta. 2014 Nov;35(11):855–865.

Tilburgs T, Crespo ÂC, van der Zwan A, et al. Human HLA-G+ extravillous trophoblasts: Immune-activating cells that interact with decidual leukocytes. Proc Natl Acad Sci U S A. 2015 Jun 9;112(23):7219-7224.

Timoshenko AV. Towards molecular mechanisms regulating the expression of galectins in cancer cells. Cell Mol Life Sci. 2015 Nov;72(22):4327–4340.

Tuckey RC. Progesterone synthesis by the human placenta. Placenta. 2005 Apr;26(4):273-281.

Tsai CM, Guan CH, Hsieh HW, et al. Galectin-1 and galectin-8 have redundant roles in promoting plasma cell formation. J Immunol. 2011 Aug 15;187(4):1643-1652.

Vladoiu MC, Labrie M, St-Pierre Y. Intracellular galectins in cancer cells: Potential new targets for therapy (Review). Int J Oncol. 2014 Apr;44(4):1001–1014.

Wang P, Mariman E, Keijer J, et al. Profiling of the secreted proteins during 3T3-L1 adipocyte differentiation leads to the identification of novel adipokines. Cell Mol Life Sci. 2004 Sep;61(18):2405-2417.

Wang XQ, Li DJ. The mechanisms by which trophoblast-derived molecules induce maternal-fetal immune tolerance. Cell Mol Immunol. 2020 Nov;17(11):1204-1207.

Yang X, Qian K. Protein O-GlcNAcylation: emerging mechanisms and functions. Nat Rev Mol Cell Biol. 2017 Jul;18(7):452-465.

Zhang W, Liu HT. MAPK signal pathways in the regulation of cell proliferation in mammalian cells. Cell Res. 2002 Mar;12(1):9-18.

Chapter 2

2 Expression, Regulation, and Functions of the Galectin-16 Gene in Human Cells and Tissues

2.1 Introduction

Galectins comprise a family of soluble β-galactoside binding proteins, which regulate key biological processes including cell growth, differentiation, apoptosis, and immune responses (Timoshenko, 2015; Allo et al., 2018; Johannes et al., 2018; Tazhitdinova & Timoshenko, 2020). Sixteen galectin genes have been identified in animal kingdoms, 12 of which are expressed in humans. Galectins share a conserved carbohydrate recognition domain (CRD) and they are subcategorized into prototype, tandem-repeat, or chimeric types according to the number of CRDs and structural features. Prototype galectins contain one CRD and include galectins -1, -2, -5, -7, -10, -11, -13, -14, -15, and -16. Tandem-repeat galectins contain two homologous CRDs connected by a linker of ~70 amino acids and include galectins-4, -6, -8, -9, and -12. The only chimera-type galectin is galectin-3, which contains one CRD linked to a non-lectin N-terminal proline/glycine-rich domain. Galectins form a network of proteins to perform glycan-dependent and glycan-independent functions both intra- and extracellularly (Vladoiu et al., 2014; Johannes et al., 2018; Tazhitdinova & Timoshenko, 2020). Intracellularly, galectins have multiple binding partners and primarily function via glycan-independent mechanisms to regulate processes such as cell growth, apoptosis, and pre-mRNA splicing among others (Vladoiu et al., 2014; Patterson et al., 2015; Tazhitdinova & Timoshenko, 2020). Extracellular galectins are secreted from cells through unconventional mechanisms (Johannes et al., 2018; Popa et al., 2018) and can bind to glycoligands on the cell surface or glycoproteins in the extracellular matrix to promote cell adhesion and migration (He et al., 2006) or bind to specific cell surface receptors to facilitate their cross-linking and transmembrane signaling (He et al., 2006; Than et al., 2012; Nabi et al., 2015; Johannes et al., 2018).

Galectin expression profiles vary significantly between different cells and tissues. Some galectins are commonly expressed with low tissue specificity, e.g., galectin-1 and galectin-3, while others are highly-tissue specific (Johannes et al., 2018). *LGALS16* was

characterized in placental tissue by Than and co-authors (Than et al., 2009) and together with two other galectins (*LGALS13* and *LGALS14*) was found to be upregulated in differentiated trophoblast cells to confer immunotolerance at the maternal–fetal interface (Than et al., 2014). These three galectin genes are located in a cluster of four human protein-coding galectin genes on chromosome 19 and they are proposed to have evolutionarily emerged to sustain hemochorial placentation in anthropoids (Than et al., 2009). The correct expression of placenta-specific galectins is an important part of proper reprogramming of the transcriptional activity of the trophoblast (Than et al., 2014). This involves the differentiation and fusion of villous cytotrophoblasts into a multinucleated syncytium that is in direct contact with maternal blood and is responsible for facilitating gas, nutrient, and waste exchange between the mother and fetus, mediating hormonal regulation, and forming an immunological barrier during pregnancy (Than et al., 2014). Differentiated extravillous trophoblasts proliferate, invade, and remodel the maternal spiral arteries to provide blood flow and nutrients to the fetus (Pollheimer et al., 2018). Dysregulation of this placenta-specific gene cluster containing *LGALS16* is associated with disorders such as preeclampsia, which can have a high rate of fatality for both the mother and fetus (Than et al., 2014; Pollheimer et al., 2018; Blois et al., 2019).

Currently, experimental studies on *LGALS16* are limited, although multiple microarray datasets and bioinformatics resources contain relevant information. Here, I use experimental and bioinformatical approaches for examining expression, regulation, and functions of *LGALS16* to position this galectin within the complex galectin network in cells and to identify directions for future studies.

2.2   Materials and methods

2.2.1   Bioinformatics data and tools

Microarray and RNA-sequencing data were extracted from the Gene Expression Omnibus (GEO) Profiles, which contained 287 datasets for *LGALS16* (accessed on 2 November 2021), considering the following criteria: (1) inclusion of only controls and untreated cell/tissue samples, (2) inclusion of only cases with positive gene expression values for

matched *ACTB* (a housekeeping gene), *LGALS1* (a low tissue specific galectin), and *LGALS16* genes, and (3) deletion of few datasets, which report enormous deviations (>100-folds) from average expression levels of *ACTB* and *LGALS1* genes. In silico prediction of transcription factor binding sites in *LGALS16* gene DNA sequence was performed with PROMO version 3.0.2 software, which utilized version 8.3 of TRANSFAC database (Messeguer et al., 2002; Farré et al., 2003). The dissimilarity index for the transcription factor search was set at 0% to limit the number of non-specific matches. Ensembl Release 104 was used to extract the sequence of the 2 kb promoter region of the gene (accessed on 24 August 2021). Four different online platforms were used and compared to predict putative miRNA targets for *LGALS16* including Diana Tools (Paraskevopoulou et al., 2013), miRabel (Quillet et al., 2020), miRDB (Chen & Wang, 2020), and TargetScan (Agarwal et al., 2015). The Human Protein Atlas (HPA) (Uhlén et al., 2015), GenBank (Clark et al., 2016), and Protein Data Bank (PDB) (Berman et al., 2000) were exploited for searching the relevant structures, sequences, and expression patterns of *LGALS16* based on the gene symbol.

2.2.2   Cell cultures

Placenta choriocarcinoma BeWo and JEG-3 cell lines (kindly provided by Dr. Renaud, Department of Anatomy and Cell Biology, Western University, London, ON, Canada) were cultured in Dulbecco's Modified Eagle Medium/Ham's F12 medium and RPMI-1640 medium, respectively, supplemented with 10% or 8% fetal bovine serum, 100 IU/mL penicillin, and 100 μg/mL streptomycin. Cell cultures were maintained in a CO_2-incubator at 37°C and 5% CO_2. To induce trophoblastic differentiation, cells were grown in 6-well plates and treated with 250 μM of 8-Br-cAMP (cat. # B7880, Sigma-Aldrich, Oakville, ON, Canada) for 48 h (BeWo cells) or 36 h (JEG-3 cells). Over the time of these treatments, cell culture media was replaced one time for BeWo cells after 24 h of growth and two times (every 12 h) for JEG-3 cells to avoid accumulation of acidic metabolites.

2.2.3   Gene expression analysis

The total RNA pools were isolated from cell monolayers using 1mL TRIzol® reagent (cat. # 15596018, Ambion, Carlsbad, CA, USA) per well of a 6-well plate and RNA quantified using the Nanodrop 2000c UV-Vis spectrophotometer (ThermoFisher, Waltham, MA, USA). RNA with a 260/280 nm ratio in the range of 1.8-2.0 was considered high quality. For cDNA synthesis with the Advanced cDNA Synthesis Kit, 1 μg of RNA sample was used (cat. # 801-100, Wisent, Montreal, QC, Canada). For both the control and 8-Br-cAMP treatments, four biological replicates (RNA isolated from different cell passages) were completed for BeWo cells and three biological replicates were completed for JEG-3 cells. The conventional and quantitative polymerase chain reaction (PCR) analyses were used to assess the mRNA expression levels for following genes: *ACTB*, *CGB3/5* (biomarkers of trophoblastic differentiation), and *LGALS16*. The oligonucleotide PCR primers for *LGALS16* (forward 5′-ATTTGCGAGTGCACTTAGGC-3′ and reverse 5′-GACACACGTAGATGCGCAAG-3′, PCR amplicon length of 132 bp) targeting exon 3 (**Figure 6**) were designed using Primer-BLAST tool at NCBI (Ye et al., 2012). Oligonucleotide primers for *ACTB* (forward 5′-TCAGCAAGCAGGAGTATGACGAG-3′ and reverse 5′-ACATTGTGAACTTTGGGGGATG-3′, PCR amplicon length of 265 bp) and *CGB3/5* (forward 5′-CCTGGCCTTGTCTACCTCTT-3′ and reverse 5′-GGCTTTATACCTCGGGGTTG-3′, PCR amplicon length of 109 bp) were available elsewhere (Timoshenko, 2011; Renaud et al., 2015). To run conventional PCR, reaction mixes (10 μL 2X Taq FroggaMix (cat. # FBTAQM, FroggaBio, Toronto, ON, Canada), 2 μL forward and reverse primer mixture from 10 μM stock, 7 μL nuclease free water, and 1 μL template cDNA) were loaded into a T100 Thermal Cycler (Bio-Rad Laboratories, Mississauga, ON, Canada) and amplified using the following PCR regime: 94°C for 3 min; 26 cycles of 94°C for 30 s, 56°C for 30 s, 72 °C for 60 s; and 72°C for 10 min; and held at 4°C. The PCR products were separated on a 2% agarose gel as described earlier (Timoshenko et al., 2016) and the gel was imaged using the Molecular Imager® Gel Doc™ XR+ (Bio-Rad) to confirm the expected size of PCR amplicons. For primer validation, bands were excised and then used with the Gel/PCR DNA Fragments Kit (Geneaid) according to the manufacturer's protocol and sent to Robarts Research Institute (London,
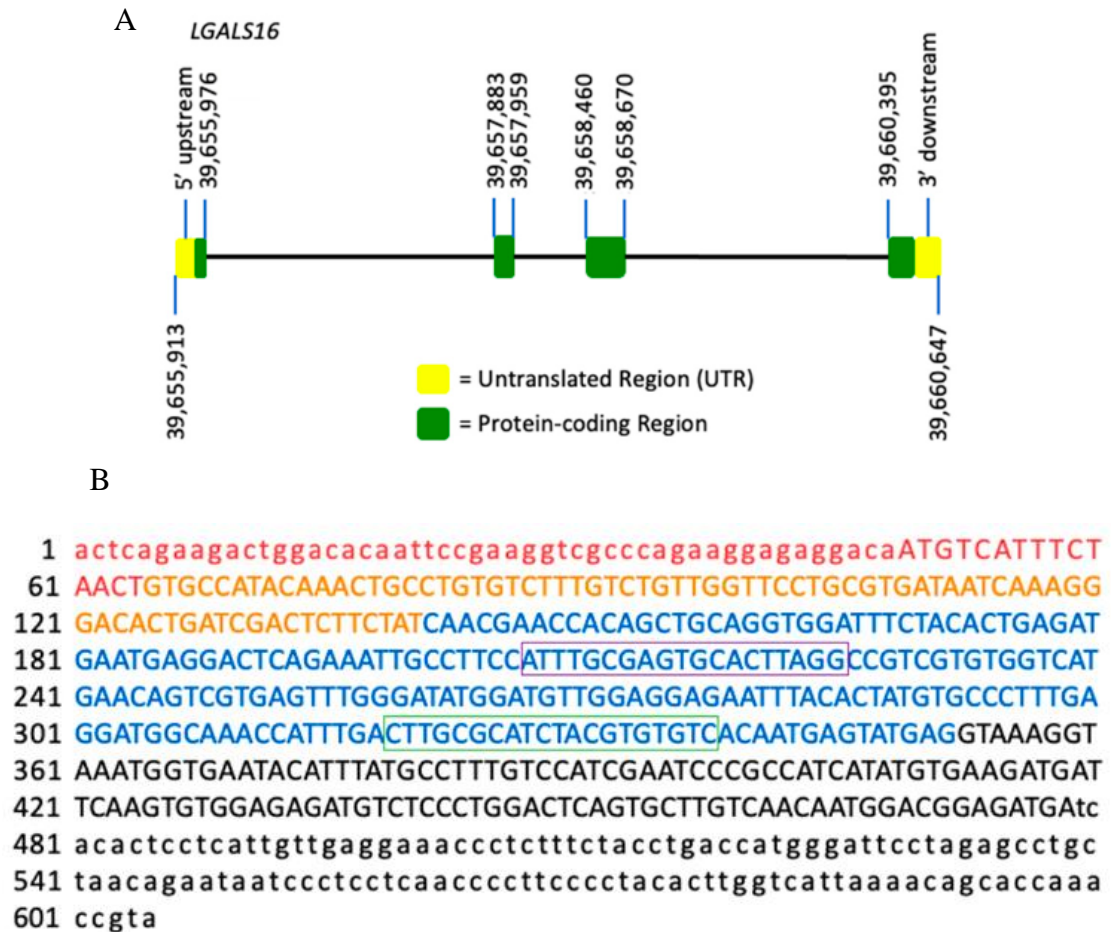
Figure 6. *LGALS16* **gene structure and the mRNA sequence.**

(A) *LGALS16* (4735 bp) is located on chromosomal band 19q13.2 and contains 4 exons (ENSG00000249861). (B) NCBI reference sequence of *LGALS16* mRNA (NM_001190441.3). Each exon is highlighted with red, orange, blue, and black representing exons 1, 2, 3, and 4, respectively. The protein coding sequence (CDS) is indicated in capitals while UTRs in small characters. The oligonucleotide sequences for PCR amplification are boxed.

ON, Canada) for sequencing. Sequences were then aligned to sequences in the BLAST®
database to verify fidelity. The quantitative PCR was performed in the CFX Connect™
Thermocycler using the SsoAdvanced Universal SYBR® Supermix kit (cat. # 1725274,
Bio-Rad Laboratories, Mississauga, ON, Canada). To quantify *ACTB*, *CGB3/5*, and
LGALS16 expression, three technical replicates were performed for each gene and sample
of control or 8-Br-cAMP treated BeWo and JEG-3 cells. Amplification specificity was
verified by the detection of a single melt peak for each PCR amplicon. Relative transcript
levels were quantified by the Livak method ($2^{-\Delta\Delta CT}$) and normalized to the reference
gene, *ACTB*. To assess the expression levels of 84 genes encoding human transcription
factors, the RT2 Profiler™ PCR Array Kit (cat. # PAHS-075ZD-2, Qiagen, Toronto, ON,
Canada) was used following the protocols provided by the manufacturer. One technical
replicate of the control and 8-Br-cAMP treated cells was completed for each gene tested.

2.2.4   Statistical analysis

Statistical analysis was performed using GraphPad Prism 9 for Windows, version 9.1.2
(GraphPad Software, San Diego, CA, USA) and the data were presented as mean ± SD.
One-way analysis of variance (ANOVA) was used to determine statistical significance
across treatments followed by Tukey's honestly significant difference test to detect which
means were statistically significant at a value of $p < 0.05$.

2.3   Results and discussion

2.3.1   Molecular characteristics of galectin-16 gene and recombinant protein

The *LGALS16* gene structure and molecular details were described by Than and co-authors
(Than et al., 2009). *LGALS16* (4735 bp) is located on chromosomal band 19q13.2, spans
from bases 39,655,913 to 39,660,647, and contains 4 exons (**Figures 6A,B**). *LGALS16* is
found only in primates and is part of the chromosome 19 gene cluster containing four
protein-coding genes (*LGALS10*, *LGALS13*, *LGALS14*, *LGALS16*) (Than et al., 2009;

A

S1   F2   S3
MSFLTVPYKLPVSLSVGSCVIIKGTLIDSSINEPQLQVDFYTEMNEDSE

S4   S5   S6   F3
IAFHLRVHLGRRVVMNSREFGIWMLEENLHYVPFEDGKPFDLRIYVCLN

F4   F5   α   S2   F1
EYEVKVNGEYIYAFVHRIPPSYVKMIQVWRDVSLDSVLVNNGRR

B
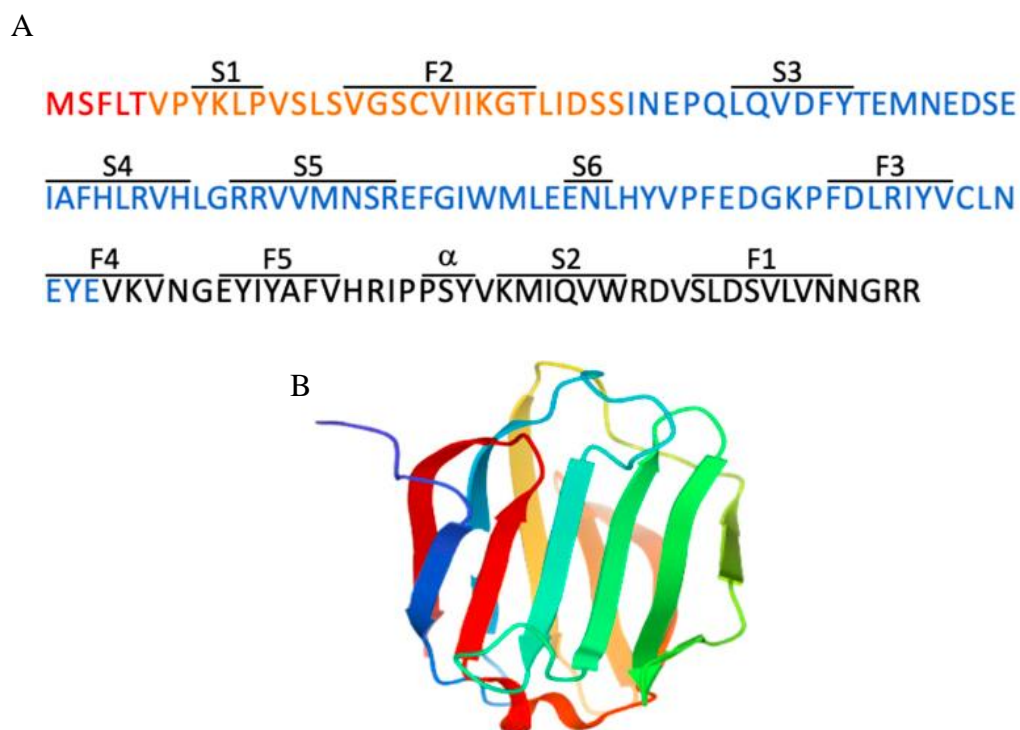
Figure 7. Protein sequence and structure of recombinant galectin-16.

(A) The 142 amino acid sequence is 16.6 kDa for the galectin-16 protein. Each color corresponds to the exon from which the amino acids were encoded with red, orange, blue, and black representing exons 1, 2, 3, and 4, respectively. The anti-parallel β-sheets of F-face (F1–F5) and S-face (S1-S6) strands as well as a short α-helix are showed. (B) The crystal structure was extracted from Protein Data Bank (available online: rcsb.org, accessed on 6 September 2021), PDB ID: 6LJP.

Than et al., 2014; Blois et al., 2019; Ely et al., 2019). The diversification and evolutionary origin of this cluster, including *LGALS16*, is thought to be related to placenta development and mediated by transposable long interspersed nuclear elements (LINEs), which are commonly found at the boundaries of large inversions and gene duplication units (Singer, 1982; Than et al., 2009; Weckselblatt & Rudd, 2015). The relevant rearrangements and subsequent gains and losses of duplicated genes and pseudogenes are proposed to have enabled anthropoids to sustain highly invasive placentation and placental phenotypes, such as longer gestation for larger offspring and an increased body to brain size ratio (Than et al., 2009).

To the best of my knowledge, no studies are available on native galectin-16 at the protein level whereas recombinant protein has been produced and tested. The crystal structure of recombinant galectin-16 and its mutants was solved by Si and co-authors (Si et al., 2021). Recombinant galectin-16 is a monomeric protein, which is composed of 142 amino acids and has a typical galectin structure of the CRD β-sandwich with two sheets formed by six β-strands on the concave side (S1–S6) and five β-strands on the convex side (F1–F5) (**Figure 7**). This group also showed that galectin-16 lacks lactose-binding ability unless arginine (Arg55) is replaced with asparagine in S4 β-strand. In comparison, an earlier report showed that recombinant galectin-16 and two other human galectins (galectin-13 and galectin-14) can bind lactose–agarose beads and are efficiently and competitively eluted by lactose (Than et al., 2009). More insights into this discrepancy are required considering multiple interfering factors, mutations/replacements of amino acids within the CRD, and different study designs. Regardless, both glycan-dependent and glycan-independent interactions might be essential for galectin-16 similar to other galectins (Johannes et al., 2018).

2.3.2   Expression patterns and functions of *LGALS16* in cells and tissues

Experimental studies focusing on *LGALS16* are limited and an essential source of relevant information about this gene is the Gene Expression Omnibus (GEO), a data repository for microarray and RNA-sequencing data (Barrett et al., 2013). Overall, 287 datasets are

available on GEO (November 2021 search) reporting *LGALS16* expression in 52 types of tissues and various cell lines based on the following platforms: Affymetrix Human Genome (n = 27), Affymetrix Human Gene (n = 151), Agilent (n = 31), Human Unigene (n = 1), Illumina Human (n = 82), MCI Human (n = 1), NuGO (n = 1), and Sentrix Human (n = 15). Quantification of differences in *LGALS16* expression between different platforms is challenging. However, evaluation of gene expression values within the same GEO datasets demonstrates that *LGALS16* can be classified as a gene with relatively low expression in comparison with *LGALS1* (a widely expressed galectin with a low tissue specificity) and *ACTB* (a common housekeeping gene) (**Table 1**). Indeed, regardless of the platform, average GEO percentile rank of expression for *LGALS16* measured with different arrays ranged 4–32% on a scale of 1–100% while the range was 63–100% for *LGALS1* and 94–100% for *ACTB*. Available GEO profiles do not contain relevant datasets with *LGALS16* for placenta for comparison, however, the Human Protein Atlas (HPA) reports tissue-specific overexpression of *LGALS16* in placenta followed by brain tissues and retina (**Figure 8A**). The biological meaning and reasons of overexpression of *LGALS16* in these diverse tissues is unknown and requires further investigations in the context of developmental biology. For instance, the complex mechanisms of the placenta–brain axis of cell development (Rosenfeld, 2021) could be addressed in terms of the unique association of *LGALS16* with these tissues.

In comparison with tissues, HPA reports the expression of *LGALS16* mRNA only in two human cell lines including placental choriocarcinoma cell line BeWo and testicular teratoma cell line SuSa, which probably can be used as appropriate systems to explore the biological role of *LGALS16* gene (**Figure 8B**). Human syncytiotrophoblasts, which are terminally differentiated placental cells, can also serve as a strong positive control for *LGALS16* overexpression (Than et al., 2009; Than et al., 2012; Than et al., 2014).

Table 1. Comparative expression of *LGALS16* in human tissues and cells from the Gene Expression Omnibus database.

Names of cells or tissues	GEO accession number	*ACTB*	*LGALS1*	*LGALS16*	Sample Size
Acetabular labrum cells	GDS5427[a]	12.682 ± 0.150	12.057 ± 0.107	2.949 ± 0.0093	3
Acute lymphoblastic leukemia cell line RS4;11	GDS4043[b]	13.861 ± 0.017	11.487 ± 0.033	0.4023 ± 0.607	2
Acute myeloblastic leukemia cell line Kasumi-1	GDS5600[a]	11.965 ± 0.025	6.455 ± 0.299	2.918 ± 0.036	3
Acute promyelocytic leukemia cell line NB4	GDS4180[a]	13.130 ± 0.035	10.823 ± 0.031	3.650 ± 0.108	3
Adipocyte progenitor cells (subcutaneous)	GDS5171[a]	13.523 ± 0.038	13.397 ± 0.112	4.597 ± 0.251	6
Adipocyte progenitors from deep neck	GDS5171[a]	13.469 ± 0.057	13.208 ± 0.177	4.505 ± 0.094	6
Bone marrow CD34+ cells (chronic myeloid leukemia)	GDS4756[a]	13.524	11.137	3.050	1
Bone marrow plasma cells	GDS4968[a]	11.990 ± 0.226	8.714 ± 0.515	3.052 ± 0.257	5
Brain frontal cortex	GDS4758[a]	13.402 ± 0.125	96.333 ± 0.840	4.632 ± 0.249	18
Brain hippocampus	GDS4758[a]	13.477 ± 0.130	11.133 ± 0.375	4.659 ± 0.300	10
Brain hippocampus	GDS4879 [a]	12.113 ± 0.409	9.076 ± 0.232	3.177 ± 0.177	19
Brain temporal cortex	GDS4758[a]	13.560 ± 0.131	11.189 ± 0.280	4.749 ± 0.193	19
Breast cancer cell line MCF-7	GDS2759[b]	15.884 ± 0.030	13.752 ± 0.153	6.053 ± 0.237	2
Breast cancer cell line MCF-7	GDS4972[a]	13.029 ± 0.038	12.439 ± 0.083	3.892 ± 0.066	3
Breast cancer cell line MCF-7	GDS4090[a]	13.087 ± 0.019	9.566 ± 0.100	2.827 ± 0.405	3
Breast cancer cell line MDA-MB-231	GDS4800[a]	13.875 ± 0.007	13.565 ± 0.042	5.189 ± 0.085	3
Bronchial smooth muscle primary cells	GDS4803[a]	11.629 ± 0.175	11.533 ± 0.041	3.181 ± 0.095	3
Bronchopulmonary neuroendocrine cell line NCI-H727	GDS4330[a]	11.978	5.715	3.808	1
Burkitt lymphoma cell line Namalwa	GDS4978[a]	13.468 ± 0.187	8.005 ± 0.073	3.916 ± 0.297	3
Burkitt lymphoma cell line Raji	GDS4978[a]	13.367 ± 0.093	8.052 ± 0.141	3.962 ± 0.019	3
Colorectal adenocarcinoma cell line SW620	GDS5416[e]	16.400 ± 0.362	17.280 ± 0.043	2.766 ± 0.554	2
Embryonic kidney cell line HEK-293	GDS4233[a]	10.330 ± 0.050	7.109 ± 0.098	3.757 ± 0.328	4
Endothelial progenitor cells	GDS3656[c]	15.397 ± 0.174	13.845 ± 0.457	8.018 ± 0.103	11
Esophagus biopsies	GDS4350[a]	12.617 ± 0.230	8.062 ± 0.507	3.255 ± 0.208	8
Gastrointestinal neuroendocrine cell line KRJ-1	GDS4330[a]	12.135	9.592	2.859	1
Germinal center B cells	GDS4977[a]	9.793 ± 0.373	8.438 ± 0.225	6.723 ± 0.538	5
Gingival fibroblasts	GDS5811[a]	13.628 ± 0.101	13.770 ± 0.174	3.674 ± 0.140	2
Heart (left ventricle)	GDS4772[a]	11.293 ± 0.361	10.672 ± 0.377	2.941 ± 0.030	5
Heart (left ventricle)	GDS4314[a]	12.142 ± 0.365	11.052 ± 0.223	3.344 ± 0.154	5
Heart (right ventricular)	GDS5610[a]	11.930 ± 0.255	10.934 ± 0.044	3.637 ± 0.181	2

Hepatocellular carcinoma cell line HepG2	GDS5340[a]	13.259 ± 0.039	11.256 ± 0.054	4.281 ± 0.327	3
Keratinocytes	GDS4426[a]	12.679 ± 0.056	11.147 ± 0.236	3.804 ± 0.138	6
Lung carcinoma cell line A549	GDS4997[a]	10.970 ± 0.044	12.187 ± 0.049	2.418 ± 0.072	3
Lung carcinoma cell line H460	GDS5247[a]	12.504 ± 0.043	11.111 ± 0.063	3.439 ± 0.117	3
Lung microvascular endothelial cell line CC-2527	GDS2987[b]	32061 ± 7366	15158 ± 2227	8.100 ± 9.051	2
Lymphoblastoid cell line TK6	GDS4915[a]	13.365 ± 0.061	11.161 ± 0.323	4.005 ± 0.327	2
Lymphoblastoid cell line TK6	GDS4916[a]	13.940 ± 0.058	12.023 ± 0.130	4.061 ± 0.357	2
Medulloblastoma tumor tissue	GDS4469[a]	13.099 ± 0.302	9.490 ± 0.801	4.005 ± 0.839	15
Melanoma cell line A-375	GDS5085[a]	13.888 ± 0.011	13.474 ± 0.101	4.618 ± 0.045	3
Melanoma cell line FEMX-I	GDS3489[d]	16.04 ± 0.354	16.04 ± 0.354	0.550 ± 1.061	2
Melanoma cell line Hs294T	GDS5670[a]	11.353 ± 0.245	10.349 ± 0.097	2.149 ± 0.585	2
Microglia cell line HMO6	GDS4151[a]	13.545	12.231	2.979	1
Myotubes from musculus obliquus internus	GDS5378[a]	13.224 ± 0.099	12.925 ± 0.114	2.840 ± 0.057	4
Pancreatic neuroendocrine cell line QGP-1	GDS4330[a]	12.057	5.749	3.031	1
Peripheral blood CD34+ cells (chronic myeloid leukemia)	GDS4756[a]	13.414 ± 0.049	11.144 ± 0.578	2.974 ± 0.140	2
Peripheral blood CD4+ T cells	GDS5544[a]	13.598 ± 0.053	9.707 ± 0.247	4.584 ± 0.126	4
Peripheral blood cells	GDS4240[a]	11.825 ± 0.084	7.307 ± 0.154	1.506 ± 0.112	7
Renal adenocarcinoma cell line 786-O	GDS5810[a]	12.902 ± 0.030	12.809 ± 0.015	5.753 ± 0.031	2
Retinal pigment epithelia primary cells	GDS4224[a]	13.407 ± 0.110	11.842 ± 0.449	3.468 ± 0.367	4
Retinal pigmented epithelium cell line ARPE-19	GDS4224[a]	13.288	11.946	3.646	1
Skeletal muscle (vastus lateralis) primary cells	GDS4920[a]	13.649 ± 0.084	13.385 ± 0.114	4.609 ± 0.136	12
Skeletal muscle tissue	GDS4841[a]	9.400 ± 0.190	11.486 ± 0.247	2.786 ± 0.355	5
Skin cancer cell line RT3Sb	GDS5381[a]	13.409 ± 0.062	8.775 ± 0.114	3.539 ± 0.252	4
Skin epidermis	GDS3806[c]	15.139 ± 0.141	9.534 ± 0.370	7.909 ± 0.469	7
Visceral adipose tissue (omentum)	GDS4857[a]	11.875 ± 0.352	11.488 ± 0.416	4.666 ± 0.754	8

Notes: The means ± SD of available gene expression values are shown. The GEO datasets originated from different platforms: [a] Affymetrix Human Gene 1.0 ST Array, [b] Sentrix Human-6 Expression BeadChip, [c] Sentrix HumanRef-8 Expression BeadChip, [d] MCI Human HEEBOChip 42k oligo array, and [e] Agilent-014850 Whole Human Genome Microarray 4 x 44K G4112F.
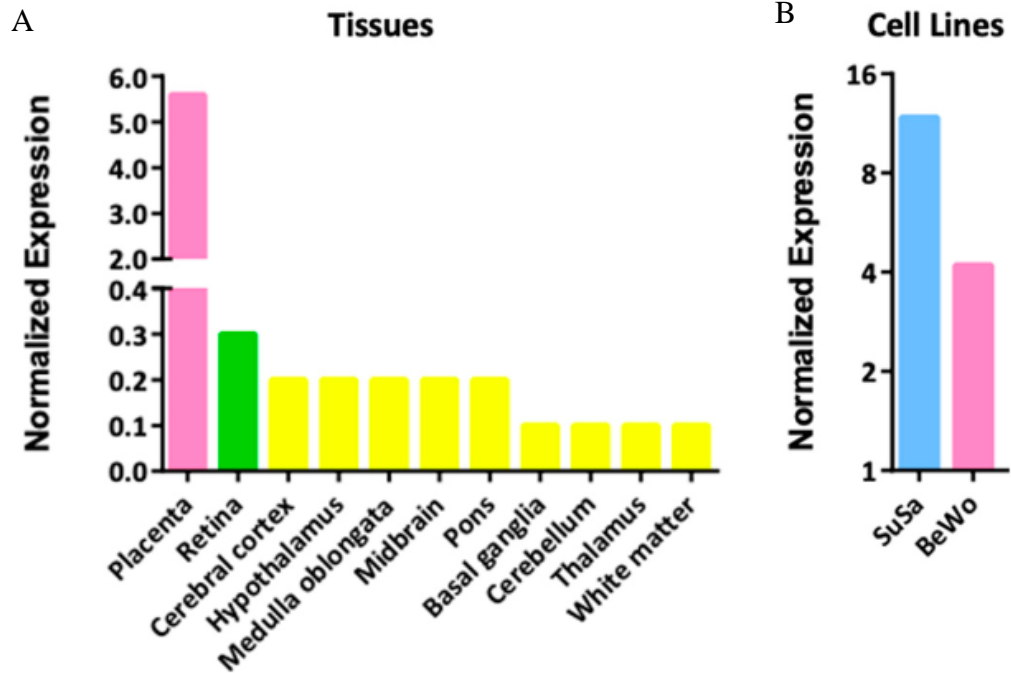
Figure 8. The normalized expression of *LGALS16* mRNA in human tissues and cells from HPA datasets.

(A) *LGALS16*-positive cases out of 55 tissue types; (B) *LGALS16*-positive cases out of 69 cell lines. The data were retrieved on 28 November 2021.

To develop experimental models for studying *LGALS16* functions and regulation, I examined gene expression in BeWo cells and an additional placental cell line JEG-3 in the context of trophoblastic differentiation. The expression of *LGALS16* mRNA was significantly increased in both cell lines after 36 h (JEG-3 cells) and 48 h (BeWo cells) treatment with a potent cell-permeable and metabolically stable activator of cAMP-dependent protein kinase 8-Br-cAMP (250 μM), which coincided with upregulation of *CGB3/5,* genes encoding chorionic gonadotropin subunits 3 and 5 (**Figure 9**). As chorionic gonadotropin is one of the biomarkers of placenta and trophoblastic differentiation, my results suggest classifying *LGALS16* to the same category of biological molecules. Other studies also reported significant upregulation of *LGALS16* in association with processes of cellular differentiation, even if the basal levels were relatively low. Thus, treatment of BeWo cells with forskolin, an inducer of cyclic adenosine 3′,5′-monophosphate (cAMP), stimulated trophoblastic differentiation and simultaneous *LGALS16* overexpression (Than et al., 2014). An interesting example of *LGALS16* upregulation was reported in a model of intestinal differentiation of Caco-2 cells induced by a combined treatment with dexamethasone and p44/42 MAPK inhibitor PD98059 (Inamochi et al., 2014). Therefore, *LGALS16* may deserve further attention as a factor associated with processes of cellular differentiation and tissue development.

An important function of galectin-16 as well as placental galectin-13 and galectin-14 is the ability to induce apoptosis of CD3+ T cells, which was detected by flow cytometry of cells double-stained with annexin-V-FITC and propidium iodide (Than et al., 2009). Considering the high expression of galectin-16 in differentiated trophoblasts, the apoptotic mechanism might contribute to the immune tolerance at the maternal-fetal interface reducing the danger of maternal immune attacks on the fetus and enabling anthropoid primates to evolve long gestation periods while retaining highly invasive placentation. The details of this regulation are obscure since there are no studies addressing the secretion of galectin-16 from trophoblasts. However, intracellular EGFP-tagged recombinant galectin-16 was readily localized in the nucleus and cytoplasm of transfected cells including, HeLa, 293T, HCT-116, SMMC-7721 and Jurkat cells (Si et al., 2021). In fact, the nuclear staining was much stronger than in the cytoplasm suggesting that the transport of galectin-16 into
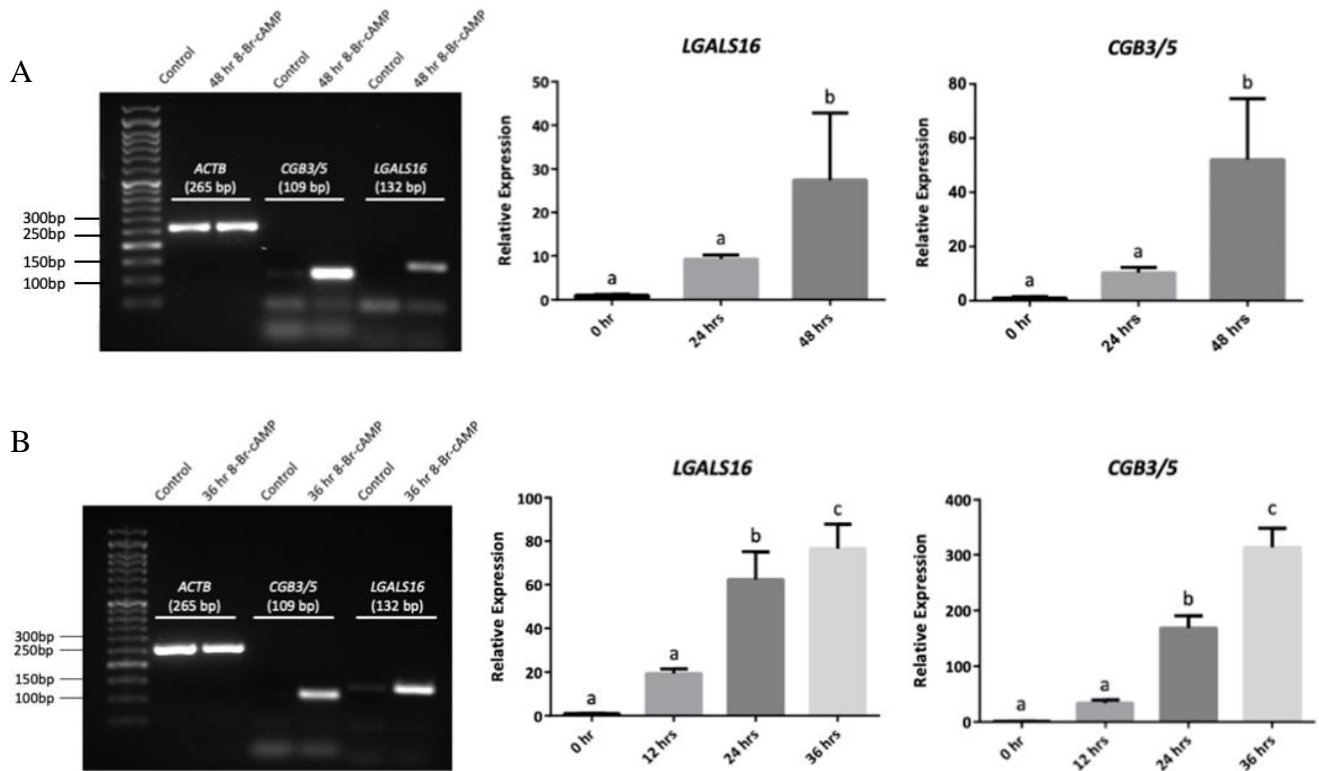
Figure 9. *LGALS16* **expression in human placental choriocarcinoma cell lines, BeWo and JEG-3.**

Cells were treated with 8-Br-cAMP (250 μM) for different periods of time to induce syncytiotrophoblast differentiation. (A) BeWo cells ($n = 4$); (B) JEG-3 cells ($n = 3$). Agarose gels on the left confirm the expected size of PCR amplicons. Bar graphs show the fold changes in the expression of *LGALS16* and *CGB3/5* genes obtained by qPCR, which were quantified by the Livak method ($2^{-\Delta\Delta CT}$) using *ACTB* as a reference gene. Data are presented as means ± SD; means with the same letter are not significantly different from each other (Tukey's post hoc HSD test, p > 0.05).

the nucleus might play a role in regulating intranuclear processes. These authors showed that the binding partner of galectin-16 is c-Rel, a member of the NF-κB family of transcription factors (TFs), which is involved in the regulation of multiple processes such as apoptosis, inflammation, immune responses, tumorigenesis, cell growth and differentiation (Park & Hong, 2016; Si et al., 2021). All NF-κB family members, including c-Rel, have a conserved N-terminal DNA-binding/dimerization domain, known as the Rel homology domain (RHD) (Hayden & Ghosh, 2011). Recombinant galectin-16 strongly binds to the RHD which might inhibit c-Rel and prevent activation of anti-apoptotic genes, such as Bcl-2 and Bcl-xL, promoting T-cell apoptosis during pregnancy (Si et al., 2021). An additional aspect of *LGALS16* functions may contribute to the rescue of glucose restriction-induced cell death in a model of a whole genome gain-of-function CRISPR activation using human mitochondrial disease complex I mutant cells (Balsa et al., 2020).

2.3.3   Transcriptional   and   post-transcriptional   regulation   of *LGALS16*

2.3.3.1   Transcription factors

Multiple TFs can be involved in the regulation of *LGALS16* expression based on the presence of specific response elements in the promoter regions of the gene. Original analysis of retrotransposons within the 10 kb 5′ UTR by Than and co-authors demonstrated that the *LGALS16* promoter has binding sites for GATA2, TEF5, and ESRRG, which are also involved in the regulation of important trophoblast-specific genes such as *ERVWE1* (marker of cell fusion), *CGA*, and *CGB3* (markers of chorionic gonadotropin production, a hormone released by differentiated trophoblasts to maintain pregnancy) (Than et al., 2014). The contribution of these TFs in regulating *LGALS16* expression was claimed to vary, especially with decreased regulation from GATA2, due to the specific layout and properties of transposable elements (L1PA6 and L1PREC2) within the 5′UTR of this gene as compared to two other placental genes, *LGALS13* and *LGALS14*. Additional shared TFs for the placental galectin gene cluster include TFAP2A and GCM1, which have binding sites within ALU transposable elements next to L1PREC2. Experimental evidence

of this regulation was confirmed in a model of forskolin-induced differentiation of primary trophoblasts, which revealed time-dependent upregulation of *LGALS16* in parallel with the expression of *TEAD3*, *ESRRG*, *GCM1*, and *ERVWE1* (Than et al., 2014). It is interesting to note that this study did not reveal the effect of 5-azacytidin on *LGALS16* expression in BeWo trophoblast cells as compared to other upregulated placental galectins, which suggested a minor role of DNA methylation in the context of *LGALS16* regulation.

To enrich this analysis, I used human choriocarcinoma cell line JEG-3 and Qiagen RT2 Profiler™ PCR Array to test changes in the mRNA transcript levels of 84 TFs during trophoblastic differentiation induced by 8-Br-cAMP. Overall, 60 TFs were upregulated in this assay including three top genes encoding Jun B proto-oncogene (*JUNB*), SMAD family member 9 (*SMAD9*), and activating transcription factor 3 (*ATF3*) (**Figure 10**). Since all of these three genes are expressed in placenta and brain tissues (Han et al., 2008; Nuzzo et al., 2014; Ma et al., 2015; Uhlén et al., 2015; Walcott et al., 2018; Knyazev et al., 2019), which are *LGALS16*-positive, this observation provides a new insight into possible transcriptional regulation of this gene. JUNB and ATF3 belong to a family of TFs with a basic leucine zipper DNA binding domain, with JUNB preferentially binding to the 12-O-tetradecanoylphorbol-13-acetate response element sequence and ATF3 binding to the cAMP response element in promoters with the consensus sequence, TGACGTCA (Garces et al., 2018). They are subunits of activating protein 1 (AP-1) TFs, which function as homodimers or heterodimers in association with other members of JUN, FOS, ATF, and MAF protein families (Garces et al., 2018). JUNB was reported to be directly involved in processes of trophoblastic cell syncytialization (Cheng et al., 2004; Shankar et al., 2015), while upregulation of ATF3 was associated with cellular stress responses (Jadhav & Zhang, 2017; Knyazev et al., 2019; Wang et al., 2021), decidualization (Wang et al., 2021), and preeclampsia (Moslehi et al., 2013). In comparison, SMAD9 is activated by bone morphogenic proteins (BMPs), a subfamily of the transforming growth factor-β (TGF-β) family (Han et al., 2008; Tsukamoto et al., 2014). Although some BMPs such as BMP-4 can be regulated in a downstream manner from the cAMP pathway (Heo & Fujiwara, 2011), the connection between SMAD9 and cAMP is still unclear. GATA2 was found to be slightly upregulated, which may suggest that the enrichment of L1PREC2 in the 5′UTR still plays a role in regulating *LGALS16* despite the insertion of L1PA6 (Than et al, 2014).

Figure 10. Changes in the expression of genes encoding TFs in JEG-3 cells.

Cells were treated with 8-Br-cAMP (250 μM) for 36 hours to induce trophoblastic differentiation and Qiagen RT2 Profiler TM PCR Array kit was used to assess fold changes in gene expression between differentiated and control cells presented as a heatmap.

Interestingly, CREB1, a major regulator downstream of the cAMP pathway was not upregulated in this RT-qPCR array analysis suggesting that post-translational modification and transcriptional activation might be essential for this TF.

I further analyzed the 2 kb region upstream from the transcription start site of *LGALS16* by extracting the sequence from Ensembl (Release 104) and performing in silico analysis of TF-binding sites using PROMO virtual laboratory with a 0% dissimilarity index. Putative binding sites for seventeen TFs were identified, which may represent specific response elements, enhancers, or silencers (**Figure 11**). To reveal common patterns in the expression of the predicted TFs, I watched for their protein levels in two *LGALS16*-positive tissues, the cerebellum and placenta, using the expression scores (high, medium, low) available at HPA. Protein expression level was determined using immunohistochemical data which was manually scored for the fraction of stained cells. The protein was then classified into one of 4 categories: not detected, low, medium, or high expression. Within this set of data, two TFs (CEBPβ and TFII-I) were characterized by high protein expression levels, seven TFs had variable levels (GR, NFAT1, p53, STAT4, TCF-4E, TFIID, and YY1), four TFs (ERα, FOXP3, Pax5, and PR A) showed low expression, and no HPA data were available for GRα, GRβ, PR B, and XBP-1 in these tissues (**Figure 12**). Thus, the role of the predicted TFs in tissue-specific transcriptional regulation of *LGALS16* can be different and remains to be studied.
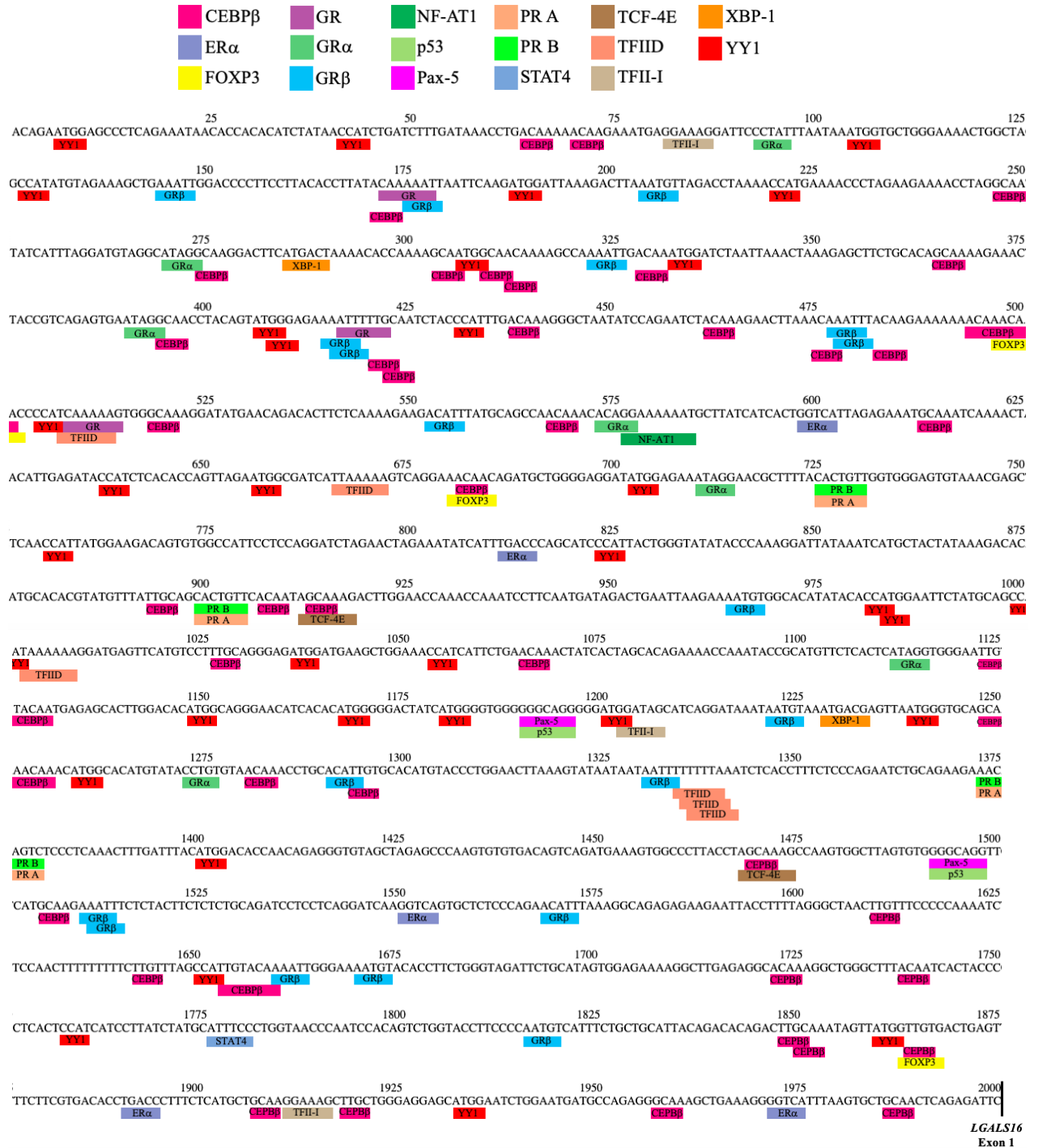
Figure 11**. In silico screening of putative transcription factor binding sites for the** *LGALS16* **gene.**

There are multiple binding sites for 17 transcription factors within the 2 kb promoter region upstream the transcription start site of *LGALS16* gene as detected by PROMO.
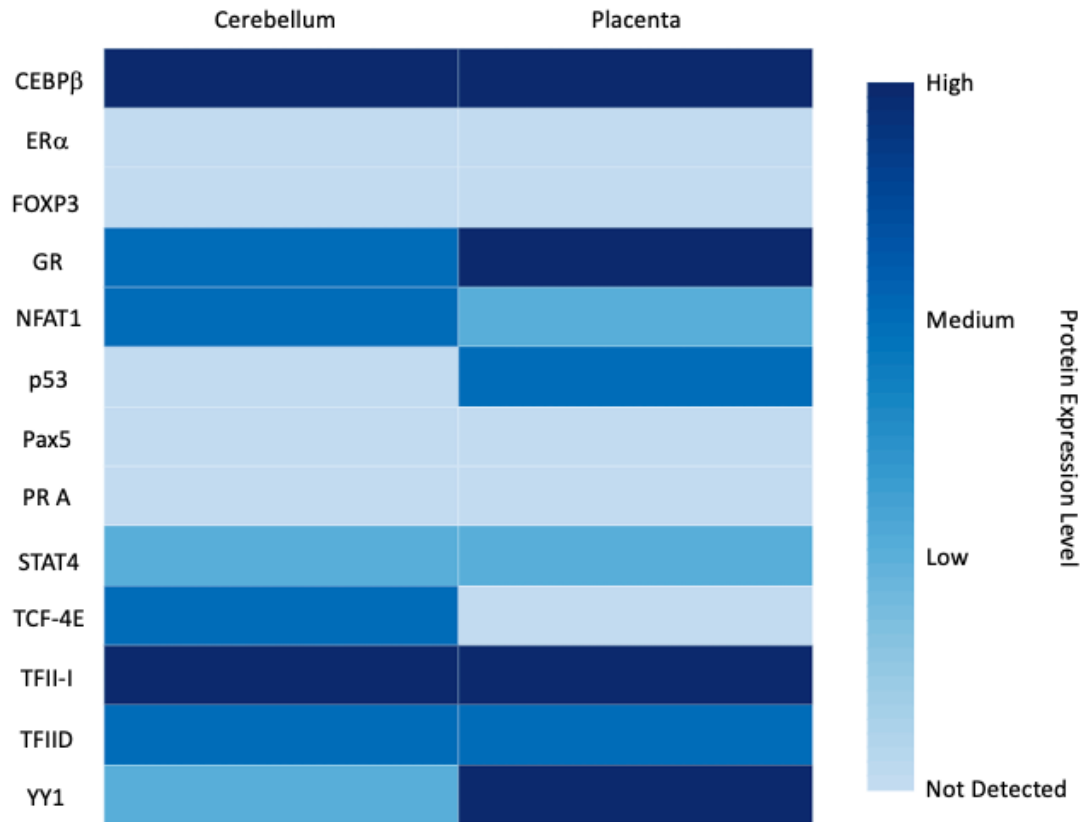
Figure 12. Protein expression patterns of predicted transcription factors for *LGALS16* **regulation in the cerebellum and placenta.**

2.3.3.2   miRNAs

Post-transcriptional control of mRNA availability for protein synthesis depends on miRNAs which can hybridize to complementary sequences in protein-coding mRNAs at the 3′ untranslated region and either block protein translation or induce mRNA degradation (Fabian et al., 2010). Multiple miRNAs were predicted to target the *LGALS16* transcript by bioinformatics tools, such as Diana Tools (Paraskevopoulou et al., 2013), miRabel (Quillet et al., 2020), miRDB (Chen & Wang, 2020), and TargetScan (Agarwal et al., 2015), which use different algorithms and methods. A robust application of these tools using default options shows that five miRNAs (hsa-miR-3155a, hsa-miR-3155b, hsa-miR-4689, hsa-miR-4778-5p, hsa-miR-6783-5p) are predicted by all four of these online platforms (**Figure 13**). These miRNAs among others can be considered as prospective candidates for regulating the stability and/or translational potential of the *LGALS16* transcripts, especially in relevant tissues such as placenta and brain. Indeed, a significant decrease in hsa-miR-4778-5p expression during gestation in exosomes from maternal blood was associated with preterm birth pregnancies (Menon et al., 2019). Expression of hsa-miR-3155a was significantly upregulated in the anterior cingulate cortex of deceased patients with major depressive disorder (Yoshino et al., 2020). In comparison, the expression of hsa-miR-4689 was downregulated in exosomes isolated from the plasma of patients with mesial temporal lobe epilepsy with hippocampal sclerosis compared to controls (Yan et al., 2017). Differential expression of exosomal hsa-miR-4689 and hsa-miR-6783-5p was reported in patients with intracranial aneurysms (Liao et al., 2020). Human miRNA tissue atlas confirms expression of hsa-miR-3155a, hsa-miR-3155b, hsa-miR-4689, and hsa-miR-4778-5p in brain among other tissues at variable levels (Ludwig et al., 2016). Unraveling possible mechanisms of miRNA-mediated regulation of galectin-16 in these tissues awaits future research.
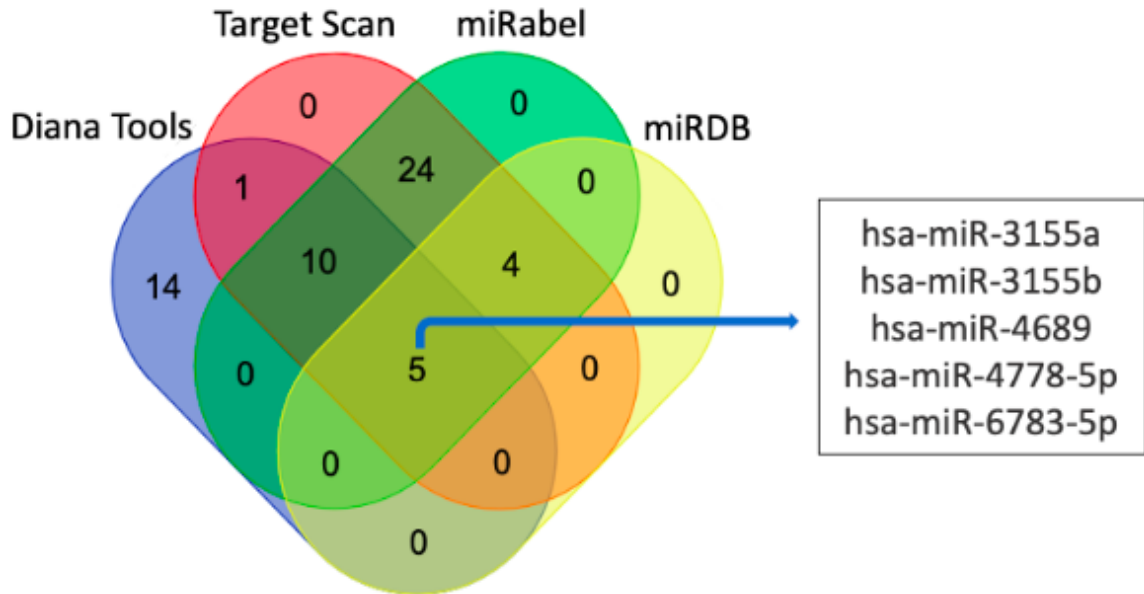
Figure 13. Putative miRNAs targeting *LGALS16* mRNA transcript.

Five miRNAs are unanimously predicted by four different online platforms such as Diana Tools, miRabel, miRDB, and TargetScan.

2.3.4 *LGALS16* and human diseases

Dysregulation of the placenta-specific gene cluster containing *LGALS16* is associated with a pregnancy complication known as preeclampsia, which can be fatal for both the mother and fetus. As such, *LGALS16* together with *LGALS13* and *LGALS14* were confirmed to satisfy the criteria of placenta enriched genes in a comprehensive study of RNA-Seq datasets from 302 placental biopsies (Gong et al., 2021). However, although increasing expression of *LGALS13*, *LGALS14*, and *LGALS16* was observed during forskolin-induced syncytialization and differentiation of primary trophoblasts and BeWo cells in culture, only *LGALS13* and *LGALS14* were downregulated in preeclampsia with no significant changes of *LGALS16* (Than et al., 2014). Remarkably, *LGALS16* does not show sex-biased expression depending on the chromosomal sex of the fetus while *LGALS13* and *LGALS14* are notably elevated in fetal male placentas based on the chorionic villus transcriptome (Braun et al., 2021). These aspects of galectin network regulation remain unclear in the context of placental disorders and development.

Alterations in the expression or mutations of *LGALS16* have been also reported for several other diseases and based mostly on microarray and RNA-Seq analysis, although the application of this gene as a biomarker is still unknown. Gene expression profiling with RNA sequencing data revealed that *LGALS16* was detected as an upregulated gene in fusiform gyrus tissue sections of 219 autopsy-confirmed Alzheimer's cases versus 70 neurologically normal age-matched controls (Vastrad & Vastrad, 2021). *LGALS16* was also recognized as a brain tissue-specific gene within genome-wide associations with several neuroimaging psychiatric traits (Zhao et al., 2021). Further, *LGALS16* was expressed two-fold higher in chronic myeloid leukemia granulocytes compared to controls (Čokić et al., 2015). Copy number variations were identified in chromosome 19 for multiple genes including *LGALS16* in association with clinical features, such as histological type, ethnicity, disease stage, and familial history of breast cancer using tumor samples from a Brazilian cohort (Rodrigues-Peres et al., 2019). In addition, *LGALS16* was determined to be a moderate impact variant associated with autism spectrum disorder, consisting of a missense single nucleotide variant (SNV), which was reported as detrimental by bioinformatic tools SIFT and PolyPhen-2 (Santos et al.,

2019). *LGALS16* also had greater SNVs within the 3′ flank region with one or more mutations in patients with diffuse large B-cell lymphoma (Arthur et al., 2018). Moreover, a *LGALS16* SNP was revealed to be associated with insulin secretion in a cohort of African Americans (Keaton et al., 2016). This study also showed that interactions between this *LGALS16* SNP and others, such as an intergenic SNP upstream of the LYPLAL1 gene, have also been associated with type 2 diabetes risk. The *LGALS16* transcript was one of the top 50 down-regulated mRNA present in the exosomes isolated from the cerebrospinal fluid in patients with meningeal carcinomatosis in comparison with healthy controls (Cheng et al., 2021).

2.4 Conclusions

Although the galectin-16 gene was described more than 10 years ago (Than et al., 2009), the regulation, functions, and clinical aspects of this tissue-specific molecule are largely unexplored. Primary association of *LGALS16* with placental tissue has been challenged by its detection in brain tissues and several cancer cell lines as followed from available microarray and RNA-seq databases. There are bioinformatics indications that the expression of *LGALS16* changes in association with Alzheimer's disease, chronic myeloid leukemia, breast cancer, B-cell lymphoma, and type 2 diabetes. Although *LGALS16* was not significantly impacted at the gene level in preeclampsia, there remain questions regarding regulation at the protein level, which cannot be properly addressed at this time due to the absence of commercially available specific galectin-16 antibodies. The results obtained with recombinant galectin-16 are promising, but there is still a gap in our understanding of why the expression of endogenous galectin-16 protein has not been reported. Nevertheless, among the possible functions of galectin-16 in these and other tissues, its contribution to the regulation of cellular differentiation and programmed cell death (apoptosis) warrants special attention. Lastly, the use of proper cell culture models and the examination of multiple factors (transcription regulators and miRNA) is evidently the first line of study to position galectin-16 within a complex galectin network in cells. The generation of galectin-16-specific antibody and *LGALS16* knockout cell lines using

CRISPR/Cas9 technology might be required steps to unravel the role and significance of this molecule in the context of cell biology.

2.5 References

Agarwal V, Bell GW, Nam JW, Bartel DP. Predicting effective microRNA target sites in mammalian mRNAs. eLife. 2015 Aug 12;4:e05005.

Allo VCM, Toscano MA, Pinto N, Rabinovich GA. Galectins: Key players at the frontiers of innate and adaptive immunity. Trends Glycosci Glycotechnol. 2018 Jan;30(172):SE97–SE107.

Arthur SE, Jiang A, Grande BM, Alcaide M, Cojocaru R, Rushton CK, Mottok A, Hilton LK, Kumar Lat P, Zhao EY. Genome-wide discovery of somatic regulatory variants in diffuse large B-cell lymphoma. Nat Commun. 2018 Oct 1;9(1):4001.

Balsa E, Perry EA, Bennett CF, Jedrychowski M, Gygi SP, Doench JG, Puigserver P. Defective NADPH production in mitochondrial disease complex I causes inflammation and cell death. Nat Commun. 2020 Jun 1;11(1):2714.

Barrett T, Wilhite SE, Ledoux P, Evangelista C, Kim IF, Tomashevsky M, Marshall KA, Phillippy KH, Sherman PM, Holko M, et al. NCBI GEO: Archive for functional genomics data sets—Update. Nucleic Acids Res. 2013 Jan;41:D991–D995.

Berman HM, Westbrook J, Feng Z, Gilliland G, Bhat TN, Weissig H, Shindyalov IN, Bourne PE. The protein data bank. Nucleic Acids Res. 2000 Jan 1;28(1):235–242.

Blois SM, Dveksler G, Vasta GR, Freitag N, Blanchard V, Barrientos G. Pregnancy galectinology: Insights into a complex network of glycan binding proteins. Front Immunol. 2019 May 29;10:1166.

Braun AE, Muench KL, Robinson BG, Wang A, Palmer TD, Winn VD. Examining sex differences in the human placental transcriptome during the first fetal androgen peak. Reprod Sci. 2021 Mar;28(3):801–818.

Chen Y, Wang X. miRDB: An online database for prediction of functional microRNA targets. Nucleic Acids Res. 2020 Jan 8;48(D1):D127–D131.

Cheng P, Feng F, Yang H, Jin S, Lai C, Wang Y, Bi J. Detection and significance of exosomal mRNA expression profiles in the cerebrospinal fluid of patients with meningeal carcinomatosis. J Mol Neurosci. 2021 Apr;71(4):790–803.

Cheng Y-H, Richardson BD, Hubert MA, Handwerger S. Isolation and characterization of the human syncytin gene promoter. Biol Reprod. 2004 Mar;70(3):694–701.

Clark K, Karsch-Mizrachi I, Lipman DJ, Ostell J, Sayers EW. GenBank. Nucleic Acids Res. 2016 Jan 4;44(D1):D67–D72.

Čokić VP, Mojsilović S, Jauković A, Kraguljac-Kurtović N, Mojsilović S, Šefer D, Mitrović Ajtić O, Milošević V, Bogdanović A, Đikić D, et al. Gene expression profile of circulating CD34(+) cells and granulocytes in chronic myeloid leukemia. Blood Cells Mol Dis. 2015 Dec;55(4):373–381.

Ely AZ, Moon JM, Sliwoski GR, Sangha AK, Shen X-X, Labella AL, Meiler J, Capra JA, Rokas A. The impact of natural selection on the evolution and function of placentally expressed galectins. Genome Biol. Evol. 2019 Sep 1;11(9):2574–2592.

Fabian MR, Sonenberg N, Filipowicz W. Regulation of mRNA translation and stability by microRNAs. Annu Rev Biochem. 2010 July 7;79:351–379.

Farré D, Roset R, Huerta M, Adsuara JE, Roselló L, Albà MM, Messeguer X. Identification of patterns in biological sequences at the ALGGEN server: PROMO and MALGEN. Nucleic Acids Res. 2003 Jul 1;31(13):3651–3653.

Garces de Los Favos Alonso I, Liang HC, Turner SD, Lagger S, Merkel O, Kenner L. The role of activator protein-1 (AP-1) family members in CD30-positive lymphomas. Cancers. 2018 Mar 28;10(4):93.

Gong S, Gaccioli F, Dopierala J, Sovio U, Cook E, Volders PJ, Martens L, Kirk PDW, Richardson S, Smith GCS, et al. The RNA landscape of the human placenta in health and disease. Nat Commun. 2021 May 11;12(1):2639.

Han YM, Romero R, Kim JS, Tarca AL, Kim SK, Draghici S, Kusanovic JP, Gotsch F, Mittal P, Hassan S.S, et al. Region-specific gene expression profiling: Novel evidence for biological heterogeneity of the human amnion. Biol Reprod. 2008 Nov;79(5):954–961.

Hayden MS, Ghosh S. NF-κB in immunobiology. Cell Res. 2011 Feb;21(2):223–244.

He J, Baum LG. Galectin interactions with extracellular matrix and effects on cellular function. Methods Enzymol. 2006 Nov 26;417:247–256.

Heo KS, Fujiwara K, Abe J. Disturbed-flow-mediated vascular reactive oxygen species induce endothelial dysfunction. Circ J. 2011 Nov 10;75(12):2722–2730.

Inamochi Y, Mochizuki K, Goda T. Histone code of genes induced by co-treatment with a glucocorticoid hormone agonist and a p44/42 MAPK inhibitor in human small intestinal Caco-2 cells. Biochim Biophys Acta. 2014 Jan;1840(1):693–700.

Jadhav K, Zhang Y. Activating transcription factor 3 in immune response and metabolic regulation. Liver Res. 2017 Sep;1(2):96–102.

Johannes L, Jacob R, Leffler H. Galectins at a glance. J Cell Sci. 2018 May 1;131(9):jcs208884.

Keaton JM, Hellwege JN, Ng MC, Palmer ND, Pankow JS, Fornage M, Wilson JG, Correa A, Rasmussen-Torvik LJ, Rotter JI, et al. Genome-wide interaction with insulin secretion loci reveals novel loci for type 2 diabetes in African Americans. PLoS ONE. 2016 Jul 22;11(7):e0159977.

Knyazev EN, Zakharova GS, Astakhova LA, Tsypina IM, Tonevitsky AG, Sukhikh GT. Metabolic reprogramming of trophoblast cells in response to hypoxia. Bull Exp Biol Med. 2019 Jan;166(3):321–325. doi: 10.1007/s10517-019-04342-1.

Liao B, Zhou MX, Zhou FK, Luo XM, Zhong SX, Zhou YF, Qin YS, Li PP, Qin C. Exosome-derived miRNAs as biomarkers of the development and progression of intracranial aneurysms. J Atheroscler Thromb. 2020 Jun 1;27(6):545–610.

Ludwig N, Leidinger P, Becker K, Backes C, Fehlmann T, Pallasch C, Rheinheimer S, Meder B, Stähler C, Meese E, et al. Distribution of miRNA expression across human tissues. Nucleic Acids Res. 2016 May 5;44(8):3865–3877.

Ma S, Pang C, Song L, Guo F, Sun H. Activating transcription factor 3 is overexpressed in human glioma and its knockdown in glioblastoma cells causes growth inhibition both in vitro and in vivo. Int J Mol Med. 2015 Jun;35(6):1561–1573.

Menon R, Debnath C, Lai A, Guanzon D, Bhatnagar S, Kshetrapal PK, Sheller-Miller S, Salomon C, Garbhini Study Team. Circulating exosomal miRNA profile during term and preterm birth pregnancies: A longitudinal study. Endocrinology. 2019 Feb 1;160(2):249–275.

Messeguer X, Escudero R, Farré D, Núñez O, Martínez J, Albà MM. PROMO: Detection of known transcription regulatory elements using species-tailored searches. Bioinformatics. 2002 Feb;18(2):333–334.

Moslehi R, Mills JL, Signore C, Kumar A, Ambroggio X, Dzutsev A. Integrative transcriptome analysis reveals dysregulation of canonical cancer molecular pathways in placenta leading to preeclampsia. Sci Rep. 2013 Aug 30;3:2407.

Nabi IR, Shankar J, Dennis JW. The galectin lattice at a glance. J Cell Sci. 2015 Jul 1;128(13):2213–2219.

Nuzzo AM, Giuffrida D, Zenerino C, Piazzese A, Olearo E, Todros T, Rolfo A. JunB/Cyclin-D1 imbalance in placental mesenchymal stromal cells derived from

preeclamptic pregnancies with fetal-placental compromise. Placenta. 2014 Jul;35(7):483–490.

Paraskevopoulou MD, Georgakilas G, Kostoulas N, Vlachos IS, Vergoulis T, Reczko M, Filippidis C, Dalamagas T, Hatzigeorgiou AG. DIANA-microT web server v5.0: Service integration into miRNA functional analysis workflows. Nucleic Acids Res. 2013 Jul;41:W169–W173.

Park MH, Hong JT. Roles of NF-κB in cancer and inflammatory diseases and their therapeutic approaches. Cells. 2016 Mar 29;5(2):15.

Patterson RJ, Haudek KC, Voss PG, Wang JL. Examination of the role of galectins in pre-mRNA splicing. Methods Mol Biol. 2015;1207:431–449.

Pollheimer J, Vondra S, Baltayeva J, Beristain AG, Knöfler M. Regulation of placental extravillous trophoblasts by the maternal uterine environment. Front Immunol. 2018 Nov 13;9:2597.

Popa SJ, Stewart SE, Moreau K. Unconventional secretion of annexins and galectins. Semin Cell Dev Biol. 2018 Nov;83:42–50.

Quillet A, Saad C, Ferry G, Anouar Y, Vergne N, Lecroq T, Dubessy C. Improving bioinformatics prediction of microRNA targets by ranks aggregation. Front Genet. 2020 Jan 28;10:1330.

Renaud SJ, Chakraborty D, Mason CW, Rumi MA, Vivian JL, Soares MJ. OVO-like 1 regulates progenitor cell fate in human trophoblast development. Proc Natl Acad Sci USA. 2015 Nov 10;112(45):E6175–E6184.

Rodrigues-Peres RM, de Carvalho BS, Anurag M, Lei JT, Conz L, Gonçalves R, Cardoso Filho C, Ramalho S, de Paiva GR, Derchain S, et al. Copy number alterations associated with clinical features in an underrepresented population with breast cancer. Mol Genet Genomic Med. 2019 Jul;7(7):e00750.

Rosenfeld CS. The placenta-brain-axis. J Neurosci Res. 2021 Jan;99(1):271–283.

Santos JX, Rasga C, Marques AR, Martiniano HFMC, Asif M, Vilela J, Oliveira G, Vicente AM. A role for gene-environment interactions in Autism Spectrum Disorder is suggested by variants in genes regulating exposure to environmental factors. BioRxiv. 2019 Jan;520544.

Shankar K, Kang P, Zhong Y, Borengasser SJ, Wingfield C, Saben J, Gomez-Acevedo H, Thakali KM. Transcriptomic and epigenomic landscapes during cell fusion in BeWo trophoblast cells. Placenta. 2015 Dec;36(12):1342–1351.

Sherazi AA, Jariwala KA, Cybulski AN, Lewis JW, Karagiannis J, Cumming RC, Timoshenko AV. Effects of global O-GlcNAcylation on galectin gene-expression profiles in human cancer cell lines. Anticancer Res. 2018 Dec;38(12):6691–6697.

Si Y, Yao Y, Ayala GJ, Li X, Han Q, Zhang W, Xu X, Tai G, Mayo KH, Zhou Y, et al. Human galectin-16 has a pseudo ligand binding site and plays a role in regulating c-Rel mediated lymphocyte activity. Biochim Biophys Acta Gen Subj. 2021 Jan;1865(1):129755.

Singer MF. SINEs and LINEs: Highly repeated short and long interspersed sequences in mammalian genomes. Cell. 1982 Mar;28(3):433–434.

Tazhitdinova R, Timoshenko AV. The emerging role of galectins and O-GlcNAc homeostasis in processes of cellular differentiation. Cells. 2020 Jul 28;9(8):1792.

Than NG, Romero R, Goodman M, Weckle A, Xing J, Dong Z, Xu Y, Tarquini F, Szilagyi A, Gal P, et al. A primate subfamily of galectins expressed at the maternal-fetal interface that promote immune cell death. Proc. Natl. Acad. Sci. USA. 2009 Jun 16;106(24):9731–9736.

Than NG, Romero R, Kim CJ, McGowen MR, Papp Z, Wildman DE. Galectins: Guardians of eutherian pregnancy at the maternal-fetal interface. Trends Endocrinol Metab. 2012 Jan;23(1):23–31.

Than NG, Romero R, Xu Y, Erez O, Xu Z, Bhatti G, Leavitt R, Chung TH. El-Azzamy H, LaJeunesse C, et al. Evolutionary origins of the placental expression of chromosome 19

cluster galectins and their complex dysregulation in preeclampsia. Placenta. 2014 Nov;35(11):855–865.

Timoshenko AV. Chitin hydrolysate stimulates VEGF-C synthesis by MDA-MB-231 breast cancer cells. Cell Biol Int. 2011 Mar;35(3):281–286.

Timoshenko AV, Lanteigne J, Kozak K. Extracellular stress stimuli alter galectin expression profiles and adhesion characteristics of HL-60 cells. Mol Cell Biochem. 2016 Feb;413(1-2):137–143.

Timoshenko AV. Towards molecular mechanisms regulating the expression of galectins in cancer cells. Cell Mol Life Sci. 2015 Nov;72(22):4327–4340.

Tsukamoto S, Mizuta T, Fujimoto M, Ohte S, Osawa K, Miyamoto A, Yoneyama K, Murata E, Machiya A, Jimi E, et al. Smad9 is a new type of transcriptional regulator in bone morphogenetic protein signaling. Sci Rep. 2014 Dec 23;4:7596.

Uhlén M, Fagerberg L, Hallström BM, Lindskog C, Oksvold P, Mardinoglu A, Sivertsson A, Kampf C, Sjöstedt E, Asplund A. Tissue-based map of the human proteome. Science. 2015 Jan 23;347(6220):1260419.

Vladoiu MC, Labrie M, St-Pierre Y. Intracellular galectins in cancer cells: Potential new targets for therapy (Review). Int J Oncol. 2014 Apr;44(4):1001–1014.

Walcott BP, Winkler EA, Zhou S, Birk H, Guo D, Koch MJ, Stapleton CJ, Spiegelman D, Dionne-Laporte A, Dion PA, et al. Identification of a rare BMP pathway mutation in a non-syndromic human brain arteriovenous malformation via exome sequencing. Hum Genome Var. 2018 Mar 8;5:18001.

Wang Z, Liu Y, Liu J, Kong N, Jiang Y, Jiang R, Zhen X, Zhou J, Li C, Sun H, et al. ATF3 deficiency impairs the proliferative-secretory phase transition and decidualization in RIF patients. Cell Death Dis. 2021 Apr 12;12(4):387.

Weckselblatt B, Rudd MK. Human structural variation: Mechanisms of chromosome rearrangements. Trends Genet. 2015 Oct;31(10):587–599.

Yan S, Zhang H, Xie W, Meng F, Zhang K, Jiang Y, Zhang X, Zhang J. Altered microRNA profiles in plasma exosomes from mesial temporal lobe epilepsy with hippocampal sclerosis. Oncotarget. 2017 Jan 17;8(3):4136–4146.

Ye J, Coulouris G, Zaretskaya I, Cutcutache I, Rozen S, Madden TL. Primer-BLAST: A tool to design target-specific primers for polymerase chain reaction. BMC Bioinform. 2012 Jun 18;13:134.

Yoshino Y, Roy B, Dwivedi Y. Altered miRNA landscape of the anterior cingulate cortex is associated with potential loss of key neuronal functions in depressed brain. Eur Neuropsychopharmacol. 2020 Nov;40:70–84.

Vastrad B, Vastrad C. Bioinformatics analyses of significant genes, related pathways and candidate prognostic biomarkers in Alzheimer's disease. BioRxiv. 2021 Jan 1

Zhao B, Shan Y, Yang Y, Zhaolong Y, Li T, Wang X, Luo T, Zhu Z, Sullivan P, Zhao H, et al. Transcriptome-wide association analysis of brain structures yields insights into pleiotropy with complex neuropsychiatric traits. Nat Commun. 2021 May 17;12(1):2878.

3   Molecular mechanisms regulating *LGALS16* expression in conjunction with trophoblastic differentiation

3.1   Introduction

Galectins are a family of multifunctional β-galactoside binding proteins that play a key role in biological processes through glycan-dependent and glycan-independent interactions both intra- and extracellularly (Sherazi et al., 2018; Tazhitdinova & Timoshenko, 2020). Intracellular galectins are involved in pre-mRNA splicing and regulate cell growth, apoptosis, and the cell cycle (Liu et al., 2002; Vladoiu et al., 2014). Extracellular galectins are non-classically secreted and localized in the extracellular matrix to facilitate transmembrane signaling for cell adhesion and migration (Johannes, 2018; He & Baum, 2006). Some galectins can be found widely throughout human tissues while others are tissue-specific. For instance, galectin-16, encoded by the gene *LGALS16*, is predominantly expressed in the placenta (Than et al., 2009; Kaminker & Timoshenko, 2021). Tissue-specific expression of galectin-16 may indicate a distinct role in cellular differentiation of the placenta. Mechanisms modulating galectin expression and function include specific transcription factors and the availability of glycan ligands (Than et al., 2014; Kamili et al., 2016).

Placental cell models can be induced to differentiate when treated with 8-bromoadenosine-3',5'-cyclic monophosphate (8-Br-cAMP) which results in the increased expression of *LGALS16* and chorionic gonadotropin beta (*CGB)*, a biomarker of placental differentiation (Burnside et al., 1985; Chen et al., 2013; Kaminker & Timoshenko, 2021). Downstream signalling molecules in the cAMP pathway, such as protein kinase A (PKA), exchange protein directly activated by cAMP (Epac), and the p38 mitogen-activated protein kinase (MAPK) pathway were included in this study to determine how cAMP mediates its effects on *LGALS16* expression during trophoblastic differentiation (Gerbaud et al., 2015; Delidaki et al., 2011). Additionally, transcription factors (TF) regulate galectin expression through unique binding sites in the promoter region (Than et al., 2014). Gene expression of 84 TFs was investigated experimentally in JEG-3 cells during placental differentiation and showed the greatest increase in 3 TFs: *JUNB*, *SMAD9*, and *GATA2* (Kaminker &

Timoshenko, 2021). In addition, analysis of binding sites in the 5' untranslated region of *LGALS16* reveals response elements for GATA2 (Than et al., 2014). The specific mechanisms through which TFs mediate *LGALS16* expression is largely unknown and warrants deeper examination.

Recent studies with a variety of cell lines have demonstrated that protein *O*-GlcNAcylation governs the localization and function of galectins. *O*-GlcNAcylation is a process involving the post-translational modification of serine and threonine residues of intracellular proteins with GlcNAc (Kim et al., 2017). Two enzymes, *O*-GlcNAc transferase and *O*-GlcNAcase are involved the addition and removal of GlcNAc, respectively (Yang & Qian, 2017). A recent model proposes high levels of *O*-GlcNAcylation are associated with galectin secretion and cellular differentiation while low levels of *O*-GlcNAcylation lead to an increase in intracellular galectins and are associated with the undifferentiated cellular state (Tazhitdinova & Timoshenko, 2020). Moreover, *O*-GlcNAcylation levels are associated with placental development and pathologies. For example, hyperglycemia is associated with an increase in *O*-GlcNAcylation and can be harmful for the fetus (Ning & Yang, 2021). The relationship between *O*-GlcNAcylation and *LGALS16* expression during trophoblastic differentiation requires further inquiry.

To date, there is little data examining the function of galectin-16 during differentiation. One suggested role of galectin-16 is the regulation of T-cell apoptosis for maternal immune tolerance at the maternal-fetal interface via interactions with c-Rel, a member of the NF-kB family of transcription factors (Than et al., 2009; Si et al., 2020). Genome editing provides a tool to target and functionally knockout a specific protein by inducing frameshift mutations with insertions/deletions (indel) of nucleotides in the nucleic acid sequence (Tuladhar et al., 2019). To gain a better understanding of galectin-16's role in placental differentiation, *LGALS16* knockout cells were produced using the CRISPR/Cas9 system to determine phenotypic changes during 8-Br-cAMP-induced differentiation.

This study investigated the upstream regulation of *LGALS16* expression, specifically by using biochemical inhibitors of transcription factors, cAMP signaling pathways, and *O*-

GlcNAc homeostasis. Additionally, the downstream effects of galectin-16 on cellular differentiation were investigated using *LGALS16* knockouts.

3.2   Materials and methods

3.2.1   Cell cultures and reagents

BeWo cells were cultured in Ham's F-12K (Kaighn's) medium (21127022, ThermoFisher, Waltham, MA) supplemented with 10% FBS, 100 IU/mL penicillin, and 100 μg/mL streptomycin. JEG-3 cells were cultured in RPMI-1640 medium (11875093, ThermoFisher) supplemented 8% FBS, 100 IU/mL penicillin, and 100 μg/mL streptomycin. Cells were subcultured at 80% confluency and maintained at 37°C and 5% CO_2.

CellTiter-Glo Luminescent Cell Viability Assay (G7571, Promega, Madison, WI) and thiazoyl blue tetrazolium bromide (MTT) assay (T0793, Bio Basic, Markham, ON) were used to assess cell viability. Inhibitors H-89 (10010556), K-7174 (32773), LDN-193189 (11802), U0126 (70970), 8-pCPT-2'-O-Me-Cyclic AMP (17143), ESI-09 (19130), and SB203580 (13067) were from Cayman Chemicals (Ann Arbor, MI).

O-GlcNAc homeostasis was altered with 2-acetamido-1,3,4,6-tetra-O-acetyl-2-deoxy-5-thio-α-D-glucopyranose (AC), which was kindly provided by Dr. David Vocadlo as per Material Transfer Agreement between Simon Fraser University and the University of Western Ontario, and thiamet G (TG) (SML0244) was from Sigma-Aldrich Canada (Oakville, ON). Trophoblastic differentiation was induced with 8-Br-cAMP (B7880, Sigma-Aldrich).

Primary antibodies used for immunodot blots and western blots included: RL2 O-GlcNAc (1:1000; MA1-072); ThermoFisher), β-actin (1:200; sc-47778; Santa Cruz, Dallas, TX), galectin-1 (1:800; sc-166618; Santa Cruz), galectin-3 (1:200; sc-20157; Santa Cruz), and CGB (1:3000; PA5-16265; Abcam, Cambridge, UK). Secondary antibodies included anti-mouse IgG HRP (1:10 000; A16066; ThermoFisher) and anti-rabbit IgG-HRP (1:10 000; A16096; ThermoFisher). Primary antibodies were diluted in TBS-T, 5% BSA, and 0.1%

NaN$_3$ and secondary antibodies were diluted in TBST-T, 3% BSA, and 1% non-fat dry milk.

For Sanger sequencing of *LGALS16* CRISPR/Cas9 knockout clonal pools, genomic DNA was isolated using QuickExtract™ DNA Extraction Solution (Lucigen, Middleton, WI). PCR was performed with 2X Amplitaq Gold 36 master mix (ThermoFisher) and samples were purified with QIAquick PCR Purification Kit (Qiagen, Hilden, Germany).

3.2.2   Cell viability assays

Cells were seeded at 2 x 10^5 cells/mL in 96-well plates with 100 μL per well and given 24 hours to adhere. Cell medium was replaced, and cells were treated every 12 hours for 36 hours. For CellTiter-Glo® Assay, cells were equilibrated to room temperature for 30 minutes and 100 μL of reagent was then added. Wells were mixed on an orbital shaker for 2 minutes, incubated at room temperature for 10 minutes, and luminescence was recorded using Instinct™ software. For MTT assays, a 2.5 mg/mL MTT solution was prepared and 20 μL were added to each well. Cells were incubated at 37°C for 4 hours. Media was aspirated and 150 μL of DMSO was added to each well. The plate was mixed on a shaker for 30 minutes and read on a BioTek 800 TS Absorbance Reader (Santa Clara, CA) at 570 nm. Dose-response curves were generated for each biochemical inhibitor to determine non-toxic concentrations for cell treatments. Three technical replicate wells were performed for every treatment and time point. Blank wells containing only media were also assayed with 3 technical replicates. Technical replicates were averaged, and the average of the blank wells was subtracted from each value. The resultant values were then normalized to the control wells which were left untreated.

3.2.3   Cell treatments

JEG-3 cells were plated at 1 x 10^5 cells/mL and 2 x 10^5 cells/mL for untreated and treated cells, respectively, in 6-well plates with 2 mL per well. JEG-3 cells were treated with 8

biochemical inhibitors including: 5 µM H-89, 2.5 µM K7174, 100 nM LDN-193189, 10 µM U0126, 5 µM SB203580, 10 µM ESI-09, and 10 µM 8-pCPT-2'-O-Me-Cyclic AMP,. Non-toxic concentrations of inhibitors were selected to target PKA, GATA2, SMAD9, JUNB, p38/MAPK, and Epac, as well as stimulate Epac, respectively. BeWo cells were plated at 5 x 10^4 cells/mL and 1 x 10^5 cells/mL for untreated and treated cells in 6-well plates with 2 mL per well. To test the effects of *O*-GlcNAcylation, BeWo cells in complete medium were treated for 24 hrs with 25 µM of AC, an OGT inhibitor, or with 10 µM of TG, an OGA inhibitor. Transcriptional and *O*-GlcNAc inhibitors were added to cell cultures with or without 250 µM of 8-Br-cAMP for 36 hours before RNA and protein collection.

3.2.4   Gene expression analysis

RNA isolation, cDNA synthesis, conventional PCR (cPCR), and real-time quantitative polymerase chain reaction (RT-qPCR) were carried out to measure mRNA expression for *ACTB*, *CGB3/5*, *LGALS1, LGALS3, LGALS8, LGALS9, LGALS12, LGALS13,* and *LGALS16* as previously described in (Kaminker & Timoshenko, 2021) using the primers synthesized at BioCorp UWO OligoFactory (**Table 2**). All primers were validated using conventional PCR and gel electrophoresis to confirm amplicon size. Bands were excised, sequenced at Robarts Research Institute (London, ON, Canada), and verified by aligning resultant sequences on BLAST®. Relative transcript levels were quantified by the Livak method ($2^{-\Delta\Delta CT}$) and normalized to the reference gene, *ACTB*.

3.2.5   Protein collection and quantification

After cell treatments, medium was aspirated and cells were washed twice with Dulbecco's phosphate buffered saline (DPBS) (0.137 M NaCl, 2.7 mM KCl, 1.1 mM KH_2PO_4, 0.5 mM $MgCl_2$•6H2O, 8.1 mM Na_2HPO_4•7H2O, 0.9 mM $CaCl_2$). Protein lysates were collected with RIPA buffer (10 mM Tris-HCl, pH 8, 1% Triton X-100, 0.1% SDS, 0.5 mM EGTA, 0.1% sodium deoxycholate, 140 mM NaCl), 100 mM sodium orthovanadate (Na_3VO_4),

Table 2. Primers for RT-qPCR to quantify gene expression.

Gene	Primer sequence, 5′ -> 3′	Forward/Reverse	Size (bp)	Melting Peak
ACTB	TCAGCAAGCAGGAGTATGACGAG	F	265	83.5°C
	ACATTGTGAACTTTGGGGGATG	R		
CGB3/5	CCTGGCCTTGTCTACCTCTT	F	109	86.0°C
	GGCTTTATACCTCGGGGTTG	R		
LGALS1	CCTGGAGAGTGCCTTCGAGTG	F	220	89.5°C
	CTGCAACACTTCCAGGCTGG	R		
LGALS3	CAGAATTGCTTTAGATTTCCAA	F	108	80.0°C
	TTATCCAGCTTTGTATTGCAA	R		
LGALS8	TGGGGACGGGAAGAGATCAC	F	172	82.0°C
	TGCCATAAATGCCCAGAGTGTC	R		
LGALS9	CTTTCATCACCACCATTCTG	F	91	83.5°C
	ATGTGGAACCTCTGAGCACTG	R		
LGALS12	TGTGAGCCTGAGGGACCA	F	111	86.5°C
	GCTGAGATCAGTTTCTTCTGC	R		
LGALS13	TATTGCCTTCCGTTTCCGAG	F	125	83.0°C
	GCTCAAATTGTTTGCCATCC	R		
LGALS16	ATTTGCGAGTGCACTTAGGC	F	132	82.5°C
	GACACACGTAGATGCGCAAG	R		

100 μM PMSF and protease inhibitor cocktail (1 mM AEBSF, 5 mM EDTA, 50 μM leupeptin, and 1 μM pepstatin). Lysates were incubated on ice for 10 minutes, passed three times through a 23G needle, and centrifuged at 10,000 x g for 15 minutes at 4°C. Supernatant was collected and protein concentrations were quantified using a DC Protein Assay™ (Bio-Rad, Hercules, CA). A Model 3550 Microplate Reader (Bio-Rad) was used to detect absorbance at 655 nm.

Immunodot blot assays were conducted to determine the *O*-GlcNAcylation level of cells using Bio-Dot® Microfiltration apparatus (Bio-Rad). Nitrocellulose membranes (GE Healthcare, Chicago, IL) were pre-wetted for 10 minutes with Tris-buffered saline (TBS) (20 mM Tris-HCl, pH 7.5, 500 mM NaCl) and then loaded into the microfiltration apparatus. Protein extracts were diluted in DPBS (20 μg/mL) and 200 μL of the diluted samples were loaded into wells and allowed to immobilize by gravity filtration for 90 minutes. The membrane was then blocked with 3% bovine serum albumin (BSA) and 1% skim milk in Tris-buffered saline with Tween (TBS-T) (20 mM Tris, pH 7.5, 500 mM NaCl, 0.05% Tween 20) for 1 hour at room temperature. The membrane was washed 3 times with TBS-T and incubated overnight at 4°C with mouse monoclonal pan-specific primary antibody to *O*-GlcNAc (RL2) (ThermoFisher). Next, the membrane was washed 3 times with TBS-T and incubated with a goat anti-mouse secondary antibody (ThermoFisher) at room temperature for 1 hour. Nitrocellulose membranes were developed with Luminata™ Forte Western HRP Substrate (Millipore) and imaged with the ChemiDoc® XRS system (Bio-Rad) and Quantity-One® 1-D analysis software (Bio-Rad) to visualize protein expression. ImageLab software version 5.2 (Bio-Rad) was used for densitometry to measure the signal intensity of each dot.

Intracellular galectins-1 and -3 as well as CGB protein levels were measured using western blots. Loading buffer (2% (w/v) SDS, 0.04% beta-mercaptoethanol) was added to protein lysates. Samples were boiled for 5 minutes, loaded on 4% polyacrylamide stacking gel (25 μg protein per lane), and electrophoretically separated by SDS-PAGE in 10% Mini-

PROTEAN TGX gels (Bio-Rad) at 100 V. Proteins were transferred to PVDF membrane (Sigma-Aldrich) overnight at 20 V in 4ºC using a transfer buffer (25 mM Tris, 190 mM glycine, 20% methanol). Membranes were blocked with 3% BSA and 1% skim milk in TBS-T for 1 hour at room temperature, washed 3 times with TBS-T, and then incubated overnight with primary antibody at 4°C. The membrane was washed 3 times the next day with TBS-T and incubated for 1 hour with secondary antibody. Membranes were imaged using the same protocols as those for immunodot blots. Western blots were normalized to β-actin.

3.2.6   *LGALS16* CRISPR/Cas9 knockouts

A JEG-3 *LGALS16* knockout cell pool was purchased from Synthego (Redwood City, CA). The single guide RNA (sgRNA) sequence, UUUCUACACUGAGAUGAAUG, targeted exon 3 of *LGALS16* near an AGG protospacer adjacent motif (PAM) sequence. To isolate knockout clones, limiting dilutions of 0.5 cells/well and 1 cell/well were performed in 96-well plates with 100 μL per well and cell growth was monitored over 8 weeks. Genomic DNA was isolated with 50 μL of QuickExtract™ and samples were placed in the thermocycler for: 68°C for 15 minutes, 95°C for 10 minutes, and 4°C hold to extract intact DNA while destroying other cellular components, such as RNA and proteins.   PCR was performed with 25 μL 2X Amplitaq Gold 36 master mix, 0.1 μM each of *LGALS16* primers designed by Synthego (forward 5′-TGAACAAGTCACAGGCCCAG-3′ and reverse 5′-ACACGTAGATGCGCAAGTCA-3′, PCR amplicon length of 392 bp), 2 μL genomic DNA, and 22 μL of water for a final volume of 50 μL. PCR samples were purified and subsequently sequenced at Robarts Research Institute (London, ON, Canada). Sanger sequencing results were analyzed using the Synthego ICE tool.

3.2.7   Statistical analysis

A minimum of three biological replicates were tested for each treatment. Statistical analysis was performed using GraphPad Prism 9 for Windows, version 9.3.1 (GraphPad Software, San Diego, CA, USA). One-way analysis of variance (ANOVA) and Tukey's honestly

significant difference test were used to determine significant differences between means, considering $p < 0.05$ as a statistical threshold.

3.3   Results

3.3.1   Effects of transcription factor and cAMP receptor inhibitors on galectin gene expression and trophoblastic differentiation in JEG-3 cells

JEG-3 cells display a significant upregulation of *LGALS16* expression during 8-Br-cAMP-induced trophoblastic differentiation (Kaminker and Timoshenko, 2021) yet the pathways underlying this mechanism are unknown. I sought to identify signaling molecules which regulate *LGALS16* expression during trophoblastic differentiation. Potential transcription factors and cAMP-dependent molecules were selected according to previous literature. Biochemical inhibitors of each molecule were used to determine how reducing their activity would affect galectin gene expression, specifically *LGALS16*. JEG-3 cells were then treated with 250 μM 8-Br-cAMP alone, inhibitor alone, or inhibitor with 8-Br-cAMP. Treatment with only 8-Br-cAMP was used as a positive control to quantify changes in galectin gene expression. Additional galectins were tested to compare whether *LGALS16* is regulated in a manner that is unique from other galectins (i.e. *LGALS1* and *LGALS3*) but more similar to placenta-specific galectins (i.e. *LGALS13*). Moreover, *CGB3/5* expression was analyzed to determine if *LGALS16* is regulated independently of this differentiation biomarker. A significant change in galectin gene expression between treatment with 8-Br-cAMP alone compared to treatment with the inhibitor in addition to 8-Br-cAMP would indicate that the galectin tested is dependent on and regulated by the inhibited molecule.

To assess these pathways, JEG-3 cell viability was measured under various concentrations of inhibitors to select non-toxic concentrations for treatments. Based on these results, JEG-3 cells were treated with 5 μM H-89, 2.5 μM K-7174, 100 nM LDN-193189, 10 μM U0126, 5 μM SB203580, 10 μM ESI-09, and 10 μM 8-pCPT-2'-O-Me-cAMP which inhibit PKA, GATA2, SMAD9, JUNB, p38/MAPK, Epac, and stimulate Epac, respectively (**Figures 14A-G**).
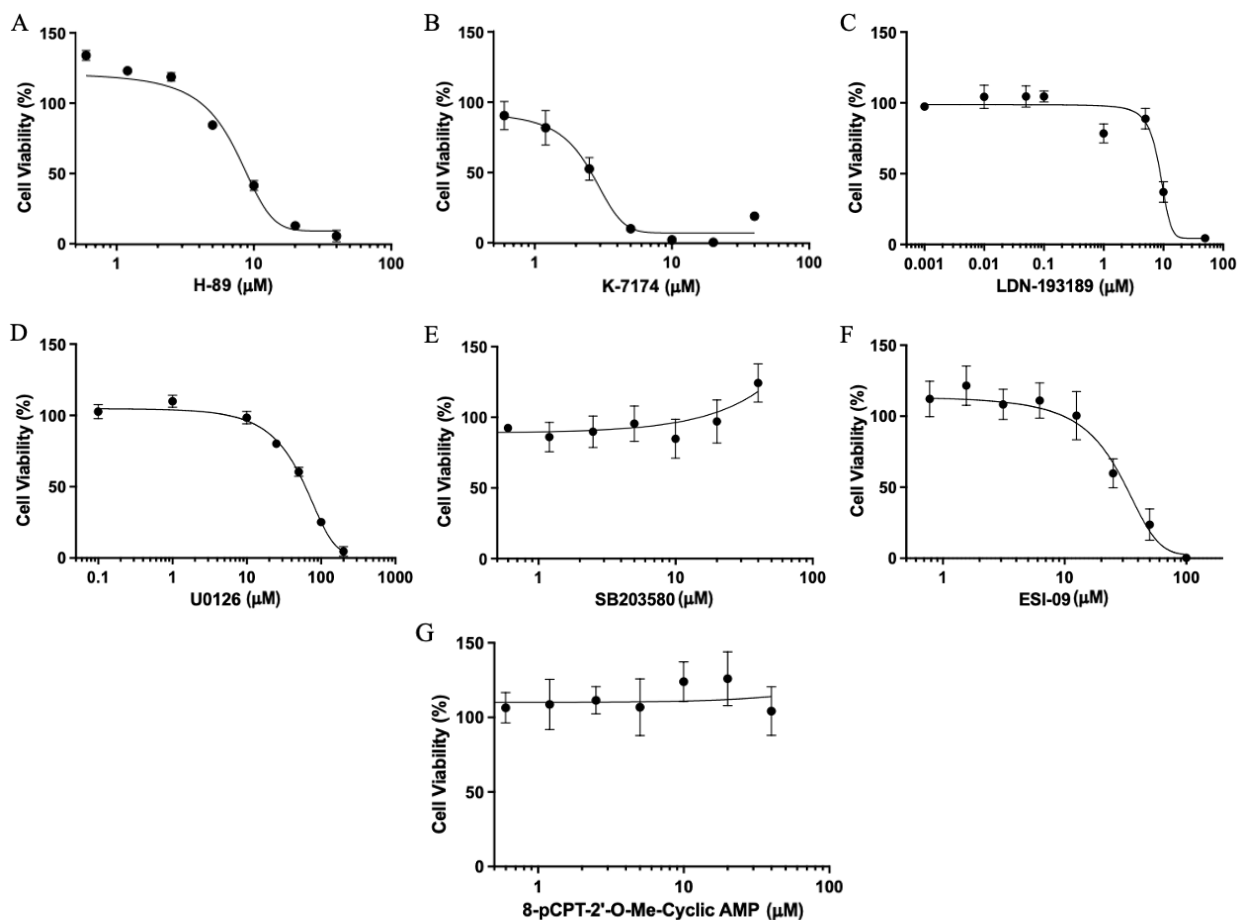
Figure 14. Cell viability of JEG-3 cells treated with varying concentrations of biochemical inhibitors.

JEG-3 cells were cultured in 96-well plates were treated with various concentrations of inhibitors with or without 8-Br-cAMP every 12 hours for 36 hours. After 36 hours, MTT assay was performed and results were used to calculate the percentage of viable cells which had been treated with (A) H-89, (B) K-7174, (C) LDN-193189, (D) U0126, (E) SB203580, (F) ESI-09, and (G) 8-pCPT-2'-O-Me-cAMP, in relation to untreated cells. Cell viability is presented as the mean ± SD (n=3).

JEG-3 cells treated with 8-Br-cAMP showed a significant 2-fold upregulation of *LGALS1* expression (**Figure 15**). Treatment with U0126, a JUNB inhibitor, led to a significant increase (P<0.05, 4-fold) in *LGALS1* expression during differentiation. Inhibition of Epac with ESI09 led to a non-significant increase of *LGALS1* expression during differentiation (P=0.5852). No significant changes were seen in cells treated with H-89, K-7174, LDN-193189, SB203580, or 8-pCPT-2'-O-Me-cAMP.

LGALS3 expression displayed a slight non-significant increase (P=0.4386) during trophoblastic differentiation (**Figure 16**). Inhibition of PKA with H-89 led to a significant upregulation (P<0.01, 2-fold) of *LGALS3* expression during differentiation. JUNB inhibition via U0126 treatment also showed an increasing trend compared to cells treated with 8-Br-cAMP alone, however it was not significant (P=0.9998). Inhibitors K-7174, LDN-193189, SB203580, ESI-09, and the stimulator 8-pCPT-2'-O-Me-cAMP resulted in no significant changes of *LGALS3* expression when used in addition to 8-Br-cAMP.

In regard to *LGALS13* expression, JEG-3 cells showed significant increases in *LGALS13* under 8-Br-cAMP treatment (P<0.05, P<0.01, P<0.001) (**Figures 17A-G**). Cells treated with 8-Br-cAMP and H-89, LDN-193189, or U0126 showed decreasing trends (P=0.1122, P=0.1122, P=0.7195) in *LGALS13* expression while cells treated with ESI-09 showed no change (P=0.2263). A significant decrease in *LGALS13* expression was observed in cells treated with 8-Br-cAMP and K-7174 (2-fold, P<0.01), SB203580 (3-fold, P<0.01), and 8-pCPT-2'-O-Me-cAMP (2-fold, P<0.05).

Similar to *LGALS1* and *LGALS13*, JEG-3 cells treated with 8-Br-cAMP displayed significant increases in *LGALS16* expression (P<0.01, P<0.001, P<0.0001) (**Figures 18A-G**). H-89, K-7174, and 8-pCPT-2-O-Me-cAMP treatment showed non-significant decreasing trends in *LGALS16* expression (P=0.1122, P=0.2449, P=0.2627) between cells treated with 8-Br-cAMP alone and cells treated with both the inhibitor and 8-Br-cAMP. No significant changes were seen in cells treated with LDN193189 and U0126 (P=0.8499, P=9790). Interestingly, JEG-3 cells treated with the p38/MAPK inhibitor, SB203580, demonstrated a significant decrease (P<0.0001) and 2.4-fold change in *LGALS16*
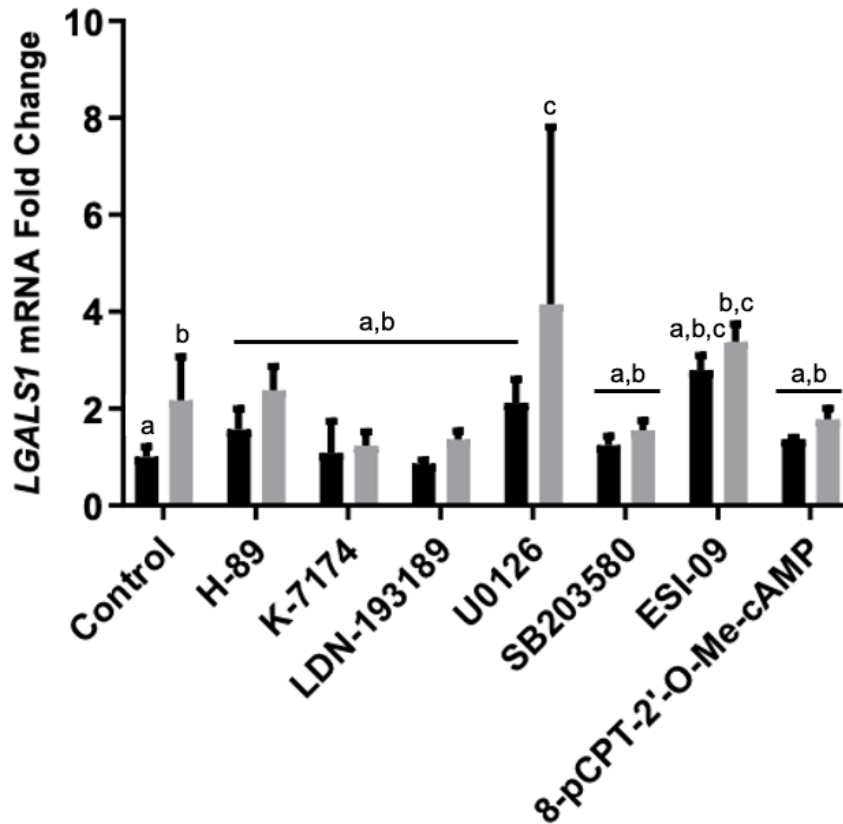
Figure 15. Effects of inhibitors on *LGALS1* expression during trophoblastic differentiation.

JEG-3 cells were cultured in 6-well plates and treated every 12 hours for 36 hours with inhibitors alone or in combination with 250 μM 8-Br-cAMP. Cells were treated with inhibitors H-89 (PKA), K-7174 (GATA2), LDN-193189 (SMAD9), U0126 (JUNB), SB203580 (p38/MAPK), ESI-09 (Epac), and stimulator 8-pCPT-2'-O-Me-cAMP (Epac). *LGALS1* was significantly upregulated during trophoblastic differentiation. Inhibition of JUNB with U0126 treatment led to a significant increase in *LGALS1* expression during differentiation while inhibition of Epac led to a non-significant increasing trend. Black bars indicate untreated cells. Grey bars indicate cells treated with 8-Br-cAMP. Values are presented as mean ± SD for control cells (n=15) and for cells treated with inhibitors (n=3). Different letters indicate significant differences.
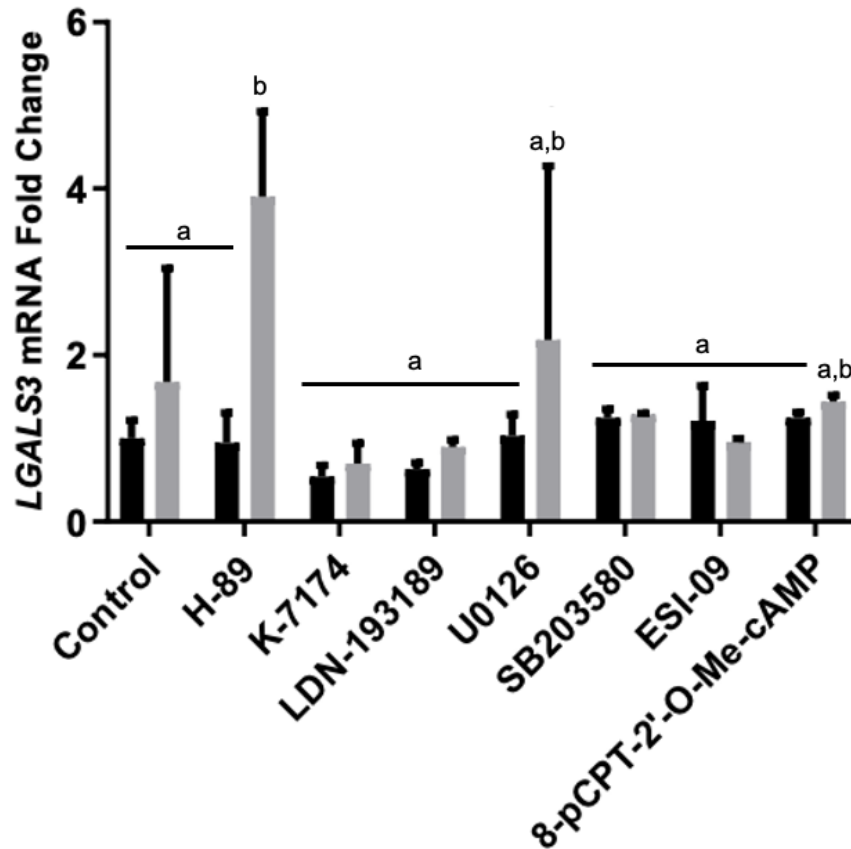
Figure 16. Effects of inhibitors on *LGALS3* expression during trophoblastic differentiation.

JEG-3 cells were cultured in 6-well plates and treated every 12 hours for 36 hours with inhibitors alone or in combination with 250 μM 8-Br-cAMP. Cells were treated with inhibitors H-89 (PKA), K-7174 (GATA2), LDN-193189 (SMAD9), U0126 (JUNB), SB203580 (p38/MAPK), ESI-09 (Epac), and stimulator 8-pCPT-2'-O-Me-cAMP (Epac). *LGALS3* did not significantly change during trophoblastic differentiation. Treatment with H-89 to inhibit PKA led to a significant increase in *LGALS3* while treatment with U0126 to inhibit JUNB resulted in a non-significant increasing trend. Black bars indicate untreated cells. Grey bars indicate cells treated with 8-Br-cAMP. Values are presented as mean ± SD for control cells (n=15) and for cells treated with inhibitors (n=3). Different letters indicate significant differences.
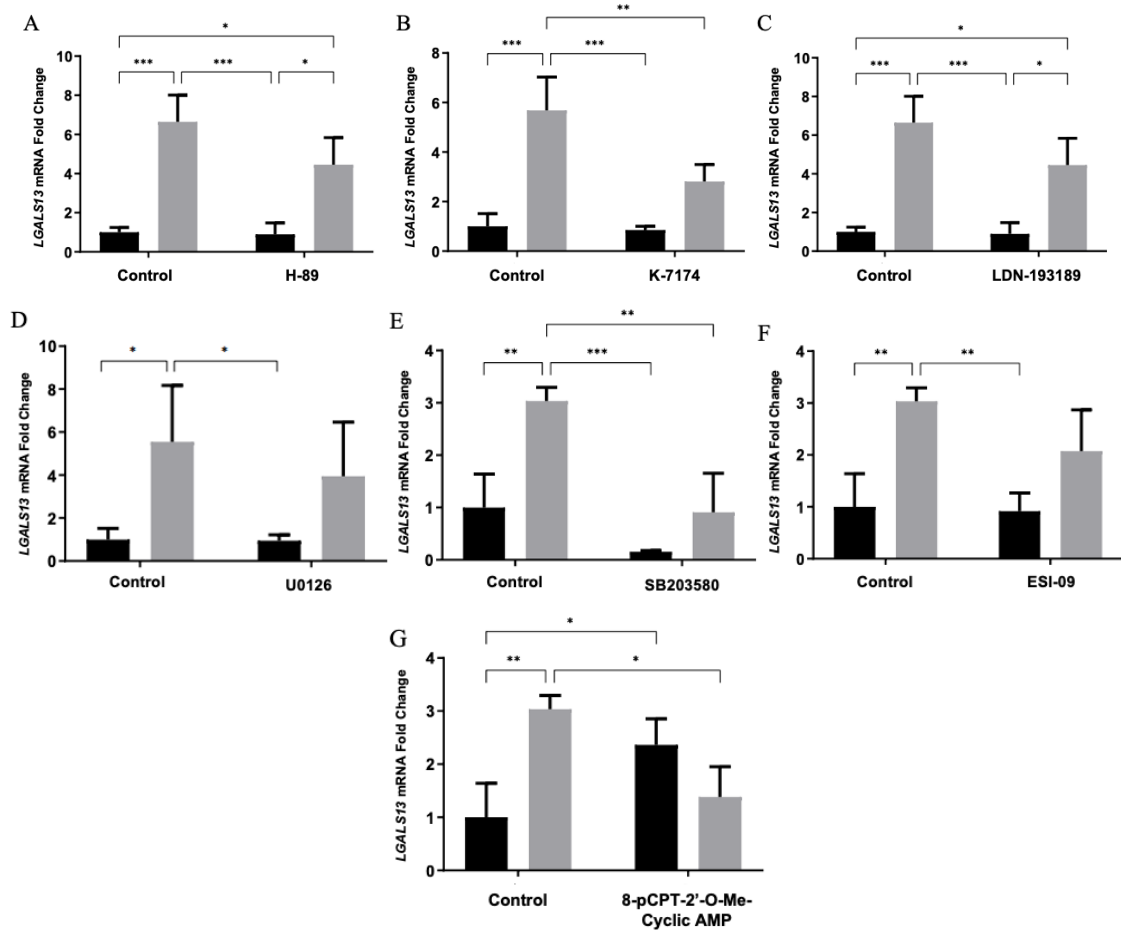
Figure 17. Effects of inhibitors on *LGALS13* expression during trophoblastic differentiation.

JEG-3 cells were cultured in 6-well plates and treated every 12 hours for 36 hours with inhibitors alone or in combination with 250 µM 8-Br-cAMP. Cells were treated with inhibitors (A) H-89 (PKA), (B) K-7174 (GATA2), (C) LDN-193189 (SMAD9), (D) U0126 (JUNB), (E) SB203580 (p38/MAPK), (F) ESI-09 (Epac), and (G) stimulator 8-pCPT-2'-O-Me-cAMP (Epac). Treatment with K-7174, SB203580, 8-pCPT-2'-O-Me-cAMP significantly decreased *LGALS13* expression. Black bars indicate untreated cells. Grey bars indicate cells treated with 8-Br-cAMP. Values are presented as mean ± SD (n=3). Relative transcript levels were quantified by the Livak method ($2^{-\Delta\Delta CT}$) and normalized to the reference gene, *ACTB*. Significance is reported according to ****$P < 0.0001$, ***$P < 0.001$, **$P < 0.01$, *$P < 0.05$.
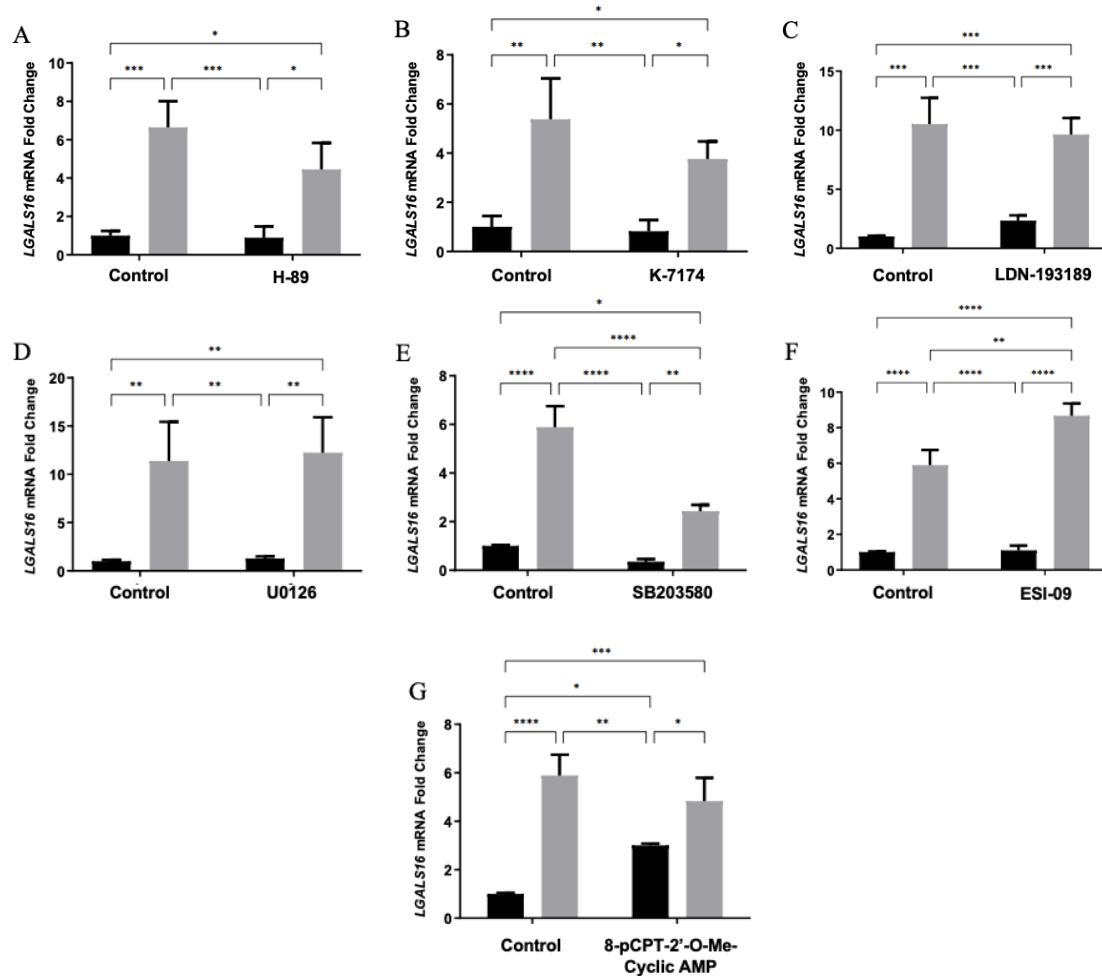
Figure 18. Effects of inhibitors on *LGALS16* expression during trophoblastic differentiation.

JEG-3 cells were cultured in 6-well plates and treated every 12 hours for 36 hours with inhibitors alone or in combination with 250 μM 8-Br-cAMP. Cells were treated with inhibitors (A) H-89 (PKA), (B) K-7174 (GATA2), (C) LDN-193189 (SMAD9), (D) U0126 (JUNB), (E) SB203580 (p38/MAPK), (F) ESI-09 (Epac), and (G) stimulator 8-pCPT-2'-O-Me-cAMP (Epac). Treatment with SB203580 significantly decreased *LGALS16* expression while ESI-09 significantly increased *LGALS16* expression during differentiation. Black bars indicate untreated cells. Grey bars indicate cells treated with 8-Br-cAMP. Values are presented as mean ± SD (n=3). Relative transcript levels were quantified by the Livak method ($2^{-\Delta\Delta CT}$) and normalized to the reference gene, *ACTB*. Significance is reported according to ****$P < 0.0001$, ***$P < 0.001$, **$P < 0.01$, *$P < 0.05$.

expression during differentiation. Additionally, JEG-3 cells treated with Epac inhibitor, ESI-09, displayed a significant increase (P<0.01) and 1.4-fold change in *LGALS16* expression during differentiation.

Untreated JEG-3 cells showed a significant 60-fold increase in *CGB3/5* expression, the biomarker of trophoblastic differentiation, when treated with 8-Br-cAMP to induce differentiation as expected (P<0.05, P<0.01, P<0.001) (**Figures 19A-G**). Treatment with H-89 showed a slight increase (P=0.6852) between control cells treated with 8-Br-cAMP and cells treated with both the inhibitor and 8-Br-cAMP while GATA2 inhibitor, K-7174, and p38/MAPK inhibitor, SB203580, demonstrated a decreasing trend (P=0.8174, P=0.2098). However, none of these changes were significant. Epac inhibitor, ESI-09, and stimulator, 8-pCPT-2'-O-Me-cAMP, displayed no changes in *CGB3/5* expression between cells only treated with 8-Br-cAMP and those treated with 8-Br-cAMP and inhibitor/stimulator. In contrast, the expression of *CGB3/5* was significantly decreased by LDN-19189 (1.5-fold, P<0.05) and U0126 (6-fold, P<0.01) which inhibit SMAD9 and U0126, respectively.

Correlation analysis reveals that *LGALS13*, *LGALS16*, and *CGB3/5* demonstrate significant positive correlations in their expression, which suggests common mechanisms in their regulation (**Figures 20A-C**).

Overall, *LGALS13*, *LGALS16*, and *CGB3/5* expression are significantly positively correlated. *LGALS13* and *LGALS16* are regulated in a similar manner that is different from *LGALS1* and *LGALS3* which supports the hypothesis. However, *LGALS13* and *LGALS16* appear to be regulated by different upstream molecules from *CGB3/5*. *LGALS16* expression during trophoblastic differentiation was only altered when cells were treated with inhibitors of p38/MAPK and Epac suggesting they may be key regulators of *LGALS16* expression.

Figure 19. Effects of inhibitors on *CGB3/5* expression during trophoblastic differentiation.

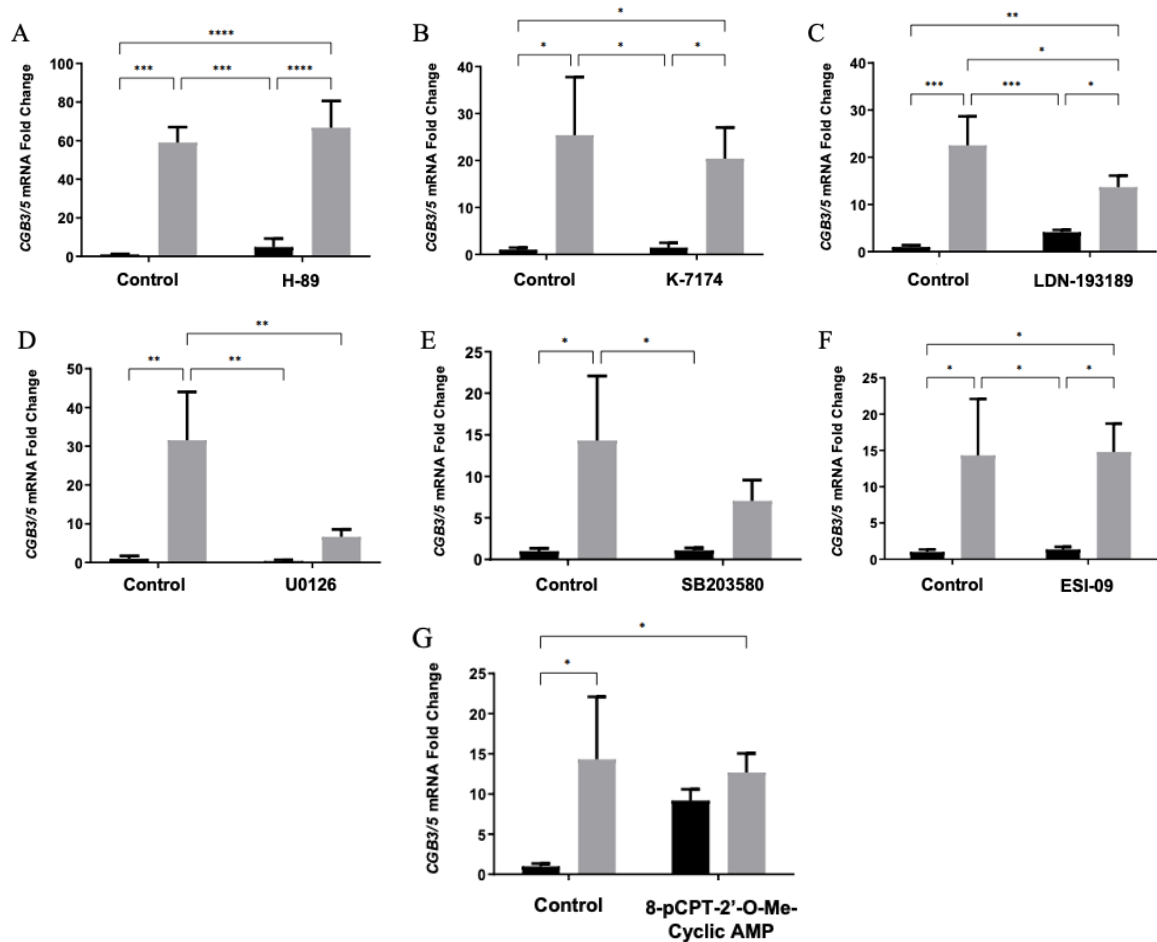JEG-3 cells were cultured in 6-well plates and treated every 12 hours for 36 hours with inhibitors alone or in combination with 250 μM 8-Br-cAMP. Cells were treated with inhibitors (A) H-89 (PKA), (B) K-7174 (GATA2), (C) LDN-193189 (SMAD9), (D) U0126 (JUNB), (E) SB203580 (p38/MAPK), (F) ESI-09 (Epac), and (G) stimulator 8-pCPT-2'-O-Me-cAMP (Epac). *CGB3/5* was significantly upregulated during trophoblast differentiation. Treatment with LDN-193189 and U0126 led to a significant downregulation of *CGB3/5* expression. Black bars indicate untreated cells. Grey bars indicate cells treated with 8-Br-cAMP. Values are presented as mean ± SD (n=3). Relative transcript levels were quantified by the Livak method ($2^{-\Delta\Delta CT}$) and normalized to the reference gene, *ACTB*. Significance is reported according to ****$P < 0.0001$, ***$P < 0.001$, **$P < 0.01$, *$P < 0.05$.

A $R^2 = 0.6117$ $p < 0.001$

B $R^2 = 0.1905$ $p < 0.001$

C $R^2 = 0.4927$ $p < 0.01$
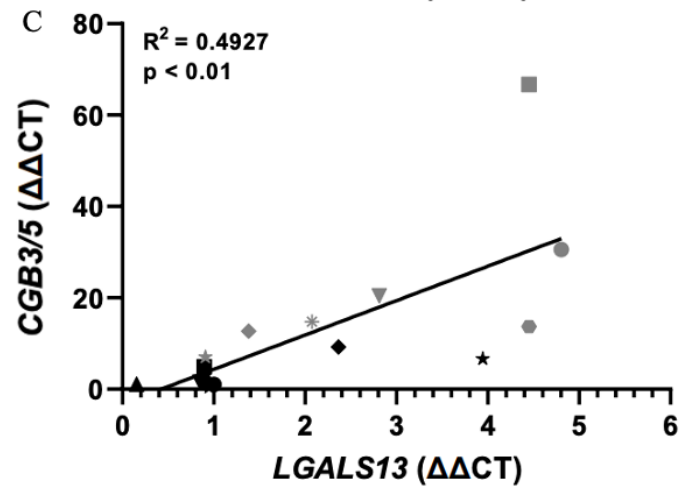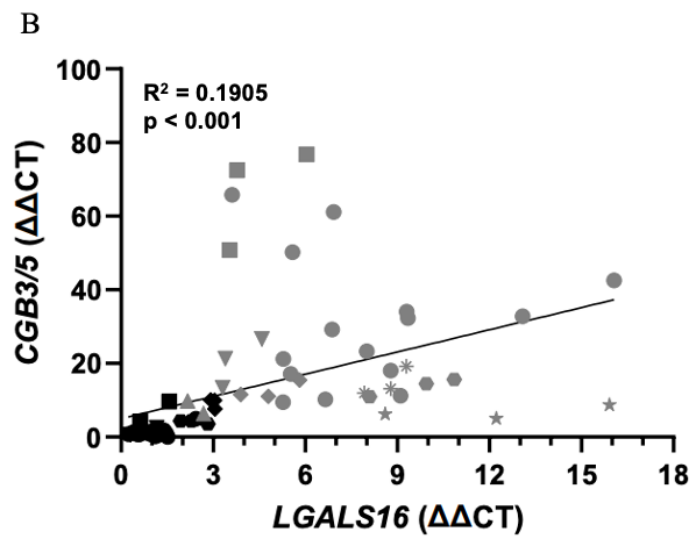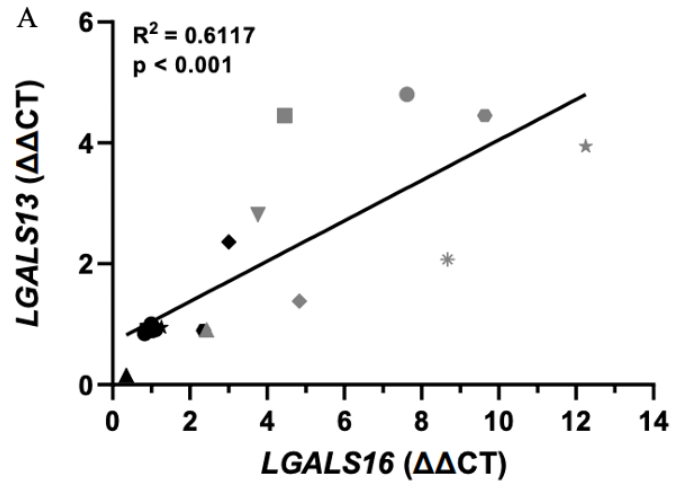
Figure 20. Correlations in gene expression between *LGALS13*, *LGALS16*, and the biomarker of trophoblastic differentiation, *CGB3/5*.

The relative expression of *LGALS13*, *LGALS16*, and *CGB3/5* in JEG-3 cells (●) untreated or treated with (■) H-89 (PKA), (▼) K-7174 (GATA2), (●) LDN-193189 (SMAD9), (★) U0126 (JUNB), (▲) SB203580 (p38/MAPK), (∗) ESI-09 (Epac), and (♦) stimulator 8-pCPT-2'-O-Me-cAMP (Epac). The correlations between (A) *LGALS13* and *LGALS16* (n=30), (B) *CGB3/5* and *LGALS16* (n=144), and (C) *CGB3/5* and *LGALS13* (n=30). Cells treated with inhibitor alone are shaded in black and cells treated with inhibitor in addition to 250 μM of 8-Br-cAMP are shaded in grey. A significant correlation was seen between *LGALS13* and *LGALS16*, *LGALS16* and *CGB3/5*, and *LGALS13* and *CGB3/5*. Relative transcript levels were quantified by the Livak method ($2^{-\Delta\Delta CT}$) and normalized to the reference gene, *ACTB*. Pearson's correlation test was used to determine the correlation between gene expression with a statistical threshold of $P < 0.05$ (n=3).

3.3.2 Galectin expression profile and *O*-GlcNAc homeostasis during trophoblastic differentiation in BeWo cells

An additional mechanism which may regulate galectins during differentiation is *O*-GlcNAcylation. I investigated whether *O*-GlcNAcylation plays a role in regulating *LGALS16* expression during trophoblastic differentiation. To do so, I first quantified changes in *O*-GlcNAcylation and the galectin expression profile of BeWo cells during 8-Br-cAMP-induced trophoblastic differentiation.

qRT-PCR was used to detect the mRNA expression levels of *LGALS1, LGALS3, LGALS8, LGALS9, LGALS12*, *LGALS13*, and *LGALS16* using cDNA from BeWo cells treated with 250 μM of 8-Br-cAMP for 0, 24, or 48 hours (**Figures 21A-H**). Significant upregulation of *LGALS1* (7-fold, P<0.01), *LGALS12* (26-fold, P<0.05), *LGALS13* (17-fold, P<0.01), and *LGALS16* (27-fold, P<0.01) expression was detected during differentiation between control cells and cells treated with 8-Br-cAMP for 48 hours. No significant changes were observed in *LGALS1* and *LGALS12* expression between the control and 24 hour treated cells. *LGALS13* and *LGALS16* expression was significantly increased (P<0.05) between cells treated for 24 hours and those treated for 48 hours indicating a time-dependent increase for both genes. *LGALS3* and *LGALS9* showed slight decreases but the changes were not significant (P=0.2947 and P=0.6885). *LGALS8* showed slight increases in gene expression between control and 24 hrs which remained consistent at 48 hrs but the changes were not significant (P=0.1968) between any time points. Additionally, intracellular galectin-1 and galectin-3 protein levels did not change significantly during differentiation (**Figure S1**).

An immunodot blot was conducted to measure the level of *O*-GlcNAcylated proteins of cells treated with 8-Br-cAMP at 0, 24, and 48 hours (**Figures 22A & B**). Quantification of the blot using ImageLab (Bio-Rad) showed no significant changes in *O*-GlcNAcylation during differentiation at 24 or 48 hrs (P=0.9919, P=0.9847). Of interest, JEG-3 cells also did not show a significant change in *O*-GlcNAc homeostasis during trophoblastic differentiation (**Figure S2**). It was also noted that JEG-3 cells showed a significantly lower basal level of *O*-GlcNAcylation than BeWo cells (**Figure S3**).
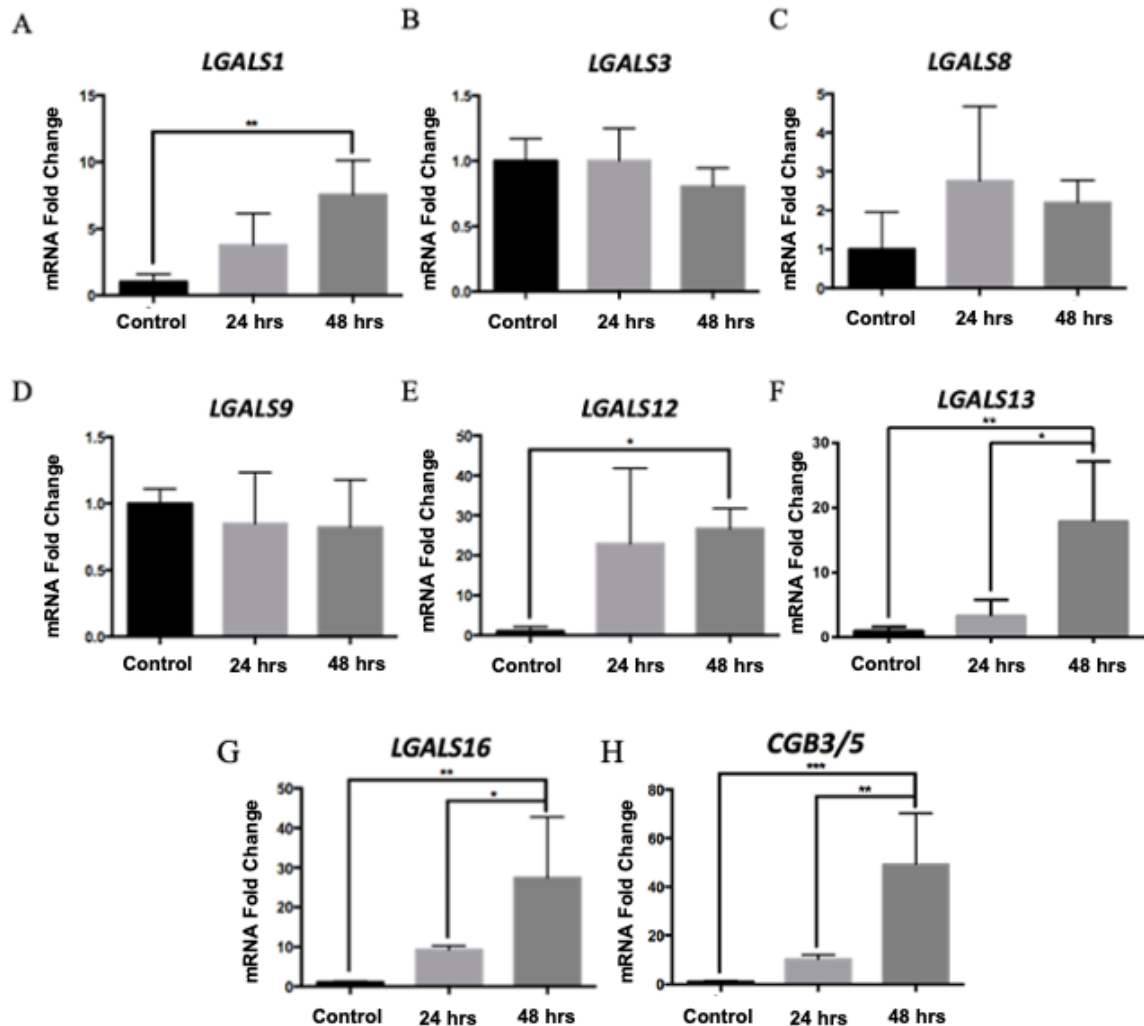
Figure 21. Galectin expression profiles of undifferentiated and differentiated BeWo placental cells.

Using RT-qPCR, relative expression levels of all galectins were determined and quantified using the 2-ΔΔCT method and normalized to housekeeping gene, *ACTB*. (A) *LGALS1*, (B) *LGALS3*, (C) *LGALS8*, (D) *LGALS9*, (E) *LGALS12*, (F) *LGALS13*, (G) *LGALS16* and (H) *CGB3/5*. Differentiation induces the expression of *LGALS1*, *LGALS12*, *LGALS13*, *LGALS16*, and *CGB3/5*. Values are presented as mean ± SD (n=4). All statistical analysis was performed using one-way ANOVA followed by Tukey's multiple comparisons test (using Prism 9.3.1). Significant differences are indicated by ****$P < 0.0001$, ***$P < 0.001$, **$P < 0.01$, *$P < 0.05$.
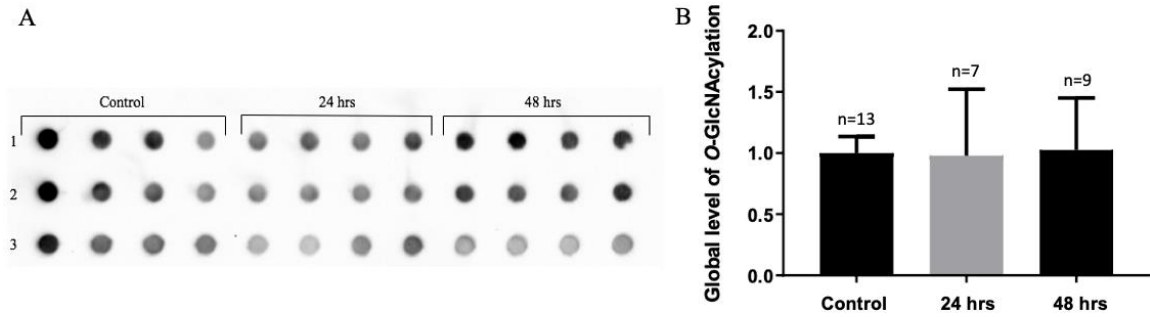
Figure 22. BeWo cells undergoing trophoblastic differentiation show no change in the global level of *O*-GlcNAcylated proteins.

Immunodot blot analysis of protein lysates from (A) BeWo cells treated with 250 μM 8-Br-cAMP for 0, 24, or 48 hours. (B) Quantification of the global level of *O*-GlcNAcylation based on densitometry analysis using ImageLab software (Bio-Rad) reveals no change in *O*-GlcNAcylation during differentiation. Values are presented as mean ± SD.

The significant increase in *CGB3/5* during 8-Br-cAMP treatment confirms differentiation of BeWo cells. These results indicate that the global level of *O*-GlcNAcylation does not change during differentiation while the expression of *LGALS1*, *LGALS12*, *LGALS13*, and *LGALS16* are significantly increased during differentiation. I next wanted to confirm whether these changes in galectin expression are dependent on *O*-GlcNAc homeostasis.

3.3.3 Expression of galectins genes and *CGB3/5* did not change in BeWo cells treated with OGA/OGT inhibitors

O-GlcNAcylation levels in BeWo cells were altered using AC, an OGT inhibitor, and TG, an OGA inhibitor, to reduce and stimulate *O*-GlcNAcylation, respectively. Galectin expression profiling was then completed to assess whether *O*-GlcNAc homeostasis affects galectin gene expression.

An immunodot blot assay was performed for cells treated with 25 μM AC or 10 μM TG (**Figures 23A & B**). This was done as a control to confirm that the OGA inhibitor promoted *O*-GlcNAcylation and the OGT inhibitor diminished global levels of *O*-GlcNAcylated proteins. Following densitometry analysis using ImageLab (Bio-Rad) and a one-way ANOVA analysis as well as Tukey test, there was a significant 2-fold increase (P<0.0001) in *O*-GlcNAcylation between control cells and TG treated cells. A significant 2-fold increase (P<0.0001) was also seen between TG treated cells and AC treated cells. However, no significant change (P=0.9901) was seen in control cells compared to AC treated cells.

Transcript gene expression levels were measured for cells treated with 25 μM AC or 10 μM TG for 24 hrs relative to untreated cells. qRT-PCR for *LGALS1, LGALS3, LGALS8, LGALS9, LGALS12*, *LGALS13*, and *LGALS16* showed no significant changes between any of the time points for any of the galectin genes tested and specifically for cells treated with TG (P=0.4732, 0.3192, 0.4979, 0.5415, 0.5834, 0.2986, and 0.4881) (**Figures 24A-F**). However, there was a slight downward trend for the expression of *LGALS3*, *LGALS8*, and *LGALS12* and a slight upward trend for *LGALS13* expression. Similarly, galectin-1 and galectin-3 levels were not altered with OGA or OGT treatment (**Figure S1**).
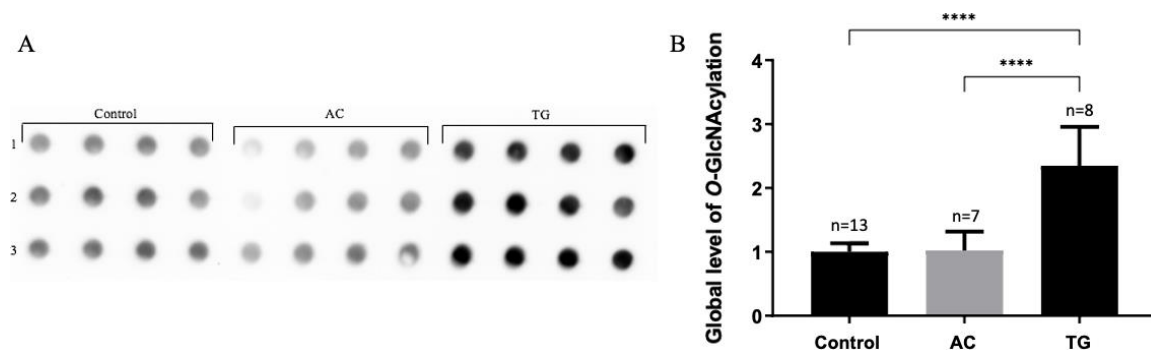
Figure 23. Global *O*-GlcNAcylation level in BeWo cells treated with AC, an OGT inhibitor, and TG, an OGA inhibitor.

Immunodot blot analysis of protein lysates from (A) BeWo cells treated with cell media, AC, or TG for 24 hours. Quantification of the global level of *O*-GlcNAcylation based on densitometry analysis using ImageLab software (Bio-Rad) reveals (B) an increase in *O*-GlcNAcylation in cells treated with TG and no change in cells treated with AC. Values are presented as mean ± SD. All statistical analysis was performed using PRISM 9.3.1 software (one-way ANOVA followed by Tukey's multiple comparisons test). Significance is reported according to ****$P < 0.0001$.
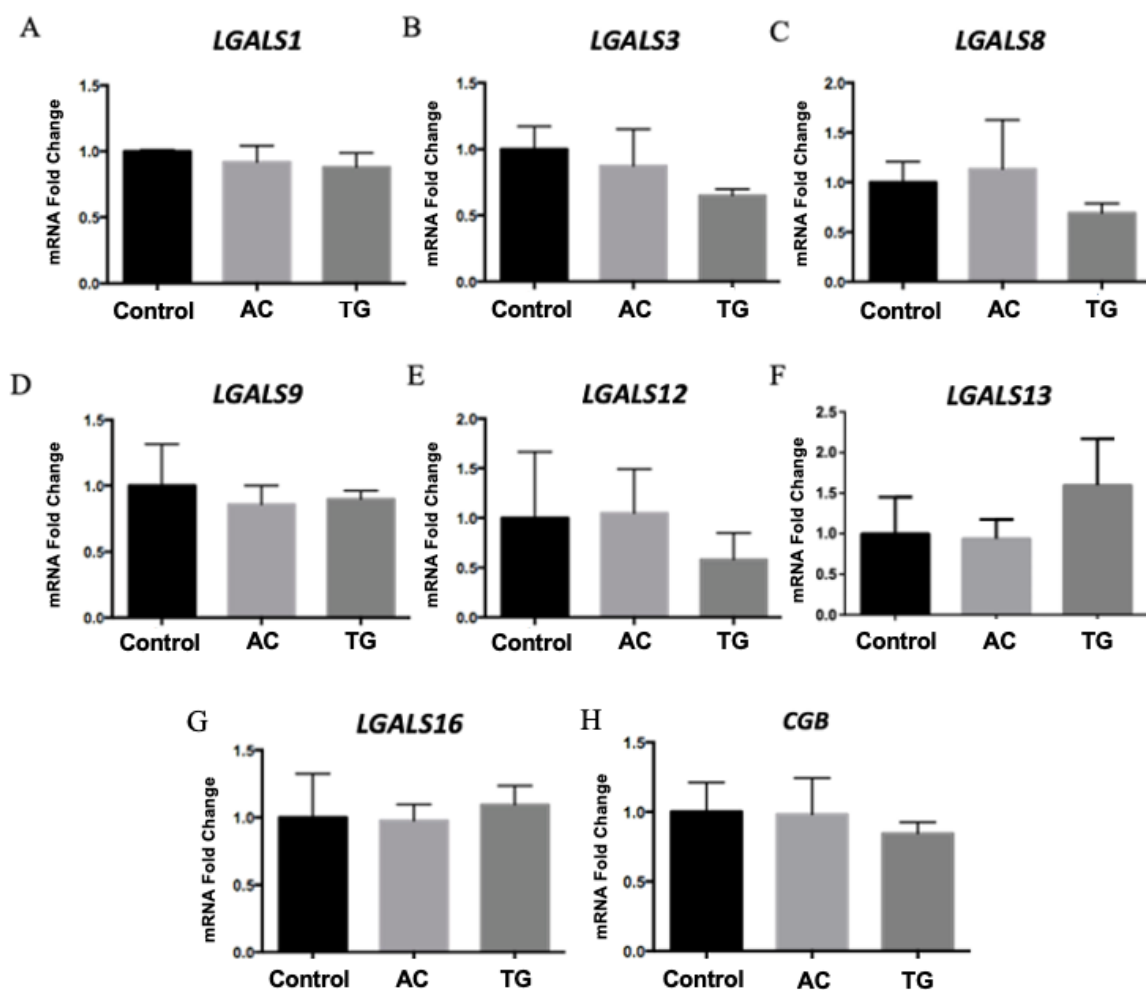
Figure 24. RT-qPCR analysis of galectin and *CGB3/5* mRNA expression in response to *O*-GlcNAc inhibitors.

Relative expression levels of BeWo placental cells treated with 25 mM AC, or 10 mM TG for 24 hours relative to untreated cells were quantified using the Livak method ($2^{-\Delta\Delta CT}$) and normalized to *ACTB* as a reference gene. (A) *LGALS1*, (B) *LGALS3*, (C) *LGALS8*, (D) *LGALS9*, (E) *LGALS12*, (F) *LGALS13*, (G) *LGALS16*, (H) *CGB3/5*. Values are presented as mean ± SD (n=3). No significant differences among treatments were detected.

mRNA levels of *CGB3/5* were tested in cells treated with *O*-GlcNAcylation enzyme inhibitors to determine whether the level of *O*-GlcNAcylation promotes the expression of *CGB3/5*, a biomarker of differentiation. qRT-PCR was used to test the transcript level of *CGB3/5* in cells treated with 25 μM AC or 10 μM TG for 24 hrs relative to untreated cells. No significant changes were observed in cells with OGA or OGT inhibitors.

These results do not support the hypothesis as *O*-GlcNAcylation appears to have no effect on *LGALS16* expression or trophoblastic differentiation of BeWo cells. Thus, other mechanisms such as p38/MAPK and Epac pathways, should be further investigated as regulatory molecules of *LGALS16*.

3.3.4   *LGALS16* knockout cell pools and their functional properties

After testing signaling mechanisms of *LGALS16* expression, I wanted to examine the functional role of galectin-16 during trophoblastic differentiation. For this analysis, a *LGALS16* knockout pool of JEG-3 cells was generated and obtained from Synthego (Menlo Park, CA). This pool contained a heterogenous mix of wildtype cells and cells with various mutations. Thus, the knockout pool needed to be diluted to create a pure genetically identical clonal population. Due to unavailable antibodies, I verified this clonal population only at the transcript level.

A limiting dilution and clonal expansion of 0.5 cells per well and 1 cell per well of JEG-3 *LGALS16* CRISPR/Cas9 knockout cell pools from Synthego was performed. Sanger sequencing was performed for 32 clonal pools. After analyzing sequencing results, 5 clonal pools were selected based on those which had the greatest proportion of mutated cells and least amount of wildtype cells (**Figure S4**). Additionally, the original knockout pool from Synthego with 50% of cells containing a knockout was included for comparison. Sequencing of clonal pool #31 using the Synthego ICE tool revealed an insertion of 1 nucleotide in 57% of the cell population (**Figure 25A**) with a model fit of 0.73 indicating that 73% of the sequences submitted were able to be read. Indels with a percentage of 5% or lower were ignored as the ICE tool is unable to differentiate these from background signals, therefore this additional 1% from a 19-nucleotide insertion was ignored. The

A

Status	Guide Target	PAM Sequence	Indel %	Model Fit (R^2)	Knockout-Score
✅ Succeeded	TTTCTACACTGAGATGAATG	AGG	58	0.73	58

POWERED BY ▸SYNTHEGO | ICE

RELATIVE CONTRIBUTION OF EACH SEQUENCE (NORMALIZED)

INDEL	CONTRIBUTION ▾	SEQUENCE
+1	57%	CAGGTGGATTTCTACACTGAGATGA⋮NATGAGGACTCAGAAATTGCCTTCCATTTGCGAGTGCACTTAGGCCGTCG
+ 0	15%	CAGGTGGATTTCTACACTGAGATGA⋮ATGAGGACTCAGAAATTGCCTTCCATTTGCGAGTGCACTTAGGCCGTCGT
+19	1%	CAGGTGGATTTCTACACTGAGATGA⋮NNNNNNNNNNNNNNNNNNNNNNNATGAGGACTCAGAAATTGCCTTCCATTTGCG

B

142 caacgaaccacagctgcaggtggatttctacactgagatgaatgaggactcag
    ||||||||||||||||||||||||||||||||||||||||||||||||||||||
    CAACGAACCACAGCTGCAGGTGGATTTCTACACTGAGATGAATGAGGACTCAG

195 aaattgccttccatttgcgagtgcacttaggccgtcgtgtggtcatgaacagtcg
    |||||||||||| |||||||||||||||||||||||||||||||||||||||||
    AAATTGCCTTCCA**N**TTTGCGAGTGCACTTAGGCCGTCGTGTGGTCATGAACAGTC

250 tgagtttgggatatggatgttggaggagaatttacactatgtgccctttgaggat
    |||
    <u>TGA</u>

305 ggcaaaccatttgacttgcgcatctacgtgtgtcacaatgagtatgag

C

INEPQLQVDFYTEMNEDSEIAFHLRVHLGRRVVMNSREFGIWMLEENLHYVPFEDGKP
||||||||||||||||||||||||
INEPQLQVDFYTEMNEDSEIAFQFASALRPSCGHEQS

FDLRIYVCHNEYEVKVNGEYIYAFVHRIPPSYVKMIQVWRDVSLDSVLVNNGRR

Figure 25. Confirmation of *LGALS16* knockout clonal pool #31 via Sanger sequencing and RT-qPCR.

A JEG-3 *LGALS16* knockout (KO) cell pool from Synthego was diluted to 0.5 cells or 1 cells per well and grown to 80% confluency in 96-well plates. Genomic DNA was extracted, PCR amplified, purified, and sequenced at Robarts Research Institute (London, ON, Canada). (A) Sanger sequencing results of clonal pool #31 were analyzed using the Synthego ICE tool demonstrating a *LGALS16* KO clonal pool with 57% containing an insertion of 1 nucleotide and 15% containing wildtype (WT) cells. A model fit of 0.7 or higher indicated high quality sequencing. Mutants less than 5% can be attributed to background noise and consequently ignored. (B) The mRNA sequence for exon 3 of the WT (lowercase) was compared with that of the knockout mRNA sequence (uppercase). Highlighted in black is the insertion of a nucleotide. This results in a frameshift mutation and a truncated protein that does not produce amino acids for exon 4. The nucleotides underlined indicate the premature stop codon. (C) The translated sequence for exon 3 of the WT was compared with that of the KO mRNA sequence (bolded). The sequence in black is the changed amino acid sequence which is prematurely terminated.

knockout (KO) score of 58 can also be reduced to 57. This score takes into account whether the mutation is a multiple of 3 to report what percentage of mutations are likely to lead to a frameshift mutation. Analysis of the mRNA sequence and translated protein sequence of clonal pool #31 in comparison to that of wildtype cells revealed a shift in the reading frame and a premature stop codon in the third exon (**Figure 25B & C**). qRT-PCR was used to measure *LGALS16* expression of all 4 selected clonal pools and the original KO pool in untreated cells and cells treated with 8-Br-cAMP for 36 hours. Clonal pool #31 significantly suppressed ($P < 0.0001$) the expression of *LGALS16* with an 8-fold change (**Figure 26**). Three of the clonal pools and the original KO pool showed a significant decrease in *LGALS16* expression ($P < 0.0001$) during differentiation while one pool showed a significant increase in *LGALS16* expression ($P < 0.01$) (**Figure S5**). Although a single pure clone was not produced, clonal pool #31 was used as a proxy for further testing.

To assess the functional effects of the JEG-3 *LGALS16* knockout clonal pool #31, I investigated *CGB3/5* expression and CGB protein levels as markers of trophoblastic differentiation. Moreover, I assessed morphological changes of the clonal pool in comparison to wildtype cells.

JEG-3 *LGALS16* KO clonal pool #31 showed a significant decrease ($P < 0.0001$) and a 2.5-fold change in *CGB3/5* expression between WT cells treated with 8-Br-cAMP and *LGALS16* KO cells treated with 8-Br-cAMP (**Figure 27A**). Other clonal pools were additionally tested and showed significant increases ($P < 0.05$, $P < 0.01$, $P < 0.001$) in *CGB3/5* expression while the original KO pool showed no significant change in *CGB3/5* expression but did show an upward trend (**Figure S6**).

To verify the changes in KO clonal pool #31 at the protein level, western blots of JEG-3 WT and clonal pool #31 cells were tested during 8-Br-cAMP-induced differentiation. The KO clonal cell pool #31 showed a decrease of CGB protein levels in comparison with WT cells (**Figure 27B**). However, additional replicates need to be completed for statistical analysis.
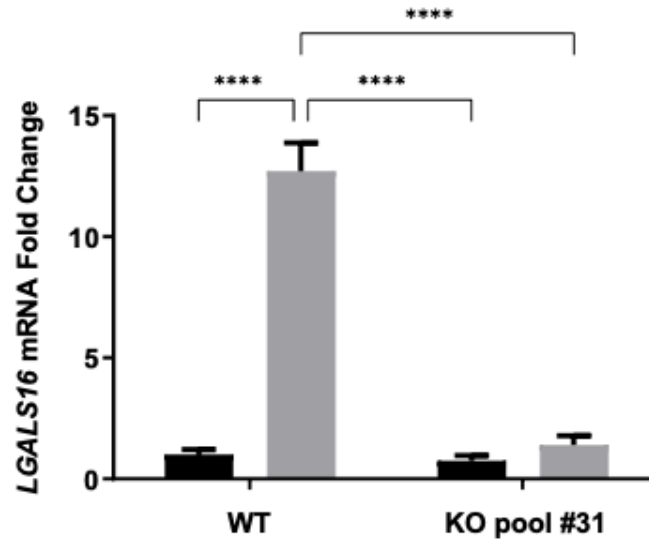
Figure 26. Confirmation of *LGALS16* knockout clonal pool #31 via Sanger sequencing and RT-qPCR.

RT-qPCR of control and *LGALS16* knockout (KO) cell mRNA untreated or treated with 8-Br-cAMP for 36 hours revealed *LGALS16* expression is inhibited under 8-Br-cAMP treatment. *LGALS16* expression was significantly decreased in JEG-3 KO cells. Black and grey columns indicate untreated and 8-Br-cAMP treated cells, respectively. The data were quantified using the Livak method ($2^{-\Delta\Delta CT}$) and normalized to *ACTB* as a reference gene. Values are presented as mean ± SD. All statistical analysis was performed using PRISM 9.3.1 software (one-way ANOVA followed by Tukey's multiple comparisons test). Significance is reported according to ****P<0.0001.
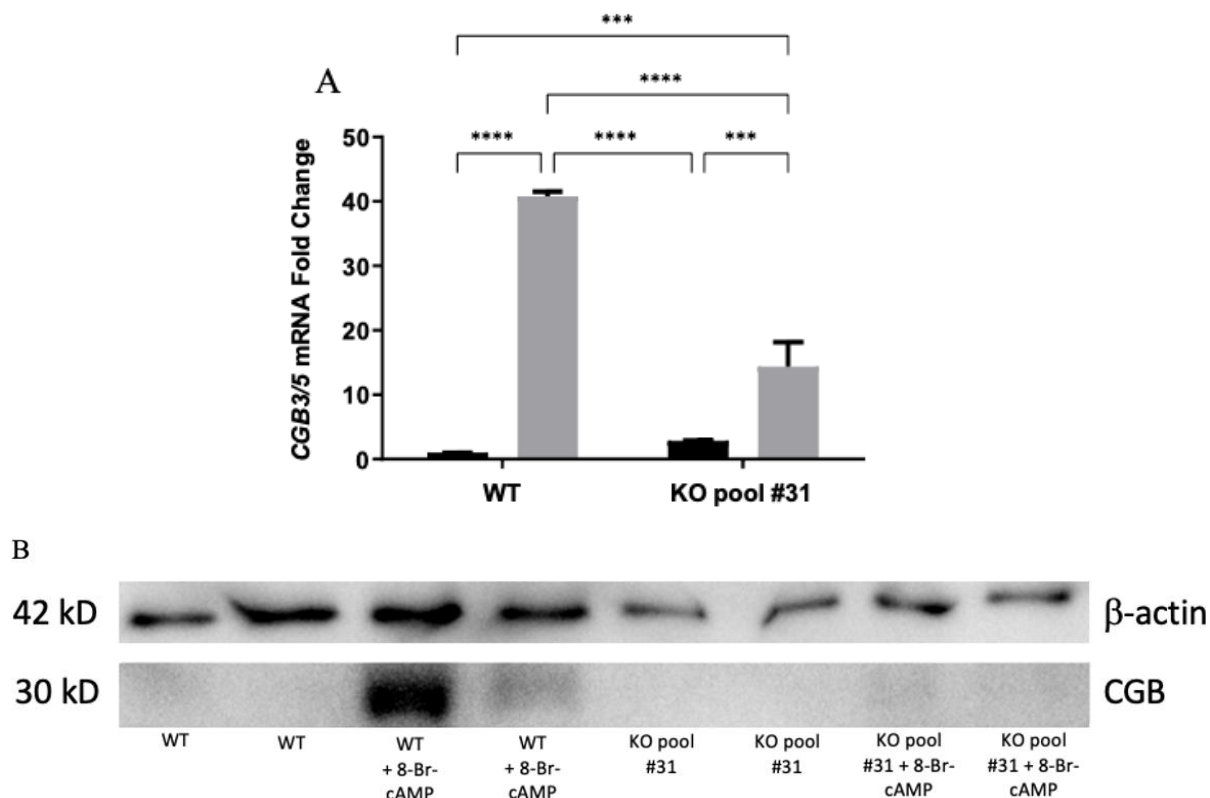
Figure 27. Functional effects of *LGALS16* knockouts on CGB gene and protein expression.

JEG-3 *LGALS16* knockout clonal pool #31 and wildtype cells were grown in 6-well plates and either left untreated or treated with 8-Br-cAMP for 36 hours. (A) RT-qPCR of samples revealed a significant decrease in *CGB3/5* expression in the knockout (KO) clonal pool when treated with 8-Br-cAMP compared to wildtype (WT) cells treated with 8-Br-cAMP. (B & C) Western blots were completed to assess CGB at the protein level. A decrease of CGB protein was observed in the KO pool of cells treated with 8-Br-cAMP compared with wildtype treated cells. However, additional replicates need to be repeated for statistical analysis. Black and grey columns indicate untreated and 8-Br-cAMP treated cells, respectively. Significance is reported according to ****P<0.0001, ***P<0.001.

WT and KO JEG-3 cells from clonal pool #31 were left untreated or treated for 36 hours with 8-Br-cAMP and imaged (**Figure 28A & B**). WT JEG-3 cells display epithelial-like morphology and grow as a confluent monolayer. WT JEG-3 cells treated with 8-Br-cAMP undergo some fusion. JEG-3 KO cells display similar epithelial-like morphology to WT cells at low confluency (0 hours). At high confluency (36 hours), untreated KO cells appear to form clusters. However, both WT and KO cells can grow into a monolayer.

Overall, these results show that the JEG-3 *LGALS16* knockout clonal pool #31 resulted in a significant decrease in *CGB3/5* expression and a decrease in CGB protein levels. Furthermore, some morphological changes are seen between the wildtype and *LGALS16* knockout cell pool. These findings support the hypothesis as knocking out *LGALS16* suppresses trophoblastic differentiation as indicated by CGB expression.
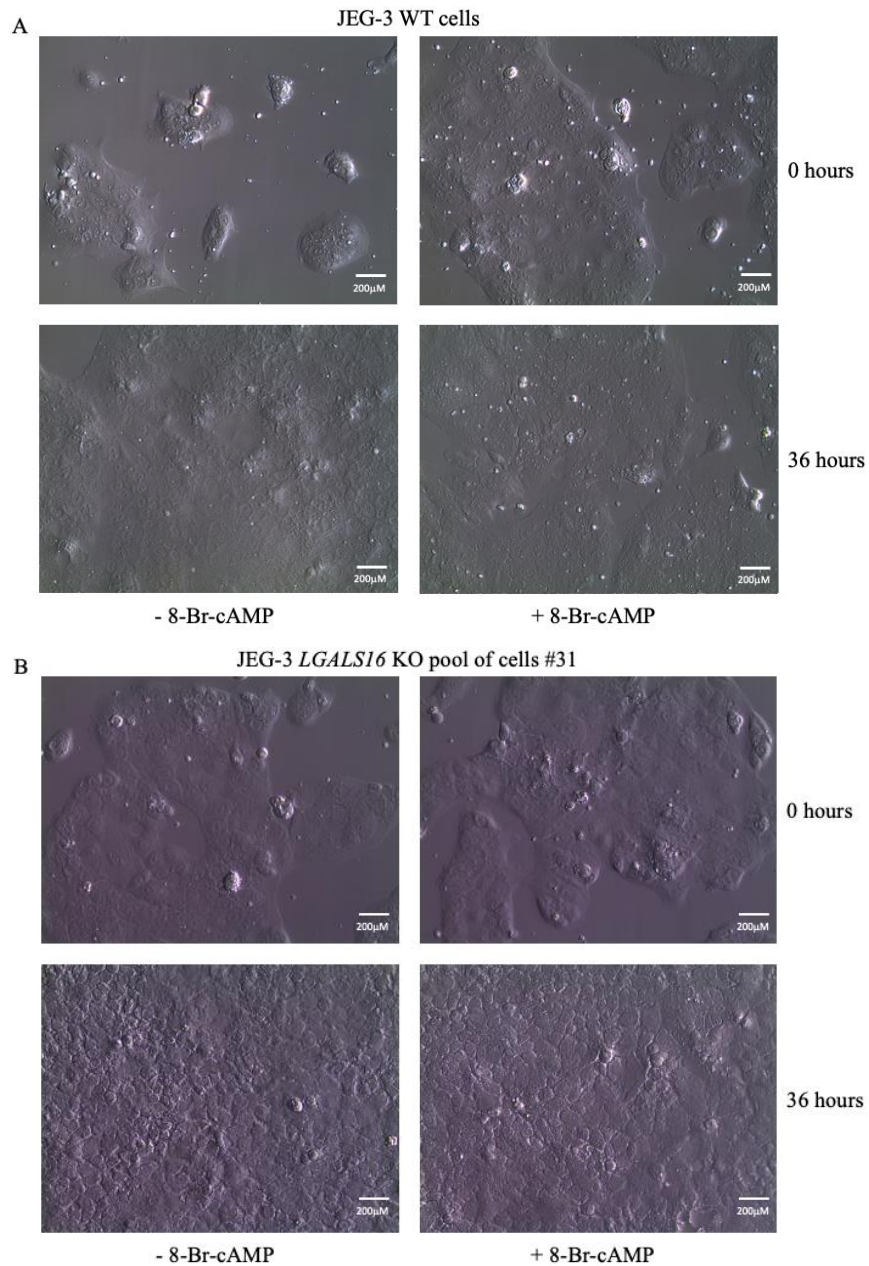
Figure 28. Images of JEG-3 WT and *LGALS16* KO clonal pool #31 cells at 0 hours of cellular differentiation vs. 36 hours of differentiation.

JEG-3 cells have epithelial-like morphology and undergo some fusion during trophoblastic differentiation. (A) Wildtype (WT) and (B) KO cells were left untreated or treated with 250 µM of 8-Br-cAMP for 36 hours. There are morphological differences, however both control and KO cells grow and form a monolayer. All images were taken at 20 × magnification.

3.4 Discussion

Trophoblastic differentiation from cytotrophoblasts to syncytiotrophoblasts is regulated by a variety of pathways including cAMP-dependent signaling pathways. cAMP activates Epac-dependent pathways as well as PKA-dependent pathways responsible for activating p38/MAPK (Gupta et al., 2015). Both lead to an increase in glial cells missing a ultimately triggering cell fusion and differentiation (Gupta et al., 2015). Galectin-16 is significantly upregulated during syncytialization in a cAMP-dependent manner along with a number of transcription factors, such as, JUNB, SMAD9, and ATF3 (Kaminker & Timoshenko, 2021). To investigate the regulation of *LGALS16*, I selected 6 inhibitors and 1 stimulator of transcription factors and signaling molecules in the cAMP pathway. For comparison with tissue-specific *LGALS16*, I included *LGALS1* and *LGALS3* which are widely expressed across different tissues as well as placenta-specific *LGALS13* for analysis.

My findings showed that during trophoblastic differentiation of JEG-3 cells, *LGALS1*, *LGALS13*, *LGALS16*, and *CGB3/5*, a biomarker of syncytialization, were significantly upregulated while *LGALS3* showed a slight non-significant increase. However, *LGALS1* and *LGALS3* were expressed at lower levels compared to *LGALS13* and *LGALS16*. *LGALS1* expression was regulated by JUNB while *LGALS3* was regulated by PKA. A lack of data exists on *LGALS1* in association with JUNB. However, previous literature has shown that galectin-1 protein induces BeWo cell fusion and differentiation through the phosphorylation of MAPK (Hutter et al., 2016). Therefore, although it was not affected by p38/MAPK inhibitor, U0126, it may instead be upstream of the p38/MAPK signaling pathway. Although my study found *LGALS3* to be regulated by PKA during trophoblastic differentiation, a study using human leukemia monocytic cell line, THP-1, showed no change in galectin-3 when cells were exposed to PKA inhibitor, H-89, in addition to phorbol 12-myristate 12-acetate treatment to induce macrophage differentiation (Kim et al., 2003). Collectively these findings suggest that galectin-3 is uniquely regulated during differentiation of different tissue types. Additionally, galectin-1 protein is abundant in syncytiotrophoblast and absent in villous cytotrophoblast (Jovanović Krivokuća et al., 2021). In contrast, galectin-3 is present in cytotrophoblasts which may explain its low level

of expression (Jovanović Krivokuća et al., 2021). Therefore, it would be interesting to see how the inhibitors affect galectin-1 and galectin-3 protein levels and their localization.

LGALS13 and *LGALS16* expression were significantly positively correlated and regulated in a similar manner by p38/MAPK and Epac. This finding aligns with literature as both galectins are evolutionarily related in the placenta-cluster of galectins through gene duplication and the insertion of transposable elements (Than et al., 2014). *LGALS13* was additionally regulated by GATA2 while *LGALS16* was not. It has been predicted that *LGALS16* is less regulated by GATA2 than *LGALS13* and *LGALS14* due to the insertion of a transposable element insertion, L1PA6, between the promoter region of *LGALS16* and GATA2 binding sites (Than et al., 2014). *LGALS13* and *LGALS14* do not have this additional transposable element and therefore, the binding site is closer to their promoter for greater regulation by GATA2 (Than et al., 2014). The decrease observed in *LGALS13* mRNA after treatment with p38 inhibitor, SB203580 has also been found in previous studies (Costa et al., 2016). Collectively, this data suggests that p38/MAPK and Epac are key regulators of *LGALS13* and *LGALS16* during trophoblastic differentiation, but these galectins can also be uniquely regulated. Interestingly, *CGB3/5* expression is significantly positively correlated with *LGALS16* and *LGALS13* expression but is regulated through SMAD9 and JUNB pathways. A study investigating galectin-13 expression in association with CGB found that these two proteins are partially expressed through independent pathways (Orendi et al., 2010). This may explain the separate regulatory pathways of *LGALS16* and *CGB3/5*. However, there may be an additional regulatory molecule signaling *LGALS13*, *LGALS16*, and *CGB3/5* which may account for their more tightly correlated expression. The same study found that *CGB3/5* expression was inhibited by H-89 treatment to inhibit PKA (Orendi et al, 2010). My findings with JEG-3 cells contradict these results. To further test these results, I treated BeWo cells with 10 μM of H-89 inhibitor which was the same concentration used by Orendi et al but *CGB3/5* expression was not affected (**Figure S7**). Moreover, they found that H-89 significantly inhibited *LGALS13* expression during differentiation while my findings did not show a significant change in *LGALS13* or *LGALS16* expression (Orendi et al, 2010). These differences may be explained through the

different differentiator inducers as I used 8-Br-cAMP while the previous paper treated with forskolin to induce cAMP.

Cellular differentiation is associated with changes in *O*-GlcNAcylation levels and galectin expression in a tissue-specific manner (Sherazi et al., 2018; Tazhitdinova & Timoshenko, 2020). Protein glycosylation is a dynamic process responsive to physiological and pathological stimuli and is regulated by the *O*-GlcNAcylation enzymes, OGA/OGT (Laderach et al., 2010; Yang & Qian, 2017). These post-translational modifications result in altered signaling pathways which are decoded by galectins, β-galactoside binding lectins (Laderach et al., 2010). In my study, I investigated the relationship between galectin expression and *O*-GlcNAcylation in a model of cytotrophoblast differentiation into syncytiotrophoblasts. To do so, I analyzed the galectin expression profile of the human placental cell line BeWo and tested the effects of *O*-GlcNAcylation stimulation and inhibition on galectin expression using OGA/OGT inhibitors, TG and AC, respectively.

Galectin expression profiling of BeWo cells during cAMP-induced differentiation revealed a significant upregulation of *LGALS1, LGALS12*, *LGALS13*, and *LGALS16*. This suggests that these four genes may play key roles in trophoblastic differentiation. Increased *LGALS1* expression and low *LGALS3* expression was consistent with what was observed in JEG-3 cells during differentiation. However, a study in which BeWo cells were treated with forskolin led to a significant upregulation of *LGALS3* (Liu et al., 2016). Currently, *LGALS12* has not been identified as showing significant changes or as having a major role in placental formation (Jeschke et al., 2013). However, the results of this study show a significant 26-fold increase in *LGALS12* expression between undifferentiated BeWo cells and those differentiated for 48 hours. Galectin-12 is primarily expressed by peripheral blood leukocytes and adipocytes and functions to block the G1 phase of the cell cycle inhibiting cell proliferation (Jeschke et al., 2013). Further investigation into the role of galectin-12 in trophoblast differentiation is therefore necessary as limited literature exists. Likewise, *LGALS16* in my study showed a 27-fold increase at 48 hrs, revealing a significant upregulation in differentiated trophoblasts. This is consistent to a study that performed RT-qPCR on *LGALS16* in normal pregnant mothers not in labour and found the

placental expression to be 1711.5-fold higher than fetal membrane expression (Than et al., 2009). No changes were seen in intracellular protein levels of galectins-1 and -3 during differentiation. A study showed that galectin-1 secretion does not change when BeWo cells undergo forskolin-induced differentiation while BeWo cells treated with chorionic gonadotropin (hCG) display increased galectin-3 expression and secretion (Yang et al., 2011; Toudic et al., 2019). Thus, it appears that galectin-1 levels do not change while the localization of galectin-3 may require further investigation.

As cells differentiated, the global level of O-GlcNAcylated proteins in BeWo and JEG-3 cells did not change. These findings are consistent with previous literature examining BeWo differentiation into syncytiotrophoblasts (Ruane et al., 2020). In my study, treatment of BeWo cells with AC showed a decreasing trend in the global O-GlcNAcylation level however it was not significant. Treatment with TG on the other hand showed the expected increase in O-GlcNAcyation levels. However, manipulation of O-GlcNAcylation levels using OGA/OGT inhibitors did not change the expression of galectins between undifferentiated and differentiated cells. Moreover, OGA/OGT inhibitors had no effect on the expression of CGB, a marker of differentiation. In a study in which hESCs were treated with AC, gene expression profiling revealed the increased expression of neuronal markers suggesting O-GlcNAcylation inhibition plays a direct role in accelerating neuronal differentiation (Andres et al., 2017). My study did not show changes in galectins that were consistent with those observed in differentiated cells. Prior investigations have found that TG does promote syncytiotrophoblast differentiation of BeWo cells (Ruane et al., 2020). These differing results may be explained as the previous study used *GCM1* and *OVOL1* which are markers of cell fusion, a characteristic found in differentiated syncytiotrophoblasts (Ruane et al., 2020). However, cell fusion has been shown to be partially independent of *CGB* expression (Orendi et al., 2010). Therefore, these genes may be distinctly regulated. Nonetheless, my results suggest that O-GlcNAcylation does not directly regulate galectin gene expression or cellular differentiation and alternative mechanisms are likely involved.

To investigate the functional importance of galectin-16 in trophoblastic differentiation, I generated JEG-3 *LGALS16* KO cells. Due to a lack of availability of galectin-16-specific antibody, the *LGALS16* knockout clonal pool was confirmed with a significant decrease in *LGALS16* expression at the mRNA level. Functional effects of the *LGALS16* KO included the suppression of CGB, the biomarker of differentiation. Additionally, KO cells appeared slightly morphologically different and formed more clusters but retained the ability to form a monolayer. Overall, these findings suggest galectin-16 is required for trophoblastic differentiation.

3.5   Conclusion

This study provides insights into the regulation and functional role of galectin-16. Trophoblastic differentiation induced by cAMP has been shown to lead to a significant increase of *LGALS16* expression. My findings reveal *LGALS16* expression to be mediated by cAMP-dependent signaling molecules, p38/MAPK and Epac. *LGALS1* and *LGALS3* appear to be predominantly regulated by JUNB and PKA, respectively. In contrast, *LGALS13* is regulated in a similar manner to *LGALS16* suggesting these signaling mechanisms are conserved with the placenta-specific galectin gene cluster. Moreover, galectin gene expression, specifically *LGALS16*, does not appear to be controlled by *O*-GlcNAc homeostasis nor does the differentiation of BeWo cells. JEG-3 *LGALS16* KO cells are a novel feature of this study and lead to a significant reduction in CGB expression. This indicates the critical role that galectin-16 serves in trophoblastic differentiation. These studies are only an initial step in elucidating the biological significance of galectin-16. Future studies using pure clones can provide a clearer picture of the regulation and functions of galectin-16. Confirmation of galectin-16 knockout cells with galectin-16-specific antibody is also a necessary verification step. Moreover, additional functional assays should be investigated, such as proliferation and apoptosis, to determine galectin-16's functional role in trophoblastic differentiation and the maternal immune tolerance during pregnancy.

3.6 References

Andres LM, Blong IW, Evans AC, et al. Chemical modulation of protein O-GlcNAcylation via OGT inhibition promotes human neural cell differentiation. ACS Chem Biol. 2017 Aug 18;12(8):2030-2039.

Burnside J, Nagelberg SB, Lippman SS, Weintraub BD. Differential regulation of hCG α and β subunit mRNAs in JEG-3 choriocarcinoma cells by 8-bromo-cAMP. J Biol Chem. 1985 Oct 15;260(23):12705-12709.

Chen Y, Allars M, Pan X, et al. Effects of corticotrophin releasing hormone (CRH) on cell viability and differentiation in the human BeWo choriocarcinoma cell line: a potential syncytialisation inducer distinct from cyclic adenosine monophosphate (cAMP). Reprod Biol Endocrinol. 2013 Apr 15;11:30.

Costa MA, Fonseca BM, Mendes A, Braga J, Teixeira NA, Correia-da-Silva G. The endocannabinoid 2-arachidonoylglycerol dysregulates the synthesis of proteins by the human syncytiotrophoblast. Biochim Biophys Acta. 2016 Mar;1861(3):205-212.

Delidaki M, Gu M, Hein A, Vatish M, Grammatopoulos DK. Interplay of cAMP and MAPK pathways in hCG secretion and fusogenic gene expression in a trophoblast cell line. Mol Cell Endocrinol. 2011 Jan 30;332(1-2):213-220.

Gerbaud P, Taskén K, Pidoux G. Spatiotemporal regulation of cAMP signaling controls the human trophoblast fusion. Front Pharmacol. 2015 Sep 15;6:202.

Gupta SK, Malhotra SS, Malik A, Verma S, Chaudhary P. Cell signaling pathways involved during invasion and syncytialization of trophoblast cells. Am J Reprod Immunol. 2016 Mar;75(3):361-371.

He J, Baum LG. Galectin interactions with extracellular matrix and effects on cellular function. Methods Enzymol. 2006 Nov 26;417:247–256.

Hutter S, Morales-Prieto DM, Andergassen U, et al. Gal-1 silenced trophoblast tumor cells (BeWo) show decreased syncytium formation and different miRNA production compared to non-target silenced BeWo cells. Cell Adh Migr. 2016 Mar 3;10(1-2):28-38.

Johannes L, Jacob R, Leffler H. Galectins at a glance. J Cell Sci. 2018 May 1;131(9):jcs208884.

Kamili NA, Arthur CM, Gerner-Smidt C, et al. Key regulators of galectin-glycan interactions. Proteomics. 2016 Dec;16(24):3111-3125.

Kaminker JD, Timoshenko AV. Expression, regulation, and functions of the galectin-16 gene in human cells and tissues. Biomolecules. 2021 Dec 20;11(12):1909.

Kim G, Cao L, Reece EA, Zhao Z. Impact of protein O-GlcNAcylation on neural tube malformation in diabetic embryopathy. Sci Rep. 2017 Sep 11;7(1):11107.

Kim K, Mayer EP, Nachtigal M. Galectin-3 expression in macrophages is signaled by Ras/MAP kinase pathway and up-regulated by modified lipoproteins. Biochim Biophys Acta. 2003 Jun 17;1641(1):13-23.

Krivokuća M, Vilotić A, Nacka-Aleksić M, et al. Galectins in early pregnancy and pregnancy-associated pathologies. Int J Mol Sci. 2021 Dec 22;23(1):69.

Laderach DJ, Compagno D, Toscano MA, et al. Dissecting the signal transduction pathways triggered by galectin-glycan interactions in physiological and pathological settings. IUBMB Life. 2010 Jan;62(1):1-13.

Liu FT, Patterson RJ, Wang JL. Intracellular functions of galectins. Biochim Biophys Acta. 2002 Sep 19;1572(2-3):263-273.

Liu M, Hassana S, Stiles J. Heme-mediated apoptosis and fusion damage in BeWo trophoblast cells. Sci Rep. 2016 Oct 31;6:36193.

Ning J, Yang H. O-GlcNAcylation in hyperglycemic pregnancies: impact on placental function. Front Endocrinol (Lausanne). 2021 Jun 1;12:659733.

Orendi K, Gauster M, Moser G, Meiri H, Huppertz B. The choriocarcinoma cell line BeWo: syncytial fusion and expression of syncytium-specific proteins. Reproduction. 2010 Nov;140(5):759-766.

Ruane PT, Tan CMJ, Adlam DJ, et al. Protein O-GlcNAcylation promotes trophoblast differentiation at implantation. Cells. 2020 Oct 6;9(10):2246.

Sherazi AA, Jariwala KA, Cybulski AN, Lewis JW, Karagiannis J, Cumming RC, Timoshenko AV. Effects of global O-GlcNAcylation on galectin gene-expression profiles in human cancer cell lines. Anticancer Res. 2018 Dec;38(12):6691–6697.

Si Y, Yao Y, Jaramillo Ayala G, et al. Human galectin-16 has a pseudo ligand binding site and plays a role in regulating c-Rel-mediated lymphocyte activity. Biochim Biophys Acta Gen Subj. 2021 Jan;1865(1):129755.

Tazhitdinova R, Timoshenko AV. The emerging role of galectins and O-GlcNAc homeostasis in processes of cellular differentiation. Cells. 2020 Jul 28;9(8).:1792.

Than NG, Romero R, Goodman M, Weckle A, Xing J, Dong Z, Xu Y, Tarquini F, Szilagyi A, Gal P, et al. A primate subfamily of galectins expressed at the maternal-fetal interface that promote immune cell death. Proc. Natl. Acad. Sci. USA. 2009 Jun 16;106(24):9731–9736.

Than NG, Romero R, Xu Y, Erez O, Xu Z, Bhatti G, Leavitt R, Chung TH. El-Azzamy H, LaJeunesse C, et al. Evolutionary origins of the placental expression of chromosome 19 cluster galectins and their complex dysregulation in preeclampsia. Placenta. 2014 Nov;35(11):855–865.

Toudic C, Vargas A, Xiao Y, et al. Galectin-1 interacts with the human endogenous retroviral envelope protein syncytin-2 and potentiates trophoblast fusion in humans. FASEB J. 2019 Nov;33(11):12873-12887.

Tuladhar R, Yeu Y, Tyler Piazza J, et al. CRISPR-Cas9-based mutagenesis frequently provokes on-target mRNA misregulation. Nat Commun. 2019 Sep 6;10(1):4056.

Vladoiu MC, Labrie M, St-Pierre Y. Intracellular galectins in cancer cells: Potential new targets for therapy (Review). Int J Oncol. 2014 Apr;44(4):1001–1014.

Yang H, Taylor HS, Lei C, Cheng C, Zhang W. Hormonal regulation of galectin 3 in trophoblasts and its effects on endometrium. Reprod Sci. 2011 Nov;18(11):1118-1127.

Yang X, Qian K. Protein O-GlcNAcylation: emerging mechanisms and functions. Nat Rev Mol Cell Biol. 2017 Jul;18(7):452-465.

4   Thesis Summary

Literature on galectin-16 is scarce with most studies focusing on its placenta-specific expression. While the structure of recombinant galectin-16 was recently elucidated, its regulation and function were largely unknown. Using bioinformatic analysis and experimental techniques, I examined the expression, regulation, and functional role of *LGALS16* gene in placental differentiation using BeWo and JEG-3 cell models. In support of my hypothesis, I have found that galectin-16 may play a critical role in placental differentiation from cytotrophoblasts to syncytiotrophoblasts which is guided through cAMP-mediated signaling pathways. Further, my studies provide a deeper understanding of these regulatory mechanisms and the functional consequences of *LGALS16* knockouts.

4.1 *LGALS16* expression is tissue-specific and may be regulated by an intricate system of transcription factors and miRNAs

Bioinformatics analysis of galectin-16 expression using data from the Human Protein Atlas revealed that *LGALS16* is most highly expressed in placental, retina, and brain tissue. Further, the Human Protein Atlas only reported *LGALS16* expression in BeWo and Susa cells, a testicular carcinoma cell line (Uhlén et al, 2015). Extraction of data from Gene Expression Omnibus, reveals *LGALS16* can be detected in a number of other tissues, however, this is at very low levels. These findings demonstrate that galectin-16 is tissue-specific and may have evolved unique, critical roles in the tissues in which it is highly expressed. I also completed an in silico analysis to determine potential regulatory mechanisms of galectin-16, including transcription factors and miRNAs. The program PROMO was used to analyze the 2 kb promoter region of *LGALS16*. This identified 17 predicted transcription factors which may be involved in the regulation of galectin-16. Four programs were used to assess miRNAs which may target galectin-16. Five miRNAs were recognized by all four programs and can be further investigated. Lastly, *LGALS16* is reported to be associated with a variety of diseases, such as Alzheimer's disease, breast cancer, and type 2 diabetes. These findings provide an introduction to the complexity

underlying the regulatory pathways of galectin-16 and downstream effects. Much of this data is predicted and needs to be confirmed and explored experimentally.

4.2 *LGALS16* expression is significantly upregulated during trophoblastic differentiation

Investigations related to my second objective confirmed that both BeWo and JEG-3 cell models undergo trophoblastic differentiation with 8-Br-cAMP treatment as observed with the significant increase in *CGB3/5* expression. RT-qPCR revealed a significant upregulation of *LGALS16* in BeWo cells which is consistent with the literature (Than et al., 2014). My findings demonstrated a significant increase in *LGALS16* expression in a time-dependent manner during trophoblastic differentiation of JEG-3 for the first time. These two placental cell lines (BeWo and JEG-3) share similarities in that they can both be differentiated towards the syncytiotrophoblast with 8-Br-cAMP. However, JEG-3 cells also express markers of extravillous trophoblasts which are responsible for proliferation and migration. The maintenance of high *LGALS16* expression between the two cell lines highlights the importance of this galectin for placental differentiation regardless of trophoblast cell type.

4.3 *LGALS16* expression is regulated by p38 and Epac

As part of my third objective, I examined transcription factor and cAMP receptor inhibitors. Transcription factors in the promoter region were first predicted using the bioinformatic tool, PROMO. A RT2 Profiler PCR array was then used to experimentally quantify the changes in gene expression for 84 transcription factors during differentiation of JEG-3 cells. Signaling molecules in the cAMP pathway were also selected by analyzing the promoter region of *LGALS16* using previous literature. This resulted in the selection of inhibitors for PKA (H-89), GATA2 (K-7174), SMAD9 (LDN-193189), JUNB (U0126), p38/MAPK (SB203580), Epac (ESI-09), and a stimulator of Epac (8-pCPT-2'-O-Me-cAMP). Only p38/MAPK and Epac were found to regulate *LGALS16* expression in JEG-3 cells. Moreover, the expression of placenta-specific galectins, *LGALS13* and *LGALS16* are

regulated in a similar manner and their expression is significantly positively correlated. This is different from *LGALS1* and *LGALS3* which are widely expressed in a variety of tissues and appear to be regulated by JUNB and PKA, respectively. *LGALS16* is not regulated by GATA2 which aligns with prior predictions based on the insertion of an additional transposable element between its promoter region and the GATA2 binding site (Than et al., 2014). Moreover, *LGALS16* and *LGALS13* expression is significantly positively correlated with *CGB3/5* expression which suggests common mechanisms in their regulation. In summary, the regulation of *LGALS16* expression is unique while sharing conserved mechanisms with its placenta-specific galectin cluster.

4.4 *LGALS16* expression is not mediated by *O*-GlcNAc homeostasis

Additional findings from investigations related to my third objective suggest that galectin expression during trophoblastic differentiation may not be directly mediated by *O*-GlcNAcylation. Galectin expression profiling during trophoblastic differentiation using the choriocarcinoma cell line, BeWo, revealed the significant upregulation of *LGALS1, LGALS12, LGALS13*, and *LGALS16*. No change in *LGALS3*, *LGALS8*, and *LGALS9* or protein levels of galectins-1 and -3 was detected. These results for *LGALS1* and *LGALS16* are consistent with previous studies while the changes for *LGALS12* have not been previously identified. This provides further support that these galectins, particularly *LGALS16*, play a critical role in the proper differentiation of cytotrophoblasts that requires further investigation. No changes in global *O*-GlcNAcylation level were seen during differentiation. Moreover, direct manipulation of OGA/OGT did not affect any of the galectin genes tested or galectins-1 and -3 at the protein level. It also did not affect gene expression of *CGB3/5*, the biomarker of differentiation. These results suggest that the expression of galectin genes and proteins in BeWo cells during differentiation is independent of *O*-GlcNAcylation.

4.5   Galectin-16 knockouts suppress CGB expression, the biomarker of trophoblastic differentiation

In regard to my fifth objective, a JEG-3 *LGALS16* knockout clonal pool was generated. Sanger sequencing of the clonal pool identified a single nucleotide insertion in 57% of the cell population that was sequenced. Further analysis showed that this results in a frameshift mutation and premature stop codon. Confirmation of the *LGALS16* knockout was detected with a significant decrease in *LGALS16* mRNA expression. Fifteen percent of the population consisted of wildtype DNA indicating the pool was not a pure clone. RT-qPCR of wildtype and knockout cells that had been treated with 8-Br-cAMP displayed a significant reduction in *CGB3/5* expression. Western blots of protein lysates from wildtype and knockout cells treated with 8-Br-cAMP also showed a decrease in CGB at a protein level. This suggests galectin-16 has a significant role in trophoblastic differentiation.

4.6   Limitations of Study Design and Future Directions

A limitation of my study is that the cell models, BeWo and JEG-3, are placental choriocarcinoma cell lines and therefore possess some differences from primary villous cytotrophoblasts. However, both are well established models and allow us to gain a deeper understanding of placental differentiation. Another model that warrants investigations is brain tissue as it demonstrates a relatively high level of expression of galectin-16. The biological significance of this specificity is unknown and no studies have been completed according to my literature search. However, the unique association of galectin-16 with the placenta-brain-axis of cell development might be a new intriguing mechanism in the context of developmental biology.

In addition, the biochemical inhibitors for investigations of transcriptional regulation may produce off-target effects. Nonetheless, these inhibitors can reveal initial insights into underlying signaling pathways. These can be examined further using silencing RNAs to provide increased accuracy in targeting specific transcription factors for inhibition.

Even though *O*-GlcNAcylation was not found to directly affect galectin gene expression of BeWo cells in this study, the galectin protein levels of all galectins included in this study should be tested. Moreover, ELISA kits can be used to assess the extracellular levels of galectins. *O*-GlcNAcylation can regulate protein trafficking between the intracellular and extracellular environments in addition to mRNA expression (Sherazi et al., 2018;). Therefore, it is possible that rather than affecting galectin gene expression, *O*-GlcNAcylation may affect galectin localization. Investigating the intracellular/extracellular distribution of galectin proteins during cytotrophoblast differentiation and with OGA/OGT inhibitors remains to be tested in future studies.

Limitations of the CRISPR/Cas9 system includes the use of a clonal pool rather than an individual clone and the lack of a primary antibody targeting galectin-16. A primary antibody from Abcam with cross reactivity for galectins-13/16 was tested. However, the resultant bands appeared weak and differentiating between the two galectins on the western blots was not possible. Despite these limitations, the clonal pool showed a significant decrease in *LGALS16* expression at the gene level which suggested it could serve as a proxy for a pure knockout. A vital step for future studies is to isolate a single clone and to verify the galectin-16 knockout at the protein level through designing and optimizing a primary antibody. This will increase the robustness of the data collected as the findings can be solely attributed to the *LGALS16* knockout as opposed to variations in knockout cell pools. Moreover, repeating the western blot should be completed. Although the bands decrease in the protein lysates of the *LGALS16* knockout clonal pool treated with 8-Br-cAMP, there is a great deal of variation. This experiment should be repeated to obtain enough samples for statistics to determine whether CGB protein levels in the knockouts significantly decrease similar to changes at the mRNA level. In the future, additional functional assays should be investigated, specifically proliferation and apoptotic assays. If galectin-16 is essential for trophoblastic differentiation, JEG-3 *LGALS16* knockouts should show increased cell proliferation as their ability to differentiate will be inhibited compared to wildtype cells which will differentiate leading to a slower growth rate. Additionally, galectin-16 is suggested to be involved in T-cell apoptosis to mediate the maternal immune response at the maternal-fetal interface (Si et al., 2021). Therefore, I would expect to see a

decrease in apoptosis if galectin-16 is knocked out. Understanding the functional consequences of *LGALS16* knockouts in terms of differentiation, cell proliferation, and apoptosis remains critical to obtaining a holistic view of the role of galectin-16 during placental differentiation.

4.7   Significance and Practical Applications

Pregnancy complications, such as preeclampsia and fetal growth restriction, are associated with improper placental development and altered levels of biomarkers. Screening for these biomarkers can allow for the prediction and diagnosis of pregnancy disorders prior to the onset of complications. Current biomarkers used include angiogenic factors, such as placental growth factor and soluble fms-like tyrosine kinase 1 (Stepan et al., 2020). This information can be applied clinically to prevent certain diseases. For example, women at high risk for preeclampsia can be administered prophylaxis with aspirin (MacDonald et al., 2022).

Galectin-13 is expressed in differentiated syncytiotrophoblasts and serves as a biomarker of preeclampsia. Previous literature has demonstrated that low levels of galectin-13 in the first trimester and mutations leading to lower *LGALS13* expression are associated with increased risk for preeclampsia (Than et al., 2014; Sammar et al., 2019). A proposed therapeutic method is to provide galectin-13 as a drug to replenish levels for individuals with galectin-13 polymorphisms (Sammar et al., 2019). My study clearly shows that galectins-13 and -16 are significantly upregulated during trophoblastic differentiation via cAMP-dependent molecules, p38/MAPK and Epac. Moreover, *LGALS16* knockout cells repress CGB expression, a biomarker of differentiation. The importance of galectin-16 for proper differentiation highlights its role as a novel genetic biomarker of placental differentiation. While studies have shown *LGALS16* expression is not associated with preeclampsia, the relationship with galectin-16 protein levels is unknown (Than et al., 2014). Additionally, altered levels of galectin-16 may serve as a biomarker for early diagnosis of pregnancy disorders other than preeclampsia to allow for preventative

treatment. Furthermore, galectin-16 may be useful for clinical applications as a therapeutic target and may be introduced exogenously.

4.8   Concluding remarks

In conclusion, these analyses deepen our understanding of the expression, regulation, and vital function of galectin-16 in placental differentiation. Importantly, these studies have illustrated some of the signaling mechanisms regulating *LGALS16* expression including p38/MAPK and Epac which are downstream cAMP receptors. Moreover, *LGALS16* is suggested to be essential for trophoblastic differentiation. Future studies can use trophoblastic models for genetic manipulation to continue to elucidate the functions of galectin-16, particularly in association with the maternal immune response. Overall, my findings indicate that *LGALS16* is a novel biomarker of placental differentiation which may be used as a diagnostic and therapeutic strategy for human choriocarcinoma and placental pathologies.

4.9   References

MacDonald TM, Walker SP, Hannan NJ, Tong S, Kaitu'u-Lino TJ. Clinical tools and biomarkers to predict preeclampsia. EBioMedicine. 2022 Jan;75:103780.

Sammar M, Drobnjak T, Mandala M, Gizurarson S, Huppertz B, Meiri H. Galectin 13 (PP13) facilitates remodeling and structural stabilization of maternal vessels during pregnancy. Int J Mol Sci. 2019 Jun 29;20(13):3192.

Sherazi AA, Jariwala KA, Cybulski AN, Lewis JW, Karagiannis J, Cumming RC, Timoshenko AV. Effects of global O-GlcNAcylation on galectin gene-expression profiles in human cancer cell lines. Anticancer Res. 2018 Dec;38(12):6691–6697.

Si Y, Yao Y, Jaramillo Ayala G, et al. Human galectin-16 has a pseudo ligand binding site and plays a role in regulating c-Rel-mediated lymphocyte activity. Biochim Biophys Acta Gen Subj. 2021 Jan;1865(1):129755.

Stepan H, Hund M, Andraczek T. Combining biomarkers to predict pregnancy complications and redefine preeclampsia: the angiogenic-placental syndrome. Hypertension. 2020 Apr;75(4):918-926.

Than NG, Romero R, Xu Y, Erez O, Xu Z, Bhatti G, Leavitt R, Chung TH. El-Azzamy H, LaJeunesse C, et al. Evolutionary origins of the placental expression of chromosome 19 cluster galectins and their complex dysregulation in preeclampsia. Placenta. 2014 Nov;35(11):855–865.

Uhlén M, Fagerberg L, Hallström BM, Lindskog C, Oksvold P, Mardinoglu A, Sivertsson A, Kampf C, Sjöstedt E, Asplund A. Tissue-based map of the human proteome. Science. 2015 Jan 23;347(6220):1260419.

Appendix A: Supplementary Material
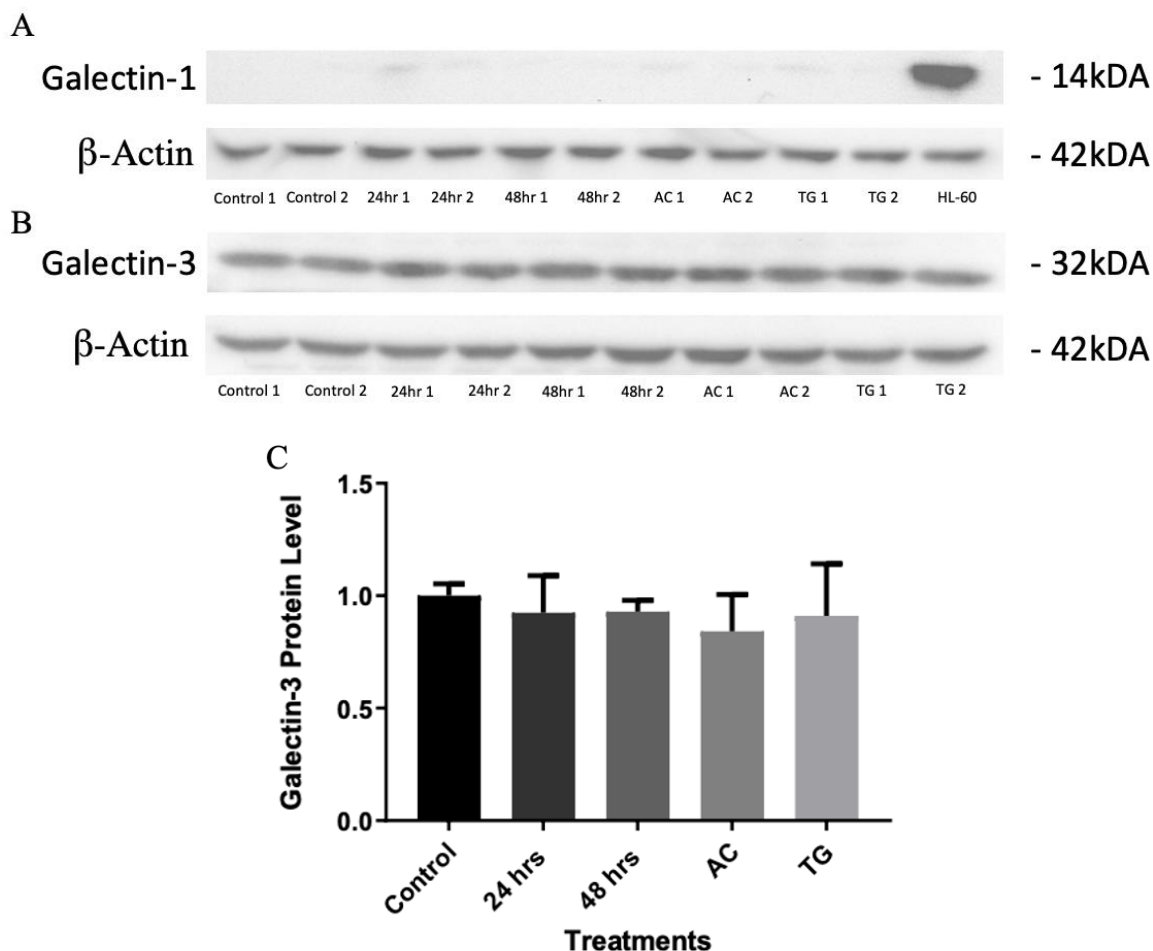
Figure S1. Western blots for intracellular protein levels of (A) galectin-1 and (B) galectin-3 in BeWo cells treated with 250 μM 8-Br-cAMP for 24 and 48 hours as well as BeWo cells treated with 25 μM AC (OGT inhibitor) or 10 μM TG (OGA inhibitor) for 24 hours, n=2. β-actin was used as the loading control. Due to low levels of galectin-1, HL60 cells were included as a positive control. (C) Band intensity of galectin-3 western blots was quantified using ImageLab software (Bio-Rad). Values are presented as mean ± SD, n=3.
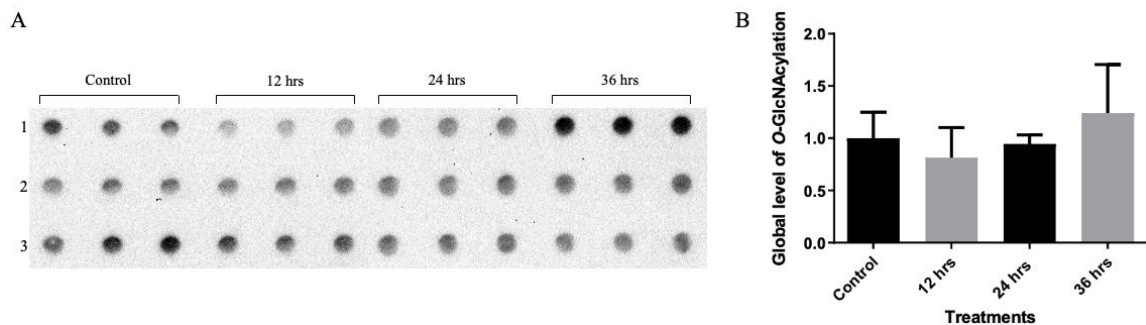
Figure S2. Immunodot blot analysis of protein lysates from (A) JEG-3 cells treated with 250 µM 8-Br-cAMP for 0, 12, 24, or 36 hours. (B) Quantification of the global level of *O*-GlcNAcylation based on densitometry analysis using ImageLab software (Bio-Rad) reveals no change in *O*-GlcNAcylation during differentiation. Values are presented as mean ± SD, n=3.
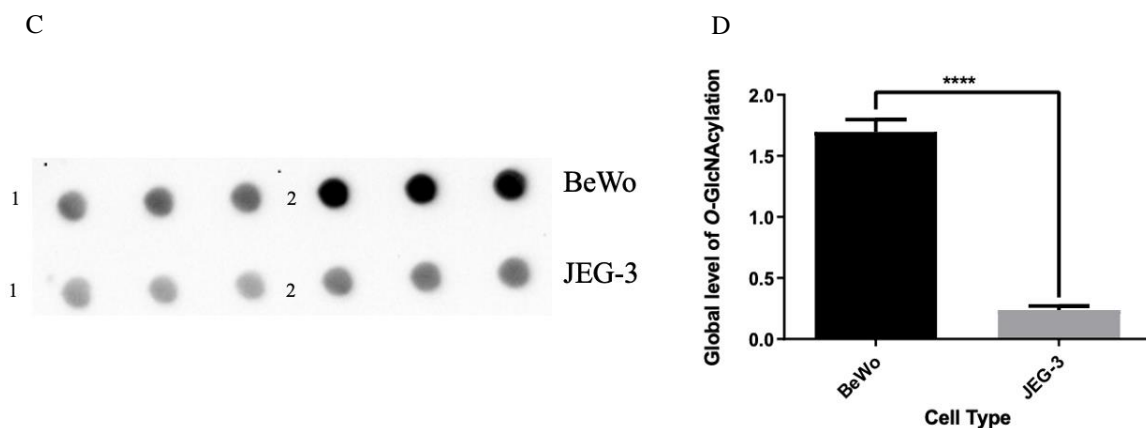
Figure S3. Immunodot blot analysis of protein lysates from untreated (A) BeWo cells or (B) JEG-3 cells. (B) Quantification of the basal level of *O*-GlcNAcylation based on densitometry analysis using ImageLab software (Bio-Rad) reveals a significantly lower level of *O*-GlcNAcylation in JEG-3 cells compared to BeWo cells. Values are presented as mean ± SD. Significance is reported according to ****$P < 0.0001$.

A

Status ⓘ	Guide Target ⓘ	PAM Sequence ⓘ	Indel % ⓘ	Model Fit (R²) ⓘ	Knockout-Score ⓘ
✅ Succeeded	TTTCTACACTGAGATGAATG	AGG	50	0.74	46

RELATIVE CONTRIBUTION OF EACH SEQUENCE (NORMALIZED)

POWERED BY ▶SYNTHEGO | ICE

INDEL	CONTRIBUTION ▾	SEQUENCE
+1	31%	CAGGTGGATTTCTACACTGAGATGA┆NATGAGGACTCAGAAATTGCCTTCCATTTGCGAGTGCACTTAGGCCGTCG
+ 0	24%	CAGGTGGATTTCTACACTGAGATGA┆ATGAGGACTCAGAAATTGCCTTCCATTTGCGAGTGCACTTAGGCCGTCGT
-11	9%	CAGGTGGATTTCTACACTGAGATGA┆-----------GAAATTGCCTTCCATTTGCGAGTGCACTTAGGCCGTCGT
+12	2%	CAGGTGGATTTCTACACTGAGATGA┆NNNNNNNNNNNNATGAGGACTCAGAAATTGCCTTCCATTTGCGAGTGCAC
-17	2%	CAGGTGGATTTCTACACTGAGAT--┆----------------TTGCCTTCCATTTGCGAGTGCACTTAGGCCGTCGT
-1	2%	CAGGTGGATTTCTACACTGAGATGA┆-TGAGGACTCAGAAATTGCCTTCCATTTGCGAGTGCACTTAGGCCGTCGT
+9	1%	CAGGTGGATTTCTACACTGAGATGA┆NNNNNNNNNATGAGGACTCAGAAATTGCCTTCCATTTGCGAGTGCACTTA
-25	1%	CAGGTGGATTTCTAC----------┆----------------TTGCCTTCCATTTGCGAGTGCACTTAGGCCGTCGT
-7	1%	CAGGTGGATTTCTACACTGAGATGA┆-------CTCAGAAATTGCCTTCCATTTGCGAGTGCACTTAGGCCGTCGT
-6	1%	CAGGTGGATTTCTACACTGAGATGA┆-------ACTCAGAAATTGCCTTCCATTTGCGAGTGCACTTAGGCCGTCGT

B

Status ⓘ	Guide Target ⓘ	PAM Sequence ⓘ	Indel % ⓘ	Model Fit (R²) ⓘ	Knockout-Score ⓘ
✅ Succeeded	TTTCTACACTGAGATGAATG	AGG	56	0.7	56

RELATIVE CONTRIBUTION OF EACH SEQUENCE (NORMALIZED)

POWERED BY ▶SYNTHEGO | ICE

INDEL	CONTRIBUTION ▾	SEQUENCE
+1	25%	CAGGTGGATTTCTACACTGAGATGA┆NATGAGGACTCAGAAATTGCCTTCCATTTGCGAGTGCACTTAGGCCGTC
+4	17%	CAGGTGGATTTCTACACTGAGATGA┆NNNNATGAGGACTCAGAAATTGCCTTCCATTTGCGAGTGCACTTAGGCC
+ 0	14%	CAGGTGGATTTCTACACTGAGATGA┆ATGAGGACTCAGAAATTGCCTTCCATTTGCGAGTGCACTTAGGCCGTCG
-17	13%	CAGGTGGATTTCTACACTGAGATGA┆------------------GCCTTCCATTTGCGAGTGCACTTAGGCCGTCG
-30	1%	CAGGTGGATTTCTAC-----------┆------------TTCCATTTGCGAGTGCACTTAGGCCGTCG

C

Status ⓘ	Guide Target ⓘ	PAM Sequence ⓘ	Indel % ⓘ	Model Fit (R²) ⓘ	Knockout-Score ⓘ
✅ Succeeded	TTTCTACACTGAGATGAATG	AGG	14	0.14	14

RELATIVE CONTRIBUTION OF EACH SEQUENCE (NORMALIZED)

POWERED BY ▶SYNTHEGO | ICE

INDEL	CONTRIBUTION ▾	SEQUENCE
-4	8%	CAGGTGGATTTCTACACTGAGATGA┆----GGACTCAGAAATTGCCTTCCATTTGCGAGTGCACTTAGGCCGTCG
-39	3%	CAGGT--------------------┆------------CTTCCATTTGCGAGTGCACTTAGGCCGTCG
-4	2%	CAGGTGGATTTCTACACTGAGA---┆-TGAGGACTCAGAAATTGCCTTCCATTTGCGAGTGCACTTAGGCCGTCG
-4	1%	CAGGTGGATTTCTACACTGAGAT--┆--GAGGACTCAGAAATTGCCTTCCATTTGCGAGTGCACTTAGGCCGTCG

D

Status	Guide Target	PAM Sequence	Indel %	Model Fit (R²)	Knockout-Score
✓ Succeeded	TTTCTACACTGAGATGAATG	AGG	62	0.75	62

RELATIVE CONTRIBUTION OF EACH SEQUENCE (NORMALIZED)

POWERED BY ▶SYNTHEGO ICE

INDEL	CONTRIBUTION	SEQUENCE
−11	38%	CAGGTGGATTTCTACACTGAGATGA‖-----------GAAATTGCCTTCCATTTGCGAGTGCACTTAGGCCGTCG
+1	20%	CAGGTGGATTTCTACACTGAGATGA‖NATGAGGACTCAGAAATTGCCTTCCATTTGCGAGTGCACTTAGGCCGTC
+ 0	13%	CAGGTGGATTTCTACACTGAGATGA‖ATGAGGACTCAGAAATTGCCTTCCATTTGCGAGTGCACTTAGGCCGTCG
−28	2%	CAGGTGGATTTCTACAC---------‖--------------------TTCCATTTGCGAGTGCACTTAGGCCGTCG
+7	1%	CAGGTGGATTTCTACACTGAGATGA‖NNNNNNNATGAGGACTCAGAAATTGCCTTCCATTTGCGAGTGCACTTAG
−19	1%	CAGGTGGATTTCTACACTGAGATGA‖--------------------CTTCCATTTGCGAGTGCACTTAGGCCGTCG

E

Status	Guide Target	PAM Sequence	Indel %	Model Fit (R²)	Knockout-Score
✓ Succeeded	TTTCTACACTGAGATGAATG	AGG	61	0.74	61

RELATIVE CONTRIBUTION OF EACH SEQUENCE (NORMALIZED)

POWERED BY ▶SYNTHEGO ICE

INDEL	CONTRIBUTION	SEQUENCE
−10	22%	CAGGTGGATTTCTACACTGAGATGA‖-----------AGAAATTGCCTTCCATTTGCGAGTGCACTTAGGCCGTCG
−25	21%	CAGGTGGATTTCTACACTGA------‖--------------------TTCCATTTGCGAGTGCACTTAGGCCGTCG
+1	17%	CAGGTGGATTTCTACACTGAGATGA‖NATGAGGACTCAGAAATTGCCTTCCATTTGCGAGTGCACTTAGGCCGTC
+ 0	13%	CAGGTGGATTTCTACACTGAGATGA‖ATGAGGACTCAGAAATTGCCTTCCATTTGCGAGTGCACTTAGGCCGTCG
+8	1%	CAGGTGGATTTCTACACTGAGATGA‖NNNNNNNNATGAGGACTCAGAAATTGCCTTCCATTTGCGAGTGCACTTA

F

Status	Guide Target	PAM Sequence	Indel %	Model Fit (R²)	Knockout-Score
✓ Succeeded	TTTCTACACTGAGATGAATG	AGG	47	0.89	46

Last guide at position 253 of 408, consider repositioning primers around the cutsites.

RELATIVE CONTRIBUTION OF EACH SEQUENCE (NORMALIZED)

POWERED BY ▶SYNTHEGO ICE

| INDEL	CONTRIBUTION	SEQUENCE
−28	42%	CAGGTGGATTTCTACAC---------‖--------------------TTCCATTTGCGAGTGCACTTAGGCCGTCGT
+ 0	42%	CAGGTGGATTTCTACACTGAGATGA‖ATGAGGACTCAGAAATTGCCTTCCATTTGCGAGTGCACTTAGGCCGTCGT
−10	2%	CAGGTGGATTTCTACACTGAGATGA‖-----------AGAAATTGCCTTCCATTTGCGAGTGCACTTAGGCCGTCGT
+19	1%	CAGGTGGATTTCTACACTGAGATGA‖NNNNNNNNNNNNNNNNNNNATGAGGACTCAGAAATTGCCTTCCATTTGCG
+6	1%	CAGGTGGATTTCTACACTGAGATGA‖NNNNNNATGAGGACTCAGAAATTGCCTTCCATTTGCGAGTGCACTTAGGC
+5	1%	CAGGTGGATTTCTACACTGAGATGA‖NNNNNATGAGGACTCAGAAATTGCCTTCCATTTGCGAGTGCACTTAGGCC

Figure S4. A JEG-3 *LGALS16* knockout (KO) cell pool from Synthego was diluted to 0.5 cells or 1 cells per well and grown to 80% confluency in 96-well plates. Genomic DNA was extracted, PCR amplified, purified, and sequenced at Robarts Research Institute (London, ON, Canada). Sanger sequencing results of (A) the original KO pool received from Synthego and 4 clonal pools, (B) pool #14, (C) pool #15, (D) pool #22, (E) pool #23, (F) pool #41 were analyzed using the Synthego ICE tool. Pools (A-E) showed mutated cells, however, none of them could be classified as pure clones due to multiple mutations in each. Only pool #41 (F) could be classified as a pure heterozygous clone of genetically identical cells. The equal contribution of sequences of 42% indicates that all cells contain one chromosome with a deletion of 28 nucleotides and one wildtype chromosome. A model fit of 0.7 or higher indicated high quality sequencing. Mutants less than 5% can be attributed to background noise and consequently ignored.
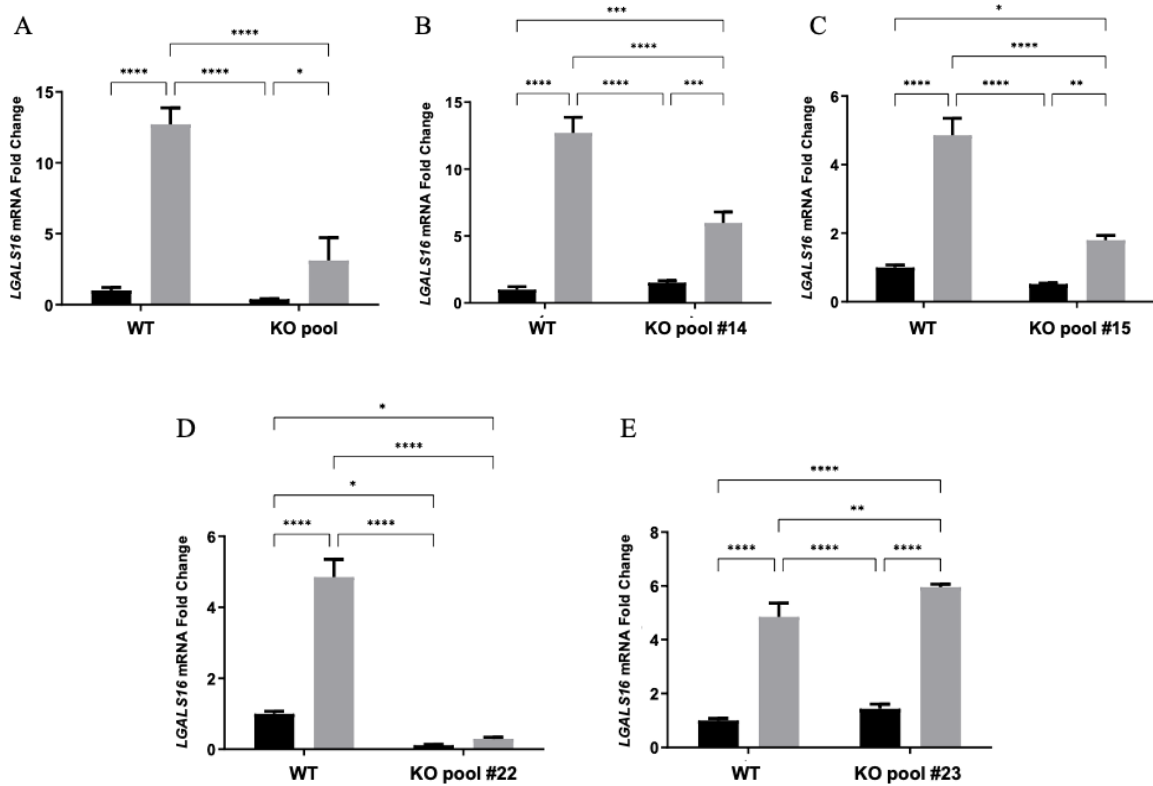
Figure S5. *LGALS16* expression during differentiation of *LGALS16* KO clonal pools. RT-qPCR of WT and *LGALS16* KO cell mRNA untreated or treated with 8-Br-cAMP for 36 hours of (A) the original KO pool received from Synthego, (B) clonal pool #14, (C) clonal pool #15, (D) clonal pool #22, and (E) clonal pool #23. Quantification revealed *LGALS16* expression was significantly inhibited under 8-Br-cAMP treatment for the KO pools and pools #14, 15, and 22 while pool #23 showed a significant increase in *LGALS16* expression. Black and grey columns indicate untreated and 8-Br-cAMP treated cells, respectively. The data was quantified using the Livak method (2-ΔΔCT) and normalized to *ACTB* as a reference gene. Values are presented as mean ± SD, n=3. All statistical analysis was performed using PRISM 9.3.1 software (one-way ANOVA followed by Tukey's multiple comparisons test). Significance is reported according to ****P<0.0001, ***P<0.001, **P<0.01, *P<0.05.
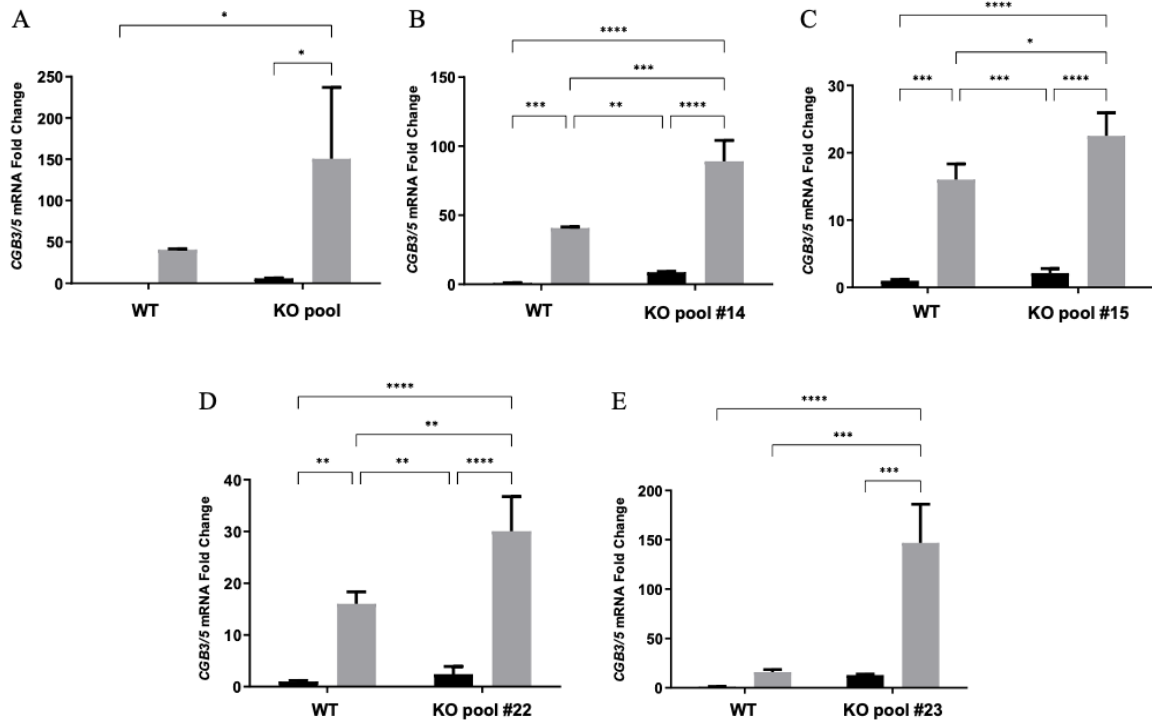
Figure S6. *CGB3/5* expression during differentiation of *LGALS16* KO clonal pools. RT-qPCR of WT and *LGALS16* KO cell mRNA untreated or treated with 8-Br-cAMP for 36 hours of (A) the original KO pool received from Synthego, (B) clonal pool #14, (C) clonal pool #15, (D) clonal pool #22, and (E) clonal pool #23. Quantification revealed *CGB3/5* expression was significantly increased under 8-Br-cAMP treatment for all clonal pools and did not change for the original KO pool. Black and grey columns indicate untreated and 8-Br-cAMP treated cells, respectively. The data was quantified using the Livak method ($2^{-\Delta\Delta CT}$) and normalized to *ACTB* as a reference gene. Values are presented as mean ± SD, n=3. All statistical analysis was performed using PRISM 9.3.1 software (one-way ANOVA followed by Tukey's multiple comparisons test). Significance is reported according to ****P<0.0001, ***P<0.001, **P<0.01, *P<0.05.
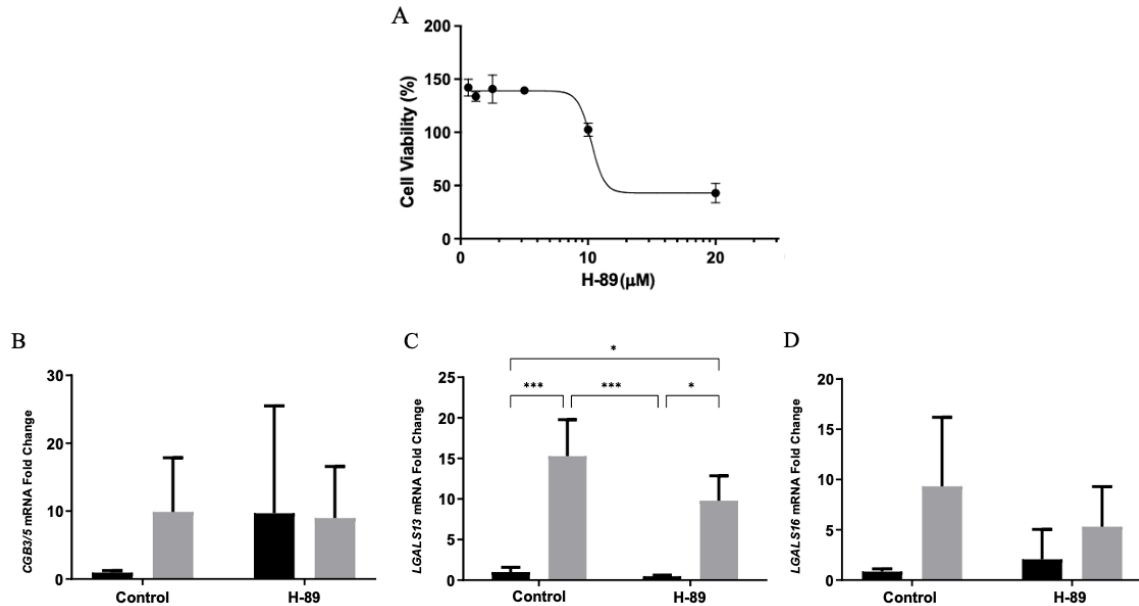
Figure S7. (A) Cell viability of BeWo cells treated with varying concentrations of H-89, a biochemical inhibitor of PKA. BeWo cells were cultured in 96-well plates and treated with various concentrations of inhibitors with or without 250 μM of 8-Br-cAMP every 12 hours for 48 hours. Control cells had medium changed every 12 hours. After 48 hours, cell viability was recorded. BeWo cells were cultured in 6-well plates and treated with 10 μM of H-89 alone or in combination with 250 μM 8-Br-cAMP for 48-hours. RT-qPCR was then used to measure the effects of H-89 on (B) *CGB3/5* expression, (C) *LGALS13* expression, and (D) *LGALS16* expression during trophoblastic differentiation. Cells treated with H-89 showed no significant affect any of the genes tested during differentiation. Black bars indicate untreated cells. Grey bars indicate cells treated with 8-Br-cAMP. Values are presented as mean $\pm$ SD (n=3). Significance is reported according to ***$P < 0.001$, *$P < 0.05$.

Curriculum Vitae

Name: Jennifer Kaminker

Post-secondary Education and Degrees:
The University of Western Ontario
London, Ontario, Canada
2020-2022 M.Sc. in Biology
2016-2020 B.Sc. Honours Specialization in Biology

Honours and Awards:
Harrypersad-Tewari Scholarship in Science
2018

Scholar Athlete Award
2018, 2019, 2020, 2021

Canada Graduate Scholarships – Masters Natural Sciences and Engineering Research Council of Canada (CGSM-NSERC)
2020-2021

Related Work Experience
Teaching Assistant
The University of Western Ontario
2020-2022

Publications:

Kaminker JD, Timoshenko AV. Expression, Regulation, and Functions of the Galectin-16 Gene in Human Cells and Tissues. Biomolecules. 2021;11(12):1909.

Abstracts and Posters:

- Kaminker J, Butt A, Timoshenko AV (2022) Insights into the molecular mechanisms regulating *LGALS16* gene expression in JEG-3 cells. 18th Annual Oncology Research and Education Day, London, Ontario, June 10, 2022, Poster #26.
- Kaminker J, Timoshenko AV (2021) *LGALS16* is a new biomarker of placental cell differentiation. Ontario Cell Biology Symposium (online), July 12-16, 2021.
- Kaminker J, Jaju G, Renaud SJ, Timoshenko AV (2021) Investigating O-GlcNAc and galectin gene expression in BeWo. 17th Annual Oncology Research and Education Day (online). June 14-18, 2021.
- Kaminker J, Jaju G, Renaud SJ, Timoshenko AV (2020) Investigating O-GlcNAc and galectin gene expression in BeWo. Canadian Glycomics Symposium (online). June 25, 2020.
- Kaminker J, Lee A, Castanov V, Duong A, Arakawa T, Agur A. Comparison of Musculotendinous Morphology of Extensor Hallucis Brevis and Extensor Digitorum Brevis. American Association of Clinical Anatomists Meeting, Minneapolis, Minnesota, July 17-21, 2017.